THE PROCEEDINGS OF
THE PHYSICAL SOCIETY

Section A

VOL. 64, PART 1 1 January 1951 No. 373 A

Cascade Theory including Ionization Loss

BY L. JÁNOSSY* AND H. MESSEL
Dublin Institute for Advanced Studies

MS. received 24th July, 1950

ABSTRACT. The Bhabha–Chakrabarty solution of the cascade equations with ionization loss is discussed, and a simplified method of numerical evaluation suggested.

§ 1.

MANY treatments of the cascade theory have been given, both in 'approximation A', i.e. using asymptotic cross sections and neglecting ionization loss, and also using asymptotic cross sections and including effects of ionization loss; for a summary of the older literature see for example Jánossy (1950). Recently two important articles have appeared (Snyder 1949, Bhabha and Chakrabarty 1948): the latter is an elaboration of the original paper by Bhabha and Chakrabarty (1943).

The treatment of the ionization term by Bhabha and Chakrabarty has, in our opinion, the great advantage that the first order correction of the effects of ionization loss is expressed as a shift of the energy spectrum by an amount of the order of the critical energy; this correction gives a direct physical insight into the mechanism of the cascade. The Bhabha-Chakrabarty treatment was criticized and it was alleged that the first approximation did not give a sufficiently accurate description of the phenomenon. In the meantime it has been shown by Bhabha and Chakrabarty (1948) that the latter criticism need not be taken too seriously: in such regions of energy where the cross sections can be relied upon, the deviations between their own treatment and the mathematically more exact treatment of, for instance, Snyder are not of importance. In our own opinion the treatment of Bhabha and Chakrabarty gives sufficient accuracy for practical purposes and has the great advantage of simplicity. For small depths, however, Bhabha and Chakrabarty sacrifice this simplicity and evaluate the average numbers of particles by a rather elaborate procedure; the object of the present paper is to show that this complicated procedure is unnecessary.

§ 2.

The first approximation to the average number of electrons of energy greater than E along a path z to which a primary energy E_0 gives rise can be written

$$T_\beta(E_0, E, z) = \frac{1}{2\pi i}\int_{y_0-i\infty}^{y_0+i\infty}\left(\frac{E_0}{E+\beta g(y,z)}\right)^{y-1} K(y,z)\frac{dy}{y-1} \qquad \ldots\ldots(1)$$

* Now at the Institute of Physics, Eötvös Loránt University, Budapest, Hungary.

where $g(y, z)$ is a slowly varying function defined by Bhabha and Chakrabarty. β is the rate of ionization loss and

$$K(y,z)=\frac{D-a_1}{a_2-a_1}\exp(-a_1 z)+\frac{a_2-D}{a_2-a_1}\exp(-a_2 z). \qquad \ldots\ldots(2)$$

For $\beta=0$ equation (1) represents the solution in approximation A. Integrals of the type (1) can be evaluated by the saddle-point method.

In some of the treatments of the cascade problem T_β is split into two terms

$$T_\beta = T^1{}_\beta + T^2{}_\beta \qquad \ldots\ldots,(3)$$

according to the terms of K given in (2) $T^1{}_\beta$ is evaluated by the saddle-point method. $T^2{}_\beta$ cannot be evaluated in this way as it possesses no suitable minimum, but $T^2{}_\beta$ is assumed to be small as compared with $T^1{}_\beta$ for sufficiently large values of z and is usually neglected.

It was pointed out by Jánossy and Tzu (1946) that it is quite unnecessary to split the integral into two parts according to (3); the integral (1) can be evaluated by using the unabridged function $K(y, z)$ in (1). The use of the unabridged function $K(y, z)$ has the advantage that saddle points are obtained right down to $z=0$; for $z=0$ one finds, for $E_0>E$, $g(y, 0)=0$ and $K(y, 0)=1$.

$$T(E_0,E,0)=\frac{1}{2\pi i}\int\left(\frac{E_0}{E}\right)^{y-1}\frac{dy}{y-1}=\begin{cases}1\ \text{(exact)}\\ \dfrac{e}{\sqrt{(2\pi)}}=1{\cdot}08\ \text{(saddle-point method),}\end{cases} \qquad \ldots\ldots(4)$$

thus for $z=0$ the error of the saddle-point method amounts to 8%. Further it was shown that for large z, i.e. whenever

$$a_1 z \ll a_2 z \quad \text{(at the saddle point)} \qquad \ldots\ldots(5)$$

the terms arising from the second term of $K(y, z)$ have a very slight effect only on either the position or height and width of the saddle; thus, provided (5) holds,

$$T_\beta \simeq T^1{}_\beta. \qquad \ldots\ldots(6)$$

The latter consideration shows that one is indeed justified in neglecting $T^2{}_\beta$ provided (5) is satisfied. Thus for small depths the method of Jánossy and Tzu gives errors of about 8% while for large depths it gives results essentially in agreement with the older procedure.

§ 3.

The method proposed by Jánossy and Tzu was criticized by Chakrabarty (1946) and therefore it appears worth while to give some justification.

From the point of view of saddle-point integration it is certainly justified to use the whole function $K(y, z)$ rather than the first exponential only. In fact the function $K(y, z)$ is analytic in the whole complex y-plane with the exception of poles along the negative y-axis; the separate terms of $K(y, z)$ given in (2) are more complicated—they are analytic only in the complex plane slit along the negative y-axis. Thus $K(y, z)$, as it must do, shows in general the analytic behaviour to be expected for the Mellin transform of T, while the separate terms have a more complicated behaviour. This consideration weighs in favour of using the whole function $K(y, z)$.

No argument against the use of $K(y, z)$ can be deduced from the fact that the second term given in (2) cannot be evaluated by a saddle; every function having

a minimum can be split into two components one possessing a minimum and the other not.

Thus from general grounds there seems to be no justification for the splitting of T_β according to (3).

§ 4.

We have thus evaluated $T_\beta(E_0, E, z)$ from (1) for $E=0$ (total number of particles), $\ln E_0/\beta = 6$, $z = 0{\cdot}5 \to 20$, using the full expression for $K(y, z)$. In course of computation it is seen immediately that without loss of accuracy it is possible to factorize the integrand into a suitable 'slowly varying function' and a 'rapidly varying function', to determine the saddle point by the latter function and replace the former by its value at the saddle thus defined. We have thus taken

$$T_\beta(E_0, E, z) = \{g(y_0, z)\}^{-\nu_s+1}\left(1+\frac{D-a_2}{a_1-D}\exp\{-(a_2-a_1)z\}\right)_{\nu_s}\frac{1}{2\pi i}$$
$$\times\int\left(\frac{E_0}{\beta}\right)^{\nu-1}\frac{D-a_1}{a_2-a_1}\exp(-a_1 z)\frac{dy}{y-1} \quad \ldots\ldots(7)$$

with
$$z = \frac{\ln\left(\frac{E_0}{\beta}\right)+\left\{\ln\frac{D-a_1}{a_2-a_1}\right\}'-\frac{1}{y_0-1}}{a_1'(y_0)} \quad \ldots\ldots(8)$$

$$\frac{1}{2\pi i}\int\left(\frac{E_0}{\beta}\right)^{\nu-1}\frac{D-a_1}{a_2-a_1}\exp(-a_1 z)\frac{dy}{y-1} = \frac{(E_0/\beta)^{\nu_s-1}}{y_0-1}\frac{D-a_1}{a_2-a_1}$$
$$\times\frac{\exp(-a_1 z)}{\left[2\pi\left\{(y_0-1)^{-2}+\left(\ln\frac{D-a_1}{a_2-a_1}\right)''-a_1''z\right\}\right]^{1/2}} \quad \ldots\ldots(9)$$

In the dotted curve of the Figure we have given results obtained from (7), (8) and (9). The full line on the same graph gives the results of Bhabha and Chakrabarty

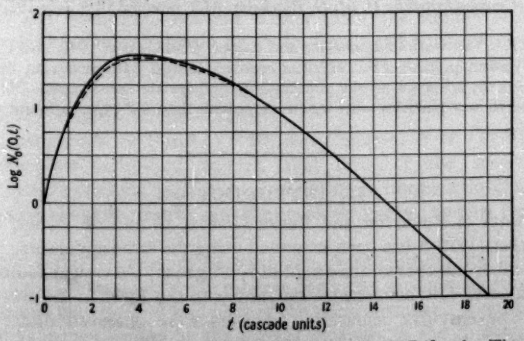

A plot of log N_e $(0, t)$ against the depth t in cascade units for $\ln E_0/\beta = 6$. The full curve is that obtained by Bhabha and Chakrabarty, the dotted one obtained by us.

obtained from (1) employing a rather elaborate method of computing the complex integral. The agreement between the two curves is excellent and therefore we conclude that the parametric representation (7), (8) and (9) gives a satisfactory method of evaluating the integral (9).

§ 5.

For most practical purposes a satisfactory approximation of T_β can be obtained with the aid of tables of T_0 and g, using the relation

$$T_\beta(E_0, E, z) \simeq T_0(E_0, E+\beta g(y_0, z), z) \qquad \ldots\ldots (10)$$

Detailed tables of T_0 using the method of Jánossy and Tzu and of the corresponding g-values have been computed by the present authors and are reproduced by Jánossy (1950, Appendix II, p. 399–407).

ACKNOWLEDGMENT

One of the authors (H. M.) wishes to thank the National Research Council of Canada for the provision of a Special Scholarship.

REFERENCES

Bhabha, H. J., and Chakrabarty, S. K., 1943, *Proc. Roy. Soc.* A, **181**, 267; 1948, *Phys. Rev.*, **74**, 1352.

Chakrabarty, S. K., 1946, *Nature, Lond.*, **158**, 166.

Jánossy, L., 1950, *Cosmic Rays*, 2nd Edition (Oxford : University Press).

Jánossy, Leonie, and Messel, H., 1949, *Tables of Cascade Functions* (circulated by the Dublin Institute for Advanced Studies).

Jánossy, L., and Tzu, H. Y., 1946, *Nature, Lond.*, **157**, 624.

Snyder, H. S., 1949, *Phys. Rev.*, **76**, 1563.

The Nuclear Interaction Length of the Particles in Penetrating Cosmic-Ray Showers

By K. H. Barker and C. C. Butler

The Physical Laboratories, University of Manchester

Communicated by P. M. S. Blackett; *MS. received* 10*th July* 1950

ABSTRACT. The work of Rochester and Butler, published in 1948, and that of Butler, Rosser and Barker, published in 1950, has been continued. In particular, the interaction properties and the spectrum of the penetrating particles are considered. The interaction length of the shower particles with momenta greater than 10^9 ev/c. is found to be 18 cm. lead ($\pm 20\%$).

§ 1. INTRODUCTION

The work of Rochester and Butler (1948 a, b) and of Butler, Rosser and Barker (1950)* has been extended using the same apparatus. The cloud chamber was operated in a field of 7,500 gauss ; the Geiger counter arrangement was a seven-fold coincidence set similar to the P-set in the arrangement B of B.R.B. Seventy-five penetrating showers were observed under 25 cm. of lead and twenty-two under 25 cm. of paraffin wax. These sea-level observations are now complete and the total data obtained during all the experiments have been analysed. A total of 164 penetrating showers has been observed which shows 240 particles penetrating the 3·4 cm. lead plate in the chamber. In order to obtain the interaction length of the secondary, or shower, particles it is necessary to measure

* Subsequently referred to as B.R.B.

the momentum spectrum of these particles. The total data for this differential momentum spectrum are given in § 2 and the interaction length is discussed in § 3. Four unusual showers obtained under 25 cm. of paraffin wax are shown in the Plate and discussed in the Description of Plate (see end of issue).

§ 2. THE DIFFERENTIAL MOMENTUM SPECTRUM OF THE PENETRATING PARTICLES

The experiments with either 25 cm. of lead or 25 cm. of paraffin wax as transition material provide considerable additional data for the momentum spectrum of the penetrating particles. That the counter selection provided a strong bias towards high-energy events is evident from the fact that 80% of the photographs obtained under 25 cm. of lead showed electrons, because Fretter (1949) shows that, in general, only very energetic interactions give rise to an appreciable electronic component. The data obtained in all the sea-level experiments are collected in Table 1; no correction has been made for ionization loss in the transition material.

Table 1

Momentum range ($\times 10^9$ ev/c.)	1–5	5–10	10–20	20–30	>30
No. of particles under lead	16	34	50	21	14
No. of particles under paraffin wax	0	6	5	2	7

Table 2

Momentum range ($\times 10^9$ ev/c.)	5–10	10–20	>20
Cloud chamber (under lead)	$3{\cdot}5 \pm 0{\cdot}7$	$2{\cdot}9 \pm 0{\cdot}7$	$2{\cdot}5 \pm 0{\cdot}8$
Photographic plate	$8{\cdot}8 \pm 1{\cdot}9$	$3{\cdot}4 \pm 0{\cdot}9$	—

A positive excess of $3{\cdot}0 \pm 0{\cdot}6$ is found among the penetrating particles under lead and a positive excess of $2{\cdot}0 \pm 1{\cdot}0$ under paraffin wax. It is generally accepted that a considerable number of the shower particles are π-mesons. On the assumption that the showers are produced equally by both neutral and charged primaries (cf. Jánossy and Rochester 1943 and Walker 1950), the number of positive and negative mesons produced should be about equal, and so the observed positive excess must be attributed to the presence of protons. Identifiable protons are strongly absorbed in the 3·4 cm. lead plate; consequently very few identified protons appear in the spectrum of Table 1.

The investigations of Fowler (1950) and Camerini *et al.* (1950), using the photographic-plate technique, suggest that 80% of the shower particles ($I/I_{\min} < 1{\cdot}5$) are π-mesons. Thus it is interesting to compare the cloud-chamber and photographic-plate results for the positive excess among the secondary particles.

In Table 2 the discrepancy between the cloud-chamber and photographic-plate data in the lowest momentum range is due to the strong absorption of protons in the transition material and lead plate of the cloud chamber. For this reason the percentage of π-mesons among the shower particles in the chamber cannot be determined and, therefore, a simple comparison with the photographic-plate data cannot be made. Between 10^9 ev/c. and 2×10^9 ev/c. agreement is good, but no comparison is possible in the highest momentum range although the cloud-chamber data provide some evidence for an appreciable component of protons among the very energetic shower particles. Individual showers of very high energy, photographed in the cloud chamber, show a very large positive excess, so it seems certain

that a process must exist whereby several protons, and presumably neutrons, can be accelerated to relativistic velocities.

Beyond momenta of 10^9 ev/c. the observed differential momentum spectrum of the penetrating particles from lead is of the form

$$N(E)\,dE \propto E^{-(2\cdot5\pm0\cdot3)}dE,$$

and is thus similar in form to the spectrum of mesons at formation.

The data obtained using paraffin wax as transition material are very meagre, but relatively more high energy particles are found under paraffin wax than under lead. This is to be expected, as fewer secondary interactions within the nucleus, made by energetic recoil nucleons from the first collision, are likely to take place in paraffin wax than in lead.

A number of primary and secondary interactions, mostly of high energy, have been observed in the lead plate. Some of the shower particles produced in the plate are suitable for measurement, and the differential momentum spectrum of 44 particles is given in Table 3.

Table 3

Momentum range ($\times 10^8$ ev/c.)	1–5	5–10	10–15	15–20	>20
No. of particles	19	9	9	5	1

The overall positive excess of these particles is $3\cdot1 \pm 1\cdot2$ and the maximum intensity occurs at a much lower momentum than is the case for the penetrating particles. This is to be expected, since the selection is made from a much wider angular distribution of particles than was possible in the results of Table 1, and also the shower particles are not required to penetrate more than about 1 cm. of lead.

§3. THE NUCLEAR INTERACTIONS OF THE SHOWER PARTICLES

The nuclear interactions of the shower particles observed in the lead plate fall into three main categories: (i) lightly ionizing particles undergoing a large-angle scattering considerably in excess of the calculated coulomb scattering appropriate to the particle momentum and the thickness of the lead plate; (ii) interactions of lightly ionizing or neutral particles with the production of both heavily and lightly ionizing secondaries; (iii) lightly ionizing particles other than electrons stopping in the lead plate.

Thirty-eight secondary interactions have been observed, consisting of 8 of type (i), 23 of type (ii), of which 14 have ionizing primaries, 5 neutral primaries and 4 either ionizing or neutral primaries, and 7 of type (iii).

The interaction length of the particles constituting penetrating showers can be deduced from the observed numbers of interactions and penetrating particles. B.R.B. found a value of 35 cm. of lead for this interaction length. Using all the data now available, the value is 26 cm. of lead. It is necessary, however, to assess the efficiency of detection of the three types of nuclear interactions in order to correct this figure.

(*a*) *Events of type* (*i*). *Anomalous scattering.*

The majority of the eight particles showing large-angle scattering in the lead plate cannot be protons because two emerge from the plate with momenta less than 6×10^8 ev/c. and with minimum ionization, and four of the remaining six particles

are negative. The variation of the scattering angle with the particle momentum is shown in the Figure; the curve corresponds to five times the probable multiple-coulomb scattering calculated using Williams' formula.

The eight examples of anomalous scattering may represent the nuclear scattering of π-mesons. On this assumption, and on the assumption that half of the shower particles are π-mesons, the cross section for this process is $2{\cdot}8 \times 10^{-27}$ cm^2 per nucleon ($\pm 50\%$) or approximately 50 cm. of lead. This is considerably larger than the cross section found by Fretter (1949) and by Brown and McKay (1950), but is in good agreement with that calculated by Heitler on the basis of damping theory. The present very limited data do not permit an examination of the variation of the cross section with energy. The value of the interaction length of all the shower particles, i.e. protons and π-mesons, indicates that π-mesons must initiate interactions of types (ii) and (iii) as well as of type (i).

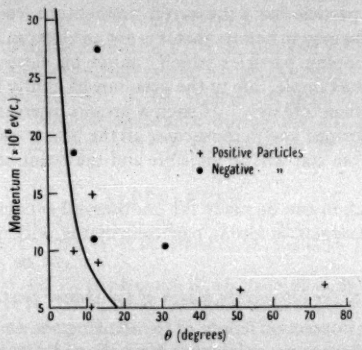

Events of type (i) are detected easily if the scattering is in the plane of the photograph, but there is considerable uncertainty when the scatter is towards or away from the camera. In addition, the geometrical form of the lead plate introduces a bias against very large-angle scattering, and if the scattering is small there is confusion with multiple-coulomb scattering. The probability of observing this type of interaction cannot be calculated, and we have to make the assumption that no events of this type are omitted from the analysis.

(*b*) *Events of type* (*ii*). *Nuclear interactions in the lead plate.*

Events of type (ii) will be detected with a high probability if lightly ionizing particles are emitted, but only with a considerably lower probability if such particles are not present, due to the fact that, for moderate excitation energies, the majority of the energy is carried by particles of intermediate ionization which are strongly absorbed in lead. In this connection the data of Brown *et al.* (1949) are useful; the average number and energy of the grey tracks, associated with 'stars' of various total energies occurring in silver and bromine nuclei, are estimated. If we assume that these data apply to stars produced in lead nuclei, a rough calculation suggests that the probability of detecting an interaction with an excitation energy of 500 Mev. is about one half in the present investigations. Below this energy the probability of detection falls quite rapidly, whilst above 500 Mev.

it rises towards unity at the energy where particle production is a frequent process, which is likely to be in the range $(1–2) \times 10^9$ ev. Thus, for the purpose of estimating an interaction length, we shall confine our attention to the interacting particles with momenta greater than 10^9 ev/c., corresponding to a proton energy of about 600 Mev., and assume that all the observed interactions of type (ii) are due to such particles, and that the probability of detecting such interactions is unity.

(*c*) *Events of type* (*iii*). *Fast particles stopped in the plate.*

All the particles which produced interactions of type (iii) have measured momenta greater than 10^9 ev/c. Electrons with similar momenta would have a high probability of producing electron cascades in the plate. The stopping particles were observed immediately below 5 cm. of lead and, since they are not accompanied by many soft electrons, are definitely not parts of cascade showers.

If the stopping particle has a measured momentum less than 10^9 ev/c. then in many cases it is less easy to be sure that it is not an electron. In fact we have not found any such stopping particles which cannot be electrons. Events of this kind must occur, for example, due to the presence of lightly ionizing protons with kinetic energy less than 500 Mev. If such a proton interacts in the plate, then a simple star will be formed and in most cases all the heavy tracks will be absorbed in the lead. Thus the star will be invisible and the event should be classified as type (iii).

Adequate correction can be made for unobserved events of type (iii) by confining attention to energetic stopping particles, that is, with momenta greater than 10^9 ev/c.

(*d*) *The calculation of the interaction length of the shower particles.*

To calculate the interaction length of the ionizing shower particles we neglect all events with incident momenta less than 10^9 ev/c. and determine the thickness of lead penetrated by the particles with momenta greater than 10^9 ev/c. From Table 1 we find that 64% of the penetrating particles have momenta greater than 10^9 ev/c., so that of the 240 penetrating particles, 153 of at least this momentum penetrate the 3·4 cm. lead plate, accompanied by 27 interactions of ionizing particles. The interaction length is thus 18 cm. of lead ($\pm 20\%$), corresponding to 1·3 times the geometrical cross section in lead. The error quoted is a purely statistical one based on the observed number of interactions. There is a further small uncertainty due to undetected nuclear interactions (mainly scatterings) of particles with momenta greater than 10^9 ev/c. Therefore it appears likely that the interaction length calculated on the foregoing assumptions will tend to be too great.

The positive excess of the shower particles with momenta above 10^9 ev/c. is $2·7 \pm 0·7$. Assuming that this positive excess is due to the presence of protons and that the proton interaction length is 14 cm. of lead, then the overall interaction length of 18 cm. of lead indicates that the high energy π-mesons possess an interaction length of the same order as that of fast protons.

Camerini *et al.* (1950) have made a determination of the interaction length of shower particles ($I/I_{\min} < 1·5$) in photographic emulsion and find a value 1·1 times the geometrical cross section.

Several workers have investigated the interactions of secondary penetrating shower particles in cloud chambers containing several thin lead plates (Fretter

1949, Lovati *et al.* 1950, Brown and McKay 1950). The values obtained for the interaction length, after applying corrections for invisible interactions, are all about the same and equal to 30 cm. of lead. This value is considerably larger than that calculated above, and a possible explanation is that a number of interactions, due to particles with energies of several hundred Mev., with the emission of heavily ionizing secondaries only, were not effectively corrected for by the procedure adopted.

§4. CONCLUSIONS

(1) The shower particles with momenta greater than 10^9 ev/c. must consist mainly of π-mesons and protons. The number of protons is likely to be between 25 and 50% of all the shower particles.

(2) The interaction length of the shower particles with momenta greater than 10^9 ev/c. is found to be 18 cm. lead ($\pm 20\%$).

ACKNOWLEDGMENTS

The authors wish to thank Professor P. M. S. Blackett for his deep interest in this work and for the laboratory facilities he has given them. They are indebted to Dr. G. D. Rochester and Dr. J. G. Wilson for helpful advice. The late Mr. C. O. Green gave valuable assistance during the last few months of the experiments; thanks are also due to Mr. A. H. Chapman for help in operating the apparatus.

REFERENCES

Brown, W. W., and McKay, A. S., 1950, *Phys. Rev.*, **77**, 342.
Brown, R. H., Camerini, U., Fowler, P. H., Heitler, H., King, D. T., and Powell, C. F., 1949, *Phil. Mag.*, **40**, 862.
Butler, C. C., Rosser, W. G. V., and Barker, K. H., 1950, *Proc. Phys. Soc.* A, **63**, 145.
Camerini, U., Fowler, P. H., Lock, W. O., and Muirhead, H., 1950, *Phil. Mag.*, **41**, 413.
Fowler, P. H., 1950, *Phil. Mag.* **41**, 169.
Fretter, W. B., 1949, *Phys. Rev.*, **76**, 511.
Heitler, W., 1949, *Cosmic Radiation* (London : Butterworth).
Jánossy, L., and Rochester, G. D., 1943, *Proc. Roy. Soc.* A, **182**, 180.
Lovati, A., Mura, A., Salvini, G., and Tagliaferri, G., 1950, *Phys. Rev.*, **77**, 284.
Rochester, G. D., and Butler, C. C., 1947, *Nature, Lond.*, **160**, 855; 1948 a, *Proc. Phys. Soc.*, **61**, 307; 1948 b, *Ibid.*, **61**, 535.
Walker, W. D., 1950, *Phys. Rev.*, **77**, 686.

The Importance of Gas Scattering in Particle Accelerators

By L. RIDDIFORD
The University, Birmingham

Communicated by P. B. Moon; *MS. received 20th July* 1950

ABSTRACT. In electron and proton synchrotrons there exists a minimum useful vertical aperture of the vacuum chamber, and for apertures less than this the beam intensity falls to zero. It is considered, on the basis of a comparison of theory and experiment, that this phenomenon is in the main due to free oscillations which arise from gas scattering. The final beam size in proton synchrotrons may be substantial for this reason also, but for cyclotrons the large spread which is known to exist must be attributed to some other phenomenon.

THE theory of gas scattering in a synchrotron has been given by Blachman and Courant (1948, 1949). The effect of this scattering is to set up vertical and horizontal free oscillations, whose mean square amplitude rises sharply to a maximum when the particles have reached four times their injection energy, and then falls asymptotically to zero. It may be shown that this maximum value is, in the vertical direction,

$$\overline{B^2} = 8{\cdot}17 \times 10^6 \frac{R^3 P}{V T_i}, \qquad \ldots\ldots(1)$$

with R the orbit radius in centimetres, P the air pressure in mm. Hg, and V and T_i the energy gained per revolution and injection energy respectively, both in electron volts. Equation (1) gives the obvious result that the vacuum should be as good as possible, and injection energy high. It is no doubt a good reason why betatron output increases so rapidly with injection voltage.

If $(\overline{B^2})^{1/2}_{\max}$ is of the order of the vertical aperture of the vacuum box, many particles will hit the walls of the doughnut and so be lost. Now it has been reported by Elder, Langmuir and Pollock (1948) and also by Lawson (1948) that an investigation of the variation of synchrotron (or betatron) beam intensity, as a function of the vertical aperture of the accelerating space, shows the existence of a minimal useful aperture of the order of 1·0 cm. in the centre of the doughnut; for apertures less than this the output from the machine falls to zero. McMillan (unpublished lecture) also has reported that a similar effect occurs in the Berkeley 300 MEV. electron synchrotron. Further, Lasich and Riddiford (1947) have noticed that for the Melbourne betatron (now a 14 MEV. synchrotron), pressures less than 2×10^{-5} mm. Hg are necessary for efficient operation. This point was also stressed by Kerst (1948) (see also Fry *et al.* 1948).

So far no reasonable explanation of this minimal useful aperture has been given although the answer has been sought in terms of resonances between the various particle oscillations (Lawson 1948). However, the reason seems clear if we substitute some figures into equation (1). The results for several accelerators are summarized in Table 1 for an operating air pressure of 1×10^{-5} mm. Hg.

It should be noted that, assuming no loss of particles due to wall collisions, the distribution about $b = B_{\max}/\sqrt{2}$ is a Rayleigh distribution, i.e. the probability that a particle has a value of B between B and $B + dB$ is

$$(\overline{b^2})^{-1} B \exp\{-(B^2/2\overline{b^2})\}\, dB. \qquad \ldots\ldots(2)$$

The integral of this distribution has a shape similar to the curves presented by Elder *et al.* and by Lawson. But equation (2) is not correct for the case in which particles are being continuously lost to the walls. If one calculates the fraction of particles P not scattered to the walls as a function of the available vertical semi-aperture from Blachman and Courant's theory, it is found that the curve has the same general shape as the integral of the Rayleigh distribution of equation (2), but that P is practically zero for values of B less than about B_{max} as defined by equation (1). This accounts for the minimal useful aperture.

A minimal aperture due to magnetic field inhomogeneities is not possible, and since the particles move in phase with the field disturbances, the curve showing the variation in beam intensity with aperture need not be symmetrical about the median plane, as it is found to be in practice. Further, with the type of gun used in electron accelerators, a wide spread of injection oscillations about the ideal orbit is to be expected, so that no minimum useful aperture would occur due to this type

Table 1

	Accelerator	R(cm.)	V^*	T_i	$2B_{max}$ (cm.)	Minimal Aperture (cm.)
Melbourne	3 MeV. betatron	7·5	20	$1{\cdot}5\times10^3$	2·2	—
Berkeley, Cornell	300 MeV. synchrotrons	100	1500	$8{\cdot}0\times10^4$	1·7	—
Malvern	30 MeV. synchrotron	10	25	$1{\cdot}0\times10^4$	1·1	0·6
G.E.C.	70 MeV. synchrotron	29	200	$3{\cdot}5\times10^4$	1·1	1·0
Oxford	16 MeV. synchrotron	20	20	$2{\cdot}5\times10^4$	2·3	—

* During betatron acceleration.

of free oscillation alone. Of course both of these phenomena occur in practice, and an investigation of the manner in which the intensity–aperture curve depends on the azimuth would permit of separation of the phenomena, in any case in which they are of comparable magnitude to the gas-scattering oscillations. Such an investigation will be an invaluable aid to efficient operation of the proton synchrotron.

It is worth while making two further points which have been investigated. The Blachman–Courant calculations, based on current design figures, indicate that proton synchrotron acceleration is quite practicable at physically realizable pressures. The operation of a model at Berkeley substantiates this conclusion (Sewell *et al.* 1950). However, gas scattering appreciably affects the final size of the beam, and may consequently make efficient extraction of the beam quite difficult. This is because the effects of damping of the free oscillations are being continuously annulled by further gas scattering throughout the acceleration cycle. For the Birmingham synchrotron (Oliphant, Gooden and Hide 1947) injecting at 500 kev. on a radius of 450 cm., with $V=200$ volts, it is estimated that the final beam size due to free gas-scattering oscillations will be 4·4 cm. horizontally and 2·5 cm. vertically, if the particles fill the vertical aperture of the vacuum box when $T_f=4T_i$, which they do unless the air pressure is less than $3{\cdot}5\times10^{-6}$ mm. Hg (see Table 2). Considering phase oscillations only, the final beam width is 0·9 cm. This does not, however, mean that the severe restrictions upon the amount that the radio frequency can slip into error in a time of the order of one phase-oscillation period can be relaxed, for although most of the particles are finally

geometrically outside the region of stable phase, they are still within that region when it is represented as a velocity–phase diagram. Table 2 shows the air pressure p (in mm. Hg) at which the vertical semi-aperture a of the vacuum box is equal to the value of $(\overline{B^2})^{1/2}_{\max}$ from equation (1), for the three proton synchrotrons at present under construction. The advantages of high injection energy and rapid acceleration are apparent. The Table also includes figures for the model accelerator. In fact it is found that, for an operating pressure of 2×10^{-6} mm. Hg, the beam intensity in this machine is very small when the vertical aperture is reduced to 10 cm. by insertion of screens.

Table 2

Laboratory	Energy (10^9 ev.)	R (cm.)	V	T_i(Mev.)	a (cm.)	p (mm.Hg)
Birmingham	1·3	450	200	0·5	5·0	$3{\cdot}5 \times 10^{-6}$
Brookhaven	3·0	1000	1040	3·0	8·9	$3{\cdot}0 \times 10^{-5}$
Berkeley	6·5	1525	1750	10·0	14·6	$1{\cdot}5 \times 10^{-4}$
Berkeley (model)	0·006	350	45	0·6	15·0	$1{\cdot}7 \times 10^{-5}$
					5·0	$1{\cdot}9 \times 10^{-6}$

Now a recent paper from Berkeley (Henrich *et al.* 1949) has stated that for 200 Mev. deuterons accelerated in the 184 in. synchro-cyclotron, the final beam is about 10 cm. wide and 3 cm. high. Further, only 2% of the beam has been successfully extracted (Powell *et al.* 1948). Since the phase oscillation amplitude at full energy is only 4·4 cm., it remains to explain the presence of free oscillations of horizontal amplitude 2·8 cm., and vertical amplitude 1·5 cm. In view of the above considerations, and the fact that the ions are formed at thermal energies, it seemed possible that gas scattering was the cause. However, an investigation based on adapting the Blachman–Courant theory to synchro-cyclotrons shows this not to be the case. But initial oscillations of the order of several centimetres arising from gas scattering will explain at least part of the factor of ten increase in beam current obtainable by shaping the central region of magnetic field (Henrich *et al.* 1949). It is possible to convince oneself that the final beam spread is not due to injection oscillations and certainly the cause is not magnetic field inhomogeneities. Possibly the vertical oscillations arise from electrostatic defocusing although this is unlikely since in a synchronous accelerator most of the phase stable particles lie on the falling part of the wave, in which case the electrostatic action is a focusing one. A solution for the horizontal oscillations particularly is most desirable from the point of view of accelerators of the cyclo-synchrotron type, as proposed by Oliphant (1950).

REFERENCES

Blachman, N. M., and Courant, E. D., 1948, *Phys. Rev.*, **74**, 140; 1949, *Ibid.*, **75**, 315.
Elder, F. R., Langmuir, R. V., and Pollock, H. C., 1948, *Rev. Sci. Instrum.*, **19**, 121.
Fry, D. W., Gallop, J. W., Goward, F. K., and Dain, J., 1948, *Nature, Lond.*, **161**, 504.
Henrich, L. R., Sewell, D. C., and Vale, J., 1949, *Rev. Sci. Instrum.*, **20**, 887.
Kerst, D. W., 1948, *Birmingham Conference on Nuclear Physics.*
Lasich, W. B., and Riddiford, L., 1947, *J. Sci. Instrum.*, **24**, 177.
Lawson, J. D., 1948, *A.E.R.E.* Memo E1/M2.
Oliphant, M. L., 1950, *Nature, Lond.*, **165**, 466.
Oliphant, M. L., Gooden, J. S., and Hide, G. S., 1947, *Proc. Phys. Soc.*, **59**, 666.
Powell, W. M., *et al.*, 1948, *Rev. Sci. Instrum.*, **19**, 506.
Sewell, D. C., *et al.*, 1950, *Phys. Rev.*, **78**, 85.

An Investigation of the Secondary Electron Spectrum of ^{198}Au

By P. E. CAVANAGH, J. F. TURNER, D. V. BOOKER and H. J. DUNSTER.
Ministry of Supply, Atomic Energy Research Establishment, Harwell, Berkshire

MS. received 8th May 1950

ABSTRACT. The secondary electron spectrum of ^{198}Au has been studied using very strong sources, up to 0·3 curie, in a magnetic lens spectrometer. In addition to the well-known γ-ray at 0·411 MeV., evidence of two much less intense higher energy γ-rays at 0·67 MeV. and 1·09 MeV. has been found, both from the Compton and photoelectric spectra. The intensities of these two γ-rays with respect to the one at 0·411 MeV. have been measured. Two photoelectric peaks at low energy, in about the region expected for Kα and Kβ x-radiation from elements in the neighbourhood of gold, have been examined with radiators of different atomic number. The radiation responsible for these peaks has been subjected to critical absorption measurements in the spectrometer. Its behaviour is compatible with the Kα and Kβ x-radiation of gold, and no evidence of platinum x-radiation, such as would suggest K-capture, has been found.

§ 1. INTRODUCTION

The 2·7-day half-life activity of ^{198}Au has been studied very extensively in recent years. It is an ideal nucleus for study because it can be obtained easily, free from all other activities, and in a form of high specific activity. It is formed by the reaction ^{197}Au (n,γ) ^{198}Au, and not only is ^{197}Au the sole stable isotope of gold, but also it has a large cross section for slow neutrons, of the order of 100 barns. Other possible reactions, such as (n, p), (n, 2p), etc., appear to have very small cross sections by comparison. It is surprising therefore that a larger measure of agreement has not been obtained by the various investigators. There is complete unanimity as to the presence of a γ-ray of energy 0·411 MeV., as evidenced both by the internal conversion lines and by the secondary electron spectrum, this being in coincidence with β-rays of maximum energy $0{\cdot}960 \pm 0{\cdot}005$ MeV. However, Levy and Greuling (1948), using a semi-circular focusing instrument, find that internal conversion lines appear, corresponding to γ-energies of 0·158 and 0·208 MeV., with an intensity of about 15% of the main γ-ray. In addition, what is believed to be an x-ray at 70 kev. has been observed and investigated by various workers, notably by Feather and Dainty (1944). Very few workers have undertaken an accurate measurement of the secondary electron spectrum; the most recent is that of Siegbahn and Hedgran (1949) who, using a double-focusing spectrometer, find evidence only for the 0·411 kev. γ-ray, and conclude that if γ-rays at 0·158 and 0·208 MeV. exist, they must be present to less than 2% of the main branch.

The present investigation of the secondary electron spectrum of ^{198}Au has been carried out using a short magnetic lens spectrometer, essentially similar in design to that described by Deutsch, Elliott and Evans (1944). Investigations have also been made on the primary β-spectrum and on β–γ and γ–γ coincidences. These will be reported at a later date.

§2. THE SPECTROMETER

The magnetic lens was used with a focal length of 25 cm. and unit magnification, and is able, with the present design of coil, to focus electrons with a maximum energy of 5 MeV. Current for the coil is supplied by a 5 kw. amplidyne generator, and is stabilized by conventional methods to a few parts in ten thousand. For γ-ray

Figure 1 (*a*). Source and radiator mountings.

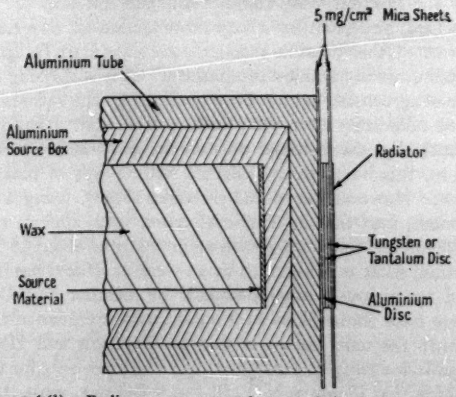

Figure 1 (*b*). Radiator arrangement for critical absorption experiment.

work heavy lead baffles are used to reduce the effect of direct γ-radiation at the counter, and also to prevent the scattering of secondary electrons into the counter window. The vacuum chamber is made of aluminium, and the baffles are aluminium clad also, to reduce electron scattering. The γ-ray source is placed in

a small cylindrical aluminium box, which is pushed into a blanked-off aluminium tube lying on the axis of the spectrometer. The tube enters the vacuum chamber via a Wilson seal, so that the axial position of the source may be varied. A three-position radiator holder is mounted before the source, and operated from outside the vacuum through a Wilson seal (Figure 1(*a*)). The radiators, which varied in thickness from 1 to 58 mg/cm² of lead and from 1 to 2 mg/cm² of tin and gold, were, with the exception of the heaviest lead radiator, made by evaporating layers of these metals on to 5 mg/cm² mica discs. The heavy lead radiator was of foil rolled to the required thickness.

For work at higher energies, the 6 mm. diameter counter window was of 2 mg/cm² mica, while for the investigation of the x-rays 0·5 mg/cm² nylon windows were used. The spectrometer was used with a transmission of 0·2% and a resolving power of about 3% at lower energies. At higher energies, where more than the outer radial section of the coil was required to focus the electrons, the resolution was somewhat worse.

§ 3. THE SOURCE

The gold used was in the form of foil 0·13 mm. thick, and discs of 5 mm. diameter were punched from it. The gold was subjected to spectrographic and chemical analysis before irradiation, and was found to contain not more than a few

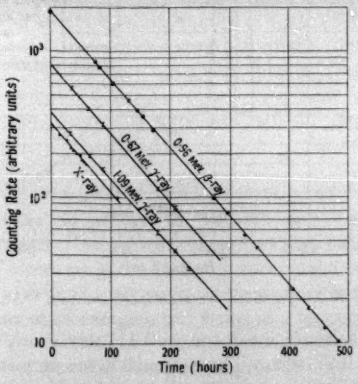

Figure 2. Lifetime measurements on gold.

parts per million of any impurity. No chemical separation was made after irradiation, and there remains the possibility that some other nuclear reaction may have occurred. However, the decay of an irradiated sample was followed over seven half-periods and compared with the uranium standard in a standard jig. The decay was found to be simple, and with half-period, obtained by least squares fitting, of $63{\cdot}86 \pm 0{\cdot}13$ hours (Figure 2). In the initial investigations sources of the order of 10 millicuries were used. These were produced by the (n, γ) reaction in the smaller Harwell pile. More detailed work at high energies required source strengths of up to 300 millicuries. For work at low energies we were able to obtain sources with an order of magnitude of greater specific activity from the larger Harwell pile.

§4. THE EXPERIMENTAL MEASUREMENTS AT HIGH ENERGIES

The entire secondary electron spectrum of ^{198}Au has been covered several times, with varying conditions, with experimental points spaced at the most at 2% intervals of momentum on a logarithmic scale, and in the regions of interest, at considerably closer spacing. All points have been taken to a statistical accuracy of within 1·5%, and most to 1%. During the investigations a total of well over ten million counts was recorded. An initial run over the spectrum of secondary electrons ejected from aluminium gave a main Compton spectrum which appeared to be due to a single γ-ray of energy about 0·41 MEV. There was also evidence of photo-electrons ejected from aluminium by the same γ-ray. However, for higher values of the momentum, the counting rate did not at once fall to the background value, but appeared to drop down in two steps. The first was partly

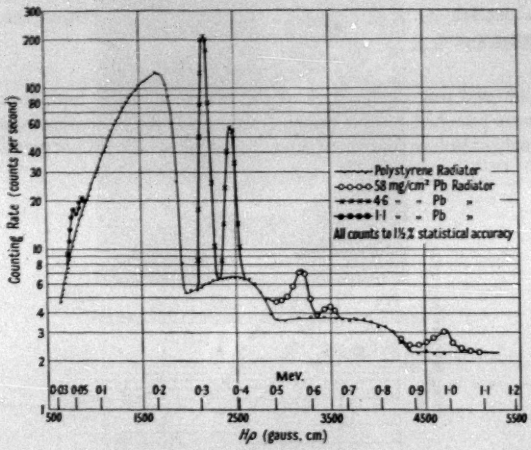

Figure 3. Secondary electron spectrum from ^{198}Au.

obscured by the photoelectric line due to the 0·411 MEV. γ-ray, and was at 0·49 MEV. The second was at 0·87 MEV. These results were confirmed when stronger sources, up to 300 millicuries, were used. A polystyrene radiator was used in place of the aluminium one, and with this no photoelectric line was observed. It was evident that the two steps represented the edges of Compton spectra due to γ-rays of energies (given by the Compton edges) of 0·67 and 1·09 MEV. (Figure 3). Concurrent measurements were made on the photoelectrons ejected from lead radiators of thickness varying from 1 to 58 mg/cm^2. The K and LM photoelectric lines due to the γ-rays of 0·411 and 0·67 MEV. were clearly resolved, and those due to the 1·09 MEV. partially resolved. In the measurements, alternate readings with and without the lead radiator were made by rotating the radiator holder. The decay of the higher energy γ-rays was followed over nearly four half-periods, check runs being made with the 0·411 MEV. γ-rays. The half-periods, as determined by a least squares fit to the data, were, for the 0·67 and 1·09 MEV. γ-rays respectively, 63·4 $\pm$ 1·2 hours and 65·8 $\pm$ 1·6 hours (Figure 2). It is therefore extremely likely that they are γ-rays originating from the decay of ^{198}Au.

§5. THE DETERMINATION OF THE ENERGY OF THE γ-RAYS

To obtain sufficient intensity in the photoelectric peaks due to the higher energy γ-rays thick radiators had to be employed, up to 58 mg/cm^2. Experiments were made with the 0·411 Mev. γ-ray with radiators of various thicknesses. For thin radiators the spectral lines were symmetrical, and of width given by the expected resolving power. As the thickness of radiator was increased, the line increased in height and developed a tail on the low energy side. However, the high energy side remained practically unchanged. For still greater thicknesses of radiator the increase in height was less marked, as also was any change in the shape of the line. Finally, for a thickness of radiator about equal to the range of photoelectrons no further change in height or line shape occurred. This we refer to as the saturation line shape, and experimentally the peak of the line, under these circumstances, was found to move down from the position of the peak for a thin radiator by only 1% in energy. Moreover the saturation line shape was very nearly the same for all three γ-rays, and a correction of 1% in energy was therefore made for the higher energy γ-rays. The spectrometer was calibrated by replacing the lead radiator by a source of Th (B + C) of the same diameter, formed by the standard technique, and determining the position of the F-line, the energy of which has been accurately determined by Ellis. A correction was made for the effect of the horizontal component of the earth's field. The γ-ray energies were determined by adding the K-binding energy of lead, 88·2 kev., to the electron energies so determined. The values were 0·410 ± 0·006 Mev., 0·671 ± 0·009 Mev., 1·092 ± 0·013 Mev. The energies were also obtained, less accurately, from a consideration of the Compton edges, correction being made for the finite resolution of the instrument, and the results were 0·412 ± 0·007 Mev., 0·668 ± 0·015 Mev., 1·075 ± 0·025 Mev.

§6. THE DETERMINATION OF THE RELATIVE INTENSITIES OF THE γ-RAYS

Estimates of the relative intensities of the γ-rays have been made both from the relative numbers of electrons in the Compton spectra and from the heights of the photoelectric lines, with good agreement. It is assumed that the relative number of Compton electrons of all energies, per γ-ray, as a function of the γ-ray energy will be given closely by the relative quantum efficiencies of a Geiger counter having a cathode of the same material as the radiator, provided that the Compton effect is very much greater than the photoelectric effect, as it is in this case. The relative efficiencies of a brass cathode counter at various quantum energies have been determined by Bradt *et al.* (1946), and the ratio of the efficiencies of counters with cathodes of various materials is given by the formula of van Droste (1936). From these we may deduce that the relative efficiencies of an aluminium-walled counter for quantum energies of 0·41, 0·67, and 1·09 Mev. are in the ratios 1 : 2·1 : 3·7. In order to determine the relative numbers of electrons in the three Compton spectra, those corresponding to the higher energy γ-rays must be extrapolated back over the greater part of their range to zero energy. This extrapolation has been made on an energy similarity basis for Compton spectra, following the work of Bleuler and Zünti, but the results are not critically dependent on the actual form of extrapolation used. On this basis the ratios of the intensities of the three γ-rays are 1 : 0·015 : 0·004. The measurements were repeated with thinner sources, down to 250 mg/cm^2, but the results obtained were within a few per cent of those with

the thicker source, indicating that the effect of differential absorption of the γ-rays within the source material is negligible with our geometry.

Our measurements of the heights of the photoelectric lines from the three γ-rays may be interpreted on the basis of an expression for the variation of line height with radiator thickness given by Deutsch, Elliott and Evans. This gives ratios of intensities of 1 : 0·012 : 0·004.

No evidence was found for γ-rays of 0·2 and 0·3 MeV. reported by other workers, and we can set an upper limit on their intensities, if present, of 2% and 4%, respectively, in agreement with Siegbahn and Hedgran.

§7. THE INVESTIGATION OF THE LOW ENERGY SECONDARY ELECTRONS

In the initial investigation of the secondary electron spectrum, using a source of superficial density 10 gm/cm², a 1·0 mg/cm² lead radiator, and a counter window of 2 mg/cm², two photoelectric peaks at energies of 52 and 63·5 kev. were observed. They were of nearly equal heights, 60–70% of the Compton background.

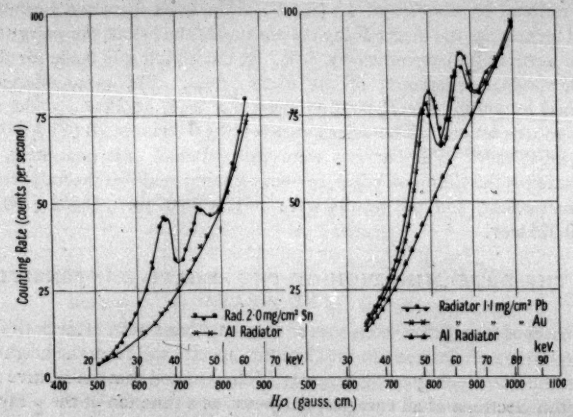

Figure 4. External conversion of low energy radiation from ^{198}Au in lead, gold and tin.

Measurements in this region were continued using sources of much higher specific activity, obtained from the larger Harwell pile, and of superficial density 1·25 gm/cm², together with a counter window of 0·5 mg/cm² nylon. Again peaks were observed, using the same radiator, at the same energies, of approximately equal intensities, but now almost equal in height to the background. The separation of the lines is approximately equal to the LM separation in the gold–lead region. It was first necessary to establish whether conversion took place in the K or L shells, especially in view of the conversion line corresponding to a γ-ray of energy 0·158 MeV., reported by Levy and Greuling. The K-conversion of this γ-ray would place it at 70 kev., just above the position of the second of the two peaks observed here. The measurements were repeated using a 1·0 mg/cm² gold radiator, and only a very small shift, of the order of 1 kev., was observed for both lines (Figure 4). The second line

appeared to be somewhat narrower with the gold than with the lead radiator. Had either of the two lines been converted in the K shell the peak would have moved to a higher energy by 8 kev. in changing from the lead to the gold radiator. The readings were carried on sufficiently far past the second peak to ensure that no larger part of it could be ascribed to the K-conversion of a γ-ray at 0·158 Mev. There was some evidence in both spectra of a third small peak lying above the second, and separated from it by about the same energy difference as between the first and second. This third peak, at 74 ± 2 kev., is rather above the position expected for the K-converted 0·158 Mev. γ-ray and, since its presence is not nearly so well marked in the case of the gold radiator, there is perhaps some possibility that it may have moved in the manner expected from K-conversion. However, it is much more likely that it corresponds to the M-conversion of a quantum radiation, the L-conversion peak of which forms part of the second spectral line.

It is evident that the first photoelectric peak is due to the L-conversion of quantum radiation of energy $66{\cdot}5 \pm 1$ kev., while the second could be due to the M-conversion of the same radiation. In view of the presence of the third low intensity peak, and also the height of the second peak in relation to the first, it seems likely that the second peak is composite, consisting, in addition, of the L-conversion of a second quantum radiation of energy $78{\cdot}0 \pm 1$ kev., while the third peak is due to the M-conversion of the same radiation. A preliminary study of the β-spectrum did not show any internal conversion peaks at low energies, which would be expected if low energy γ-rays were emitted. On the other hand the energies of the two quantum radiations indicated by the secondary electron spectrum are compatible with their being Kα and Kβ x-rays of an element in the neighbourhood of gold. These x-rays would not be expected to give internal conversion in the β-spectrum, even if they were emitted as a result of the internal conversion of one of the higher energy γ-rays, because the Auger effect is small for high atomic numbers. If the x-rays were emitted as a result of external conversion, there is even less likelihood of their giving rise to conversion peaks in the β-spectrum.

The emission of x-rays can arise in a number of ways. It is known that the 0·411 Mev. γ-ray is internally converted to the extent of 2·5-3%, and this will give rise to the same fraction per disintegration of mercury x-rays. The source is comparatively thick for the 0·411 Mev. γ-rays, and a calculation of the absorption of this γ-ray within the source, based on the model of a point source embedded in the middle of a disc of absorbing material, and using the photoelectric cross section given by Heitler (1936), gives a value of 15% of gold x-rays per disintegration. This is unlikely to differ by more than 30% from the result for a distributed source. Gold x-rays will therefore be present to about six times the intensity of mercury x-rays. There remains the possibility that ^{198}Au disintegrates by an alternative mode of decay, viz. K-capture to ^{198}Pt, in which case the emission of platinum x-rays would be expected. This latter possibility has been investigated by Feather and Dainty (1944) using critical absorption and coincidence absorption methods. They concluded that K-capture did not take place in more than 15% of the disintegrations. However, in view of the fact that they reported a nuclear γ-ray of energy 65 kev., present to the extent of about one per disintegration, it was thought desirable to re-examine the problem.

§8. CRITICAL ABSORPTION MEASUREMENTS ON ^{198}Au X-RAYS IN THE SPECTROMETER

It was thought that critical absorption measurements could be made much more accurately in conjunction with the spectrometer, because not only is the Compton background on which the absorption is superimposed reduced very considerably, but also x-rays which differ in energy by more than a few kev. will be resolved, and their absorption followed separately. Moreover, the secondary x-radiation from the critical absorber may also be resolved and studied separately. Figure 5 shows the K-absorption edges for tantalum and tungsten, together with the $K\alpha_1$, $K\alpha_2$, $K\beta_1$, $K\beta_2$ x-ray lines for platinum, gold and mercury, as well as for tantalum and tungsten. Let us consider just the $K\alpha_1$ and $K\alpha_2$ lines. Those for platinum at 66·9 and 65·2 kev., respectively, both lie below the K-absorption edge of tantalum at 67·5 kev., and hence will not be critically absorbed in either tantalum or tungsten.

The $K\alpha_2$ of gold at 67·1 kev. will similarly not be critically absorbed in either, but the $K\alpha_1$ of gold at 68·8 kev. will be critically absorbed in tantalum but not in tungsten. Both mercury x-rays at 68·8 and 70·6 kev. will be critically absorbed in tantalum, but only the $K\alpha_1$ in tungsten. This difference in behaviour of the

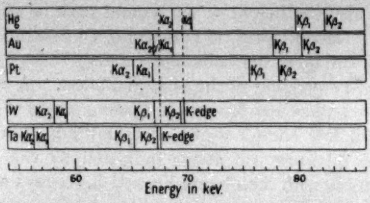

Figure 5. X-ray energies of Hg, Au, Pt, W and Ta.

K x-rays of platinum, gold and mercury should enable us to distinguish between them, or even to separate out the effects of each, if they are present to a comparable extent.

A set of piles of absorbers of the same thickness, 0·3 mm., and of diameter 5 mm. was made up with varying proportions of aluminium and tantalum, from all aluminium to all tantalum. A similar set of aluminium and tungsten absorbers was made up.

The absorber piles were stuck on to the centres of one-inch mica discs of weight 5·0 mg/cm². These were placed in turn behind the 5 mm. diameter 1 mg/cm² lead radiator, which was also mounted on the front of a similar mica disc, so as to shield it from the source. The sandwich was mounted in the radiator holder, and the aluminium tube containing the source was pushed forward until it came in contact with, and slightly bent forward, the mica discs (Figure 1(*b*)). This was to ensure that both absorbers and radiator always took up the same position in relation to source. The 5 mg/cm² mica backing to the radiator is sufficient to stop any low energy photoelectrons from the absorber. Usually two absorbers with two radiators of nominally the same thickness were placed in two of the positions of the radiator holder and alternate readings taken. The two radiators were afterwards calibrated against each other. An attempt was made to measure the Compton background by placing a plain mica disc in the third position of the radiator holder, but this was unsatisfactory because the curve so obtained, although similar in shape, did not fit the spectrum obtained with the radiator, away from the neighbourhood of the conversion peaks. This led to an uncertainty in the actual heights of

the peaks above the background. Finally it was found that, by reversing the radiator, the backing of which was sufficiently thick to stop the low energy photoelectrons from the radiator, a background spectrum could be obtained which was identical with that for a radiator in its normal position, away from the conversion peaks.

The results of this set of experiments are shown in Figure 6, where spectra are given for the region of the first photoelectric peak, for the thickness of tantalum of 0, 84, 168, and 500 mg/cm². Besides reducing the height of the photoelectric peak, the introduction of the absorber also results in the appearance of a small peak at $42{\cdot}5 \pm 0{\cdot}8$ kev., which may be ascribed to the L-conversion in lead of the Kα radiation of tantalum. It is also to be expected that there should be peaks due to L-conversion in lead of tantalum Kβ and the M-conversion in lead of the tantalum

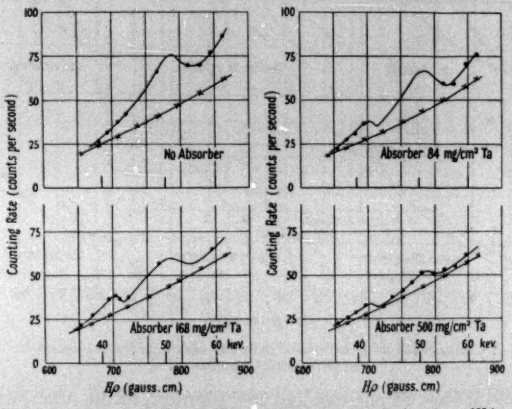

Figure 6. Absorption in tantalum of low energy radiation from ^{198}Au (1·1 mg/cm² lead radiator).

Kα. Both of these are centred about 53 kev., i.e. almost exactly at the position of the photoelectric peak under investigation at 52 ± 1 kev. It is evident therefore that the true absorption of this peak is greater than would be deduced immediately from the heights of peaks at various absorber thicknesses. A correction for the effect of the secondary x-rays from tantalum may be made in the following way: if we are correct in assuming that the second of the two primary photoelectric peaks is made up in a similar way to the second of the secondary photoelectric peaks due to tantalum, viz. as an L-conversion of Kβ plus the M-conversion of Kα, then the ratio of the two primary photoelectric peaks will be very nearly the same as that for the secondaries, since all the energies are very much higher than the L-absorption edge of lead. So the height of the first secondary peak may be used to deduce the height of the second. They are of nearly equal heights. For large thicknesses of absorber, however, the height of the secondary peak is as much as two-thirds that of the primary, and consequently the difference becomes rather inaccurate.

It was decided to repeat the experiments using a tin radiator, so that the K-conversion lines could be studied. This would have the advantage of moving the lines to lower energies, so improving the height-to-background ratio. An initial spectrum was measured under the same conditions as for the lead and gold radiators, but using a 2 mg/cm² tin radiator. This is shown in Figure 4. Again

two conversion lines were observed in the region investigated, at $38 \pm 0{\cdot}8$ and 48 ± 1 kev., but the second line was now only about 50% of the height of the first. They may be ascribed to the K-conversion in tin of the Kα and Kβ lines from elements in the neighbourhood of gold. The use of the tin radiator therefore splits up the composite second photoelectric peak. Critical absorption experiments were then carried out in the same manner as before, using 0, 84, 168 and 335 mg/cm^2 tantalum absorbers and 196 and 390 mg/cm^2 tungsten absorbers. The results are given in Figure 7. Again the introduction of the absorber results in the appearance

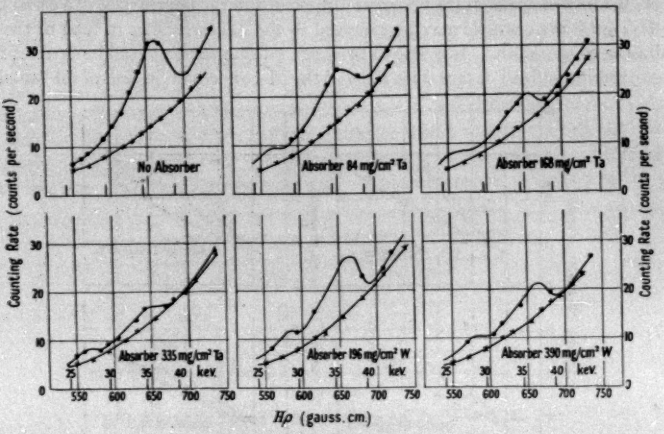

Figure 7. Absorption in tantalum and tungsten of low energy radiation from ^{198}Au (2 mg/cm^2 tin radiator).

of lines at $28 \pm 0{\cdot}6$ kev. in one case and $29{\cdot}7 \pm 0{\cdot}6$ kev. in the other, which may be ascribed to the K-conversion in tin of the Kα radiation of tantalum and tungsten respectively. Other smaller peaks at approximately 54 kev. could be ascribed to the L-conversion of the same Kα radiation. Again a peak from the K-conversion of the Kβ radiation is to be expected at 37 kev. for tantalum and 38 kev. for tungsten, i.e. just at the position of the primary peak, but this time it is only 50% of the first secondary peak, and the correction factor for the height of the primary peak is never large. It is evident from an inspection of the curves that the absorption in tantalum is very much greater than that in tungsten. This at once suggests that gold or mercury x-radiation very much predominates over platinum x-radiation, or that of any other nucleus higher in atomic number than mercury.

We must now consider the spectra in more detail. Since we are working not far from the cut-off of the counter window at 15 kev., considerable corrections must be applied for window absorption. However, this will only affect us as far as the estimation of the height of the secondary peak, due to the K-conversion in tin of the tantalum or tungsten Kβ, is concerned. The correction is greater with tin than with the lead radiator. It was applied on the basis of an exponential law of attenuation, with the exponent inversely proportional to the fourth power of the electron velocity.* Although the attenuation of the lowest energy peak, viz. the K-conversion of the Kα of the absorber, due to this cause is large (a factor of nearly three in the case of the tantalum Kα), the effect on the estimated height of the tantalum

* W. Bothe, *Handbuch der Physik*, 1933, Vol. 22/2, p. 41.

Kβ peak is such as to reduce the height of the primary photoelectric peak by only about 10% in the worst case. All the peaks contain more than one unresolved component, and to compare relative average intensities, the areas of the peaks should be used, divided by the mean $H\rho$ value, to take into account the resolution of the instrument. With these corrections the relative intensities of the two primary photoelectric peaks for the tin radiator become 3 : 1, which is just what would be expected on the basis of their being Kα and Kβ x-radiations. Applying the same

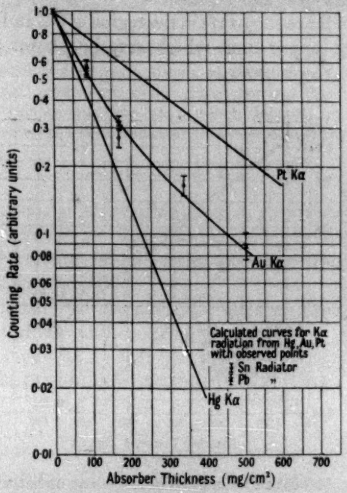

Figure 8. Absorption in tantalum of low energy radiation from ^{198}Au.

corrections to the lead radiator results, on the basis of the second peak being composite, the components being the L-conversion of a Kβ and an M-conversion of a Kα x-ray, the ratio of conversions in the L and M shells is 2 : 1.

Attenuation curves calculated on the above basis are shown in Figures 8 and 9, where the results for both the lead and the tin radiators are shown, together with attenuation curves expected on the basis of the radiation being the $K\alpha_2$ and $K\alpha_1$ of platinum, or gold, or mercury alone, in tantalum and tungsten, the latter being obtained from standard textbooks. Let us consider first the absorption in tungsten.

The experimental points lie somewhat above the absorption curve for gold x-rays, or even for a frequency just at the foot of the K-absorption edge. However, it is possible that the experimental determinations on which the published absorption curves are based may be in error. The absorption in tungsten therefore gives a strong indication of gold or, perhaps, platinum K x-radiation. Mercury radiation can only be present to a small extent. The experimental points for tantalum, however, lie just about on the absorption curve expected for gold K x-radiation and very considerably different from either platinum or mercury K x-radiation. Again the absorption is rather smaller than would be expected on the basis of a 6 : 1 mixture of gold and mercury x-radiation, arising from external and internal conversion of the 0·411 Mev. γ-ray, but nevertheless it is evident that platinum K x-radiation, if present, must be much less intense than the gold

K x-radiation. The upper limit which can be set on the K-capture process, from this evidence, is 6%.

§9. CONCLUSIONS

1. In addition to the 0·411 MeV. γ-ray there are two higher energy γ-rays at $0{\cdot}670 \pm 0{\cdot}008$ MeV. and $1{\cdot}089 \pm 0{\cdot}012$ MeV. present to the extent of 1·5 and 0·4% respectively. The sum of the energies of the first two γ-rays is approximately equal to that of the third. This would suggest that there are energy levels of the ^{198}Hg nucleus at 0·411 MeV. and 1·09 MeV.

2. There is no evidence for γ-rays in the region of 0·2 and 0·3 MeV. as reported by other workers. The upper limit which may be placed on their intensities, if present, is 2 and 4% respectively.

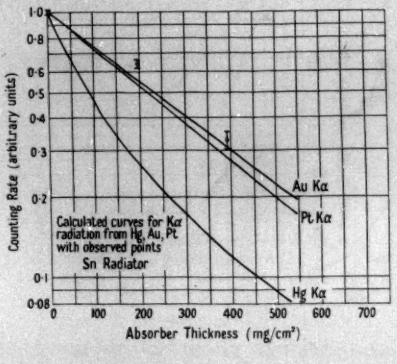

Figure 9. Absorption in tungsten of low energy radiation from ^{198}Au.

3. There is no evidence for the reported γ-ray at 0·158 MeV.

4. There in no evidence for the nuclear γ-ray at 65 kev. reported by Feather and Dainty.

5. There is no evidence for K-capture, in agreement with Feather and Dainty. The maximum branching ratio for such a mode of disintegration compatible with our results is 6%.

ACKNOWLEDGMENTS

Acknowledgment is made to the Director, Atomic Energy Research Establishment, for permission to publish this paper. We wish to acknowledge the work of Messrs. E. H. Cooke-Yarborough and H. Bisby, of the Electronics Division, A.E.R.E., who were responsible for the design of the electronic equipment used in conjunction with the spectrometer.

REFERENCES

BRADT, H., *et al.*, 1946, *Helv. Phys. Acta*, **19**, 77.
DEUTSCH, M., ELLIOTT, L. G., and EVANS, R. G., 1944, *Rev. Sci. Instrum.*, **15**, 178.
VAN DROSTE, G. F., 1936, *Z. Phys.*, **100**, 529.
FEATHER, N., and DAINTY, J., 1944, *Proc. Camb. Phil. Soc.*, **40**, 57.
HEITLER, W., 1936, *Quantum Theory of Radiation* (Oxford : University Press).
LEVY, P. W., and GREULING, E., 1948, *Phys. Rev.*, **73**, 83.
SIEGBAHN, K., and HEDGRAN, A., 1949, *Phys. Rev.*, **75**, 523.

A Method for Determining Uranium and Thorium in Rocks by the Nuclear Photographic Plate

By J. W. BREMNER
Imperial Chemical Industries, General Chemicals Division, Runcorn, Cheshire

MS. received 20th June 1949, and in final form 5th July 1950

ABSTRACT. A nuclear photographic emulsion which has been in contact with material containing traces of uranium and thorium shows on processing α-ray stars arising from atoms which have undergone several successive disintegrations during the exposure. The relative frequency of the various multiple stars, which depends on the uranium/thorium ratio, is here evaluated on simple assumptions to show the possibility of determining these elements by star counting.

THE use of the nuclear photographic plate in determining small quantities of uranium and thorium in rocks has been suggested (Joliot-Curie 1946), and subsequently results of the technique have been given (Poole and Bremner 1948, 1949, Coppens 1950).

From the α-track density on the plate, we have an equation for c_U and c_{Th}, the concentrations of uranium and thorium (Evans 1934):

$$\text{number of } \alpha\text{-tracks per cm}^2 \text{ per sec.} = \left(\frac{n_U d}{4\mu}\sum_U R\right)c_U + \left(\frac{n_{Th} d}{4\mu}\sum_{Th} R\right)c_{Th}, \quad \ldots\ldots(1)$$

where n_U, n_{Th} are the total numbers of α-particles emitted per second per gramme from uranium I and thorium, d is the density of the rock,

$$\mu = (\text{range of } \alpha\text{-particles in air})/(\text{range in rock}),$$

and $\sum_U R$, $\sum_{Th} R$ are the sums of the ranges of the α-particles from the uranium and thorium families. Radioactive equilibrium is assumed, and the actinium family is neglected. The necessary modification to the equation to allow for the existence of a minimum observable range ρ is obtained by replacing each R in the summations by the effective range $R-\rho$.

Another equation is required. This can be obtained by finding the density of 2, 3, 4, 5 stars. These stars arise from atoms in or near the surface which have undergone several successive disintegrations in the time of exposure of the plate. The ratio of the density of, say, 3 stars to the track-density gives an equation for c_U, c_{Th} independent of (1).

As a first step in obtaining such an equation we require the number per cm³ of atoms which have emitted 2, 3, 4 particles in time T. β-particles may be regarded as α-particles of range zero. We consider the general case of a primary element A whose amount may be taken as constant during the exposure giving rise successively to elements B, C, ...N...., the respective decay constants being λ, λ_1, λ_2, ...λ_n.... and the elements being present in amounts ν, ν_1, ν_2, ...ν_n.... atoms per cm³.

The number of A atoms breaking up in the interval dt is $\nu\lambda\,dt$, and if they have broken up at time t (within the interval 0 to T), the number of these which break

up further before time T is $\nu\lambda\,dt[1-\exp\{-\lambda_1(T-t)\}]$, therefore the total number of at least double emissions from A atoms is

$$\int_0^T \nu\lambda[1-\exp\{-\lambda_1(T-t)\}]\,dt=\nu\lambda\left(T-\frac{1}{\lambda_1}+\frac{\exp(-\lambda_1 T)}{\lambda_1}\right).$$

The number of double emissions from A formed in dt at time t is

$$\frac{d}{dt}\left\{\nu\lambda\left(t-\frac{1}{\lambda_1}+\frac{\exp(-\lambda_1 t)}{\lambda_1}\right)\right\}dt=\nu\lambda\{1-\exp(-\lambda_1 t)\}\,dt.$$

Therefore the total number of at least triple emissions from A in time T is

$$\int_0^T \nu\lambda[1-\exp(-\lambda_1 t)][1-\exp\{-\lambda_2(T-t)\}]\,dt$$
$$=\nu\lambda\left\{T-\frac{1}{\lambda_1}-\frac{1}{\lambda_2}+\frac{\lambda_2}{\lambda_1(\lambda_2-\lambda_1)}\exp(-\lambda_1 T)+\frac{\lambda_1}{\lambda_2(\lambda_1-\lambda_2)}\exp(-\lambda_2 T)\right\},$$

and by induction it can be shown that the number of at least $r+1$ emissions

$$E_r=\nu\lambda\left\{T-\sum_1^r\frac{1}{\lambda_i}+\sum_1^r\frac{\lambda_1\lambda_2\lambda_3\ldots.\lambda_r}{\lambda_i^2(\lambda_1-\lambda_i)(\lambda_2-\lambda_i)\ldots.(\lambda_r-\lambda_i)}\exp(-\lambda_i T)\right\}.$$

The term $(\lambda_i-\lambda_i)$ does not appear in the difference product.

The number of r emissions per cm³ from A is therefore

$$E_{r-1}-E_r=\frac{\nu\lambda}{\lambda_r}\left\{1-\sum_1^r\frac{\lambda_1\lambda_2\ldots.\lambda_r}{\lambda_i(\lambda_1-\lambda_i)(\lambda_2-\lambda_i)\ldots.(\lambda_r-\lambda_i)}\exp(-\lambda_i T)\right)\right\}. \quad \ldots\ldots(2)$$

If the lth member of the family is stable, so that there can be no more than $(l-1)$ α-particles emitted from an A atom, the number of at least $(l-1)$ emissions E_{l-2} is the number of $(l-1)$ emissions per cm³ from A.

This approximates to $\nu\lambda T$ for large T as would be expected. The expressions (2), on the other hand, rise exponentially to a constant value which will eventually be negligible in comparison with $\nu\lambda T$.

So far only multiple emissions provided by A have been considered. At the beginning of the exposure, however, there will be present the ν_1, ν_2.... atoms per cm³ of B, C..... These will gradually disappear, giving rise to multiple stars; new atoms of B, C.... will form to replace them, but the break-up of such an atom of B, for example, is a further disintegration of an A atom. Similarly, if the number of multiple emissions from A and the original ν_1 atoms of B present at the beginning of the exposure have been found, we have only to take account of the multiple emissions from the original ν_2 atoms of C, for new C atoms can only be formed from B or from A via B, and so on. In an exposure long compared with the half-lives of B, C...., such multiple emissions will be negligible in number compared with those from A.

In the case of B, the number of at least double emissions is found by the same procedure as before: the number of atoms of the original ν_1 which decay in dt at time $t=\nu_1\lambda_1\exp(-\lambda_1 t)\,dt$.

The number of at least double emissions by the end of time T is

$$\nu_1\lambda_1\int_0^T \exp(-\lambda_1 t)[1-\exp\{-\lambda_2(T-t)\}]\,dt.$$

By a repetition of the process, the number of at least triple emissions by time T is found.

The number of double emissions is equal to the number of at least double minus the number of at least triple, i.e.

$$=\nu_1\lambda_1\lambda_2\left\{\frac{\exp(-\lambda_1 T)}{(\lambda_2-\lambda_1)(\lambda_3-\lambda_1)}+\frac{\exp(-\lambda_2 T)}{(\lambda_1-\lambda_2)(\lambda_3-\lambda_2)}+\frac{\exp(-\lambda_3 T)}{(\lambda_1-\lambda_3)(\lambda_2-\lambda_3)}\right\}.$$

In general, the number of $(n-1)$ emissions corresponding to the number of N atoms formed in time T from ν_1 atoms of B, is

$$\nu_1\lambda_1\lambda_2\ldots\lambda_{n-1}\sum_1^n\frac{\exp(-\lambda_i T)}{(\lambda_1-\lambda_i)(\lambda_2-\lambda_i)\ldots(\lambda_n-\lambda_i)}, \qquad \ldots\ldots(3)$$

the difference products as before not involving a $(\lambda_i-\lambda_i)$ term, as can be proved by an inductive argument.

It should be said that many of the above results have been obtained (Bateman 1910) by solving in the general case the simultaneous differential equations for the rate of growth of the members of a radioactive family by the method of the Laplace transform. It is necessary for the present theory, however, to terminate his equations by one expressing the formation of a stable member.

We now turn to consider the problem: if there are N atoms per cm^3 which have emitted α-particles of range in air R_1, $R_2\ldots R_r$ in exposure time T, how many of the various multiple stars per cm^3 are to be expected from these atoms? These ranges are supposed to be placed in ascending order of magnitude, so the subscripts $1, 2\ldots$ do not denote association with elements A, B$\ldots$. Let the layers lying between depths 0 and R_1, R_1 and R_2, R_2 and R_3, $\ldots$ be labelled layers 1, 2, 3, $\ldots$. It will also be convenient in the following to use $R_1, R_2\ldots R_r$ for the ranges in the rock ($=\mu^{-1}\times$ range in air).

Take layer 1: it is possible for all the r particles emitted from each atom to emerge from the rock, that is, be registered as an r star. The probability of emergence of the R_1 particle at depth x intermediate between 0 and R_1 is $\frac{1}{2}(1-x/R_1)$ (Evans 1934). The number of r stars due to the atoms between x and $x+dx$ is, therefore,

$$\frac{N}{2^r}\left(1-\frac{x}{R_1}\right)\left(1-\frac{x}{R_2}\right)\ldots\left(1-\frac{x}{R_r}\right)dx,$$

so that the number of r stars due to these atoms per cm^2 is

$$\frac{N}{2^r}\int_0^{R_1}\left(1-\frac{x}{R_1}\right)\left(1-\frac{x}{R_2}\right)\ldots\left(1-\frac{x}{R_r}\right)dx$$
$$=\frac{N}{2^r}\left\{R_1-\frac{R_1^2}{2}\sum_1^r\frac{1}{R_i}+\frac{R_1^3}{3}\sum_{(i<j)}^r\frac{1}{R_iR_j}-\frac{R_1^4}{4}\sum_{(i<j<k)}^r\frac{1}{R_iR_jR_k}\right.$$
$$\left.+\ldots\ldots\frac{(-1)^r}{r+1}\frac{R_1^{r+1}}{R_1R_2\ldots R_r}\right\}. \qquad \ldots\ldots(4)$$

To find the density of $(r-1)$ stars from these atoms due to layer 1, we calculate the chance at depth x that the $R_2, R_3, R_4, \ldots R_r$ particles or the $R_1, R_3, R_4\ldots R_r$, or the $R_1, R_2, R_4\ldots R_r, \ldots$ or the $R_1, R_2, R_3, R_4\ldots R_{r-1}$ proceeding from the same atom shall emerge. Integrating as above over $x=0$ to R_1, we obtain

$$\frac{N}{2^{r-1}}\left\{{}^rC_{r-1}R_1-{}^{r-1}C_{r-2}\frac{R_1^2}{2}\sum_1^r\frac{1}{R_i}+{}^{r-2}C_{r-3}\frac{R_1^3}{3}\sum_{(i<j)}^r\frac{1}{R_iR_j}\ldots\right.$$
$$\left.\ldots(-1)^{r-1}\frac{R_1^r}{r}\sum_1^r\frac{R_i}{R_1R_2R_3,\ldots R_r}\right\}. \qquad \ldots\ldots(5)$$

This gives the density of $(r-1)$ stars; it also includes, however, the r stars, each of which is counted ${}^{r}C_{r-1}$ times in this process. So to obtain the density of $(r-1)$ stars from layer 1, we must subtract from this ${}^{r}C_{r-1}$ times the density of r stars.

Using the same process for the $(r-2)$ star density, we obtain

$$\frac{N}{2^{r-2}}\left\{{}^{r}C_{r-2}R_1-{}^{r-1}C_{r-3}\frac{R_1^2}{2}\sum_{1}^{r}\frac{1}{R_i}+{}^{r-2}C_{r-4}\frac{R_1^3}{3}\sum_{\substack{1\\(i<j)}}^{r}\frac{1}{R_iR_j}\cdots\right.$$

$$\left.\cdots(-1)^{r-2}R_1{}^{r-1}\sum_{\substack{1\\(i<j)}}^{r}\frac{R_iR_j}{R_iR_2,\ldots R_r}\right\}\ldots\ldots(6)$$

which gives the density of $(r-2)$ stars when we subtract ${}^{r-1}C_{r-2}$ times the $(r-1)$ star density, and ${}^{r}C_{r-2}$ times the r star density.

The same process can be followed down to the 2 stars.

Layer 2 can now be considered: the R_1 particle cannot emerge from this layer, so that the maximum possible is an $(r-1)$ star. The integration is now carried over the range of x from R_1 to R_2; thus the density of $(r-1)$ stars from layer 2 is found by writing $N/2^{r-1}$ outside the braces in (4) in place of $N/2^{r}$, replacing ${R_1}^{n}$ outside the summations by ${R_2}^{n}-{R_1}^{n}$ and allowing the summations to range from 2 to r. If we make the last two changes in (5) and (6) also, and replace $N/2^{r-1}$ and $N/2^{r-2}$ outside by $N/2^{r-2}$ and $N/2^{r-3}$ respectively, we obtain two expressions appropriate for calculating the $(r-2)$ star and the $(r-3)$ star densities. From the first we must subtract ${}^{r-1}C_{r-2}$ times the $(r-1)$ star density, giving the $(r-2)$ star density, from the second ${}^{r-2}C_{r-3}$ times the $(r-2)$ star density and ${}^{r-1}C_{r-3}$ times the $(r-1)$ star density, giving the $(r-3)$ star density. We may proceed in this way down to the 2 stars.

The $(r-2)$, $(r-3)\ldots$. star densities due to lower strata can be found by the same method.

If, say, two β-particles are among the r particles emitted, on writing $R_1=R_2=0$, the above expressions become just what would be obtained if the atoms had been treated from the start as emitting $(r-2)$ particles, ranges $R_3, R_4\ldots R_r$ in order of magnitude. The only part played by the β-particles is that they, to some extent, determine N, the number of $(r-2)$ emitters per cm^3, by reason of the time which elapses before they are emitted. In the following, in calculating these range functions, β-particles will therefore be ignored.

All that is required has now been obtained: if we wish to calculate the ratio of, say, 3 star density to the total α-track density, we collect the 3, 4, 5.... emitters, multiply each by its appropriate range function and add, obtaining

$$n\lambda\,\Sigma\,\{f_i(\lambda_1,\lambda_2\ldots,T)f_i'(R_1,R_2\ldots)\},$$

where f_i and f_i' are functions calculated as above. The total α-density is $\frac{1}{4}n\lambda T\Sigma R$, where ΣR is the sum of all the ranges. The ratio is therefore independent of n and λ as is to be expected. Also the dimensions of all the f_i' are those of length, so that if the ratio is multiplied above and below by μ, it is seen to be unaltered by writing everywhere air ranges for rock ranges. Correction for minimum observable range may be made by replacing these air ranges by the effective air ranges.

This theory can now be applied to uranium and thorium. In the case of uranium, no chain of quickly disintegrating α-particle emitters occurs except following radium. This may be taken as ending as RaD for, though this is not

stable and will supply single α-particles, its half-life (22 years) is so long that the chance that any RaD atom formed during the exposure will disintegrate before the exposure is completed is negligible. Similar reasons justify our neglecting all members except those in the Ra–RaD chain. Further, the branching ratio at RaC is so much in favour of RaC′ that all the atoms may be regarded as disintegrating by this route; also the half-life of RaC′ ($1{\cdot}5 \times 10^{-4}$ sec.) is so short that RaC may be regarded as turning to RaD by the simultaneous ejection of an α- and a β-particle. We therefore have the following scheme, treating radium as the primary element, which gives a maximum possible emission per atom of six (four α- and two β-particles)

$$\mathrm{Ra} \xrightarrow{\alpha} \mathrm{Rn} \xrightarrow{\alpha} \mathrm{RaA} \xrightarrow{\alpha} \mathrm{RaB} \xrightarrow{\beta} \mathrm{RaC} \xrightarrow{\alpha+\beta} \mathrm{RaD}.$$

The values for λ_1, λ_2, λ_3, λ_4 calculated from the half-lives given in a recent review (Seaborg 1944) are as follows: $\lambda_1 = 0{\cdot}174$ days^{-1}, $\lambda_2 = 328$ days^{-1}, $\lambda_3 = 37{\cdot}3$ days^{-1}, $\lambda_4 = 50{\cdot}7$ days^{-1}. The Table shows the density per cm^3 of the various kinds of emitter for different exposures, and the total number of α-particles emitted per cm^3; it is calculated for $n\lambda = 2{\cdot}78 \times 10^3$ days^{-1} corresponding to a decay constant for U I of $4{\cdot}21 \times 10^{-13}$ day^{-1}, a concentration of 10^{-6} gm. uranium per gramme of rock, and a rock-density of 2·6 gm/cm^3. In the sense used in this Table, the almost simultaneous ejection of an α- and a β-particle from RaC is a single emission.

Weeks	1	2	3	5	10	20
Double emissions per cm^3 from						
Ra	5·98	7·75	8·26	8·46	8·49	8·49
Rn	22·2	6·54	2·01	0·17	0	0
RaA	0	0	0	0	0	0
RaB	74·6	74·6	74·6	74·6	74·6	74·6
Triple emissions per cm^3 from						
Ra	52·5	68·0	72·5	74·4	74·6	74·6
Rn	16·3	4·83	1·49	0·12	0	0
RaA	8·49	8·49	8·49	8·49	8·49	8·49
Quadruple emissions per cm^3 from						
Ra	38·6	50·1	53·4	54·7	54·9	54·9
Rn	$11{\cdot}3 \times 10^3$	$1{\cdot}46 \times 10^4$	$1{\cdot}56 \times 10^4$	$1{\cdot}60 \times 10^4$	$1{\cdot}60 \times 10^4$	$1{\cdot}60 \times 10^4$
Quintuple emissions per cm^3 from						
Ra	$8{\cdot}06 \times 10^3$	$2{\cdot}42 \times 10^4$	$4{\cdot}26 \times 10^4$	$8{\cdot}12 \times 10^4$	$1{\cdot}78 \times 10^5$	$3{\cdot}73 \times 10^5$
Total number of particles emitted per cm^3	$1{\cdot}56 \times 10^5$	$3{\cdot}11 \times 10^5$	$4{\cdot}67 \times 10^5$	$7{\cdot}78 \times 10^5$	$1{\cdot}56 \times 10^6$	$3{\cdot}11 \times 10^6$

It is obvious that Rn is the only one of Rn, RaA, RaB, RaC with a small enough decay constant to play an appreciable part; the atoms of it present at the beginning of the exposure supply many quadruple emissions since its equilibrium proportion is large, and by its delay in disintegrating, it holds up the production of quintuple emissions from Ra.

In the case of thorium, we have the following system, where half-lives are written below each element:

$$\underset{1{\cdot}39\times10^{10}\text{ yr.}}{\mathrm{Th}} \xrightarrow{\alpha} \underset{6{\cdot}7\text{ yr.}}{\mathrm{MsTh_1}} \xrightarrow{\beta} \underset{6{\cdot}13\text{ hr.}}{\mathrm{MsTh_2}} \xrightarrow{\beta} \underset{1{\cdot}9\text{ yr.}}{\mathrm{RdTh}} \xrightarrow{\alpha} \underset{3{\cdot}64\text{ days}}{\mathrm{ThX}} \xrightarrow{\alpha} \underset{5{\cdot}45\text{ sec.}}{\mathrm{Tn}} \xrightarrow{\alpha} \underset{0{\cdot}158\text{ sec.}}{\mathrm{ThA}} \xrightarrow{\alpha}$$

$$\underset{10{\cdot}6\text{ hr.}}{\mathrm{ThB}} \xrightarrow{\beta} \underset{60{\cdot}5\text{ min.}}{\mathrm{ThC}} \begin{cases} \xrightarrow{\beta} \underset{3\times10^{-7}\text{ sec.}}{\mathrm{ThC'}} \xrightarrow{\alpha} \\ \xrightarrow{\alpha} \underset{3{\cdot}1\text{ min.}}{\mathrm{ThC''}} \xrightarrow{\beta} \end{cases} \mathrm{ThD}.$$

We take RdTh as the primary element: it will be seen that this is justifiable even though its decay constant is quite large. Such a primary atom can emit seven particles, five α and two β, and, applying the principle seen to operate in the case of the uranium series, that for the exposures considered an element with half-life less than about half-an-hour may be taken as disintegrating as soon as it is formed, we have the following system:

$$\text{RdTh} \xrightarrow{\alpha} \text{ThX} \xrightarrow{3\alpha} \text{ThB} \xrightarrow{\beta} \text{ThC} \xrightarrow{\alpha+\beta} \text{ThD}.$$

The branching need only be taken into account now in the calculation of the range functions.

We may reduce this further to

$$\text{RdTh} \xrightarrow{\alpha} \text{ThX} \xrightarrow{3\alpha} \text{ThB} \xrightarrow{\alpha+2\beta} \text{ThD}.$$

The error caused by this in the number of emissions in 1 week is 1·6% for quintuple emissions and less than 1% for quadruple or less. It is also easily shown that less than $1{\cdot}36 \times 10^{-3}$ of the RdTh atoms formed during a 20 weeks exposure have come from Th, and of these very few will have time to disintegrate further. That is, the decay of RdTh is made good almost entirely by β-emission from $MsTh_1$ even in long exposures, so that the objection of large decay-constant in the case of RdTh as primary element has been met. This gives the following results for 4α and 5α emitters:

Weeks	1	2	3	5	10	20
(no. of transitions per cm³ from ThX to ThD)/$n\lambda$	3·68	4·85	5·16	5·26	5·27	5·27
(no. of transitions per cm³ from RdTh to ThD)/$n\lambda$	2·68	8·51	15·2	29·1	64·1	134·1

For thorium, the branching ratio has to be taken into account in calculating the range function; 65% of the atoms traverse one branch and 35% the other in any exposure; if f_1 is any range function for the set of ranges corresponding to the first branch, and f_2 the same function for the set corresponding to the second, the correct range function will be $0{\cdot}65 f_1 + 0{\cdot}35 f_2$.

We adopt the following values for the ranges required (Joliot-Curie 1946) Ra 3·30 cm., Rn 4·05 cm., RaA 4·66 cm., RaC′ 6·91 cm., RdTh 3·98 cm., ThX 4·28 cm., Tn 5·00 cm., ThA 5·64 cm., ThC 4·66 cm., ThC′ 8·57 cm.

Thus the ratios to the total track density are, for the uranium family alone:

Weeks	1	2	3	5	10	20
4 stars per cm³ ($\times 10^{-3}$)	2·78	4·16	4·89	5·59	6·13	6·42
3 stars per cm³ ($\times 10^{-2}$)	2·81	3·26	3·50	3·72	3·90	4·00
2 stars per cm³ ($\times 10^{-1}$)	1·02	1·05	1·07	1·09	1·10	1·11

and for the thorium family alone:

Weeks	1	2	3	5	10	20
5 stars per cm³ ($\times 10^{-3}$)	1·93	3·07	3·67	4·20	4·62	4·84
4 stars per cm³ ($\times 10^{-2}$)	1·50	1·93	2·14	2·35	2·50	2·57
3 stars per cm³ ($\times 10^{-2}$)	5·73	6·46	6·78	7·07	7·30	7·41
2 stars per cm³ ($\times 10^{-1}$)	1·33	1·40	1·43	1·45	1·47	1·47

No correction for minimum visible range is made.

The required equation additional to (1) is now easily obtained: if, for instance, a three weeks exposure is used, the total number of α-tracks per cm² in this time from the uranium is, from (1),

$$\left(\frac{n_U \times 60^2 \times 24 \times 21 \times d}{4\mu} \sum_U R\right) c_U,$$

so that, referring to the Table above, the number of 2 stars per cm² due to uranium is

$$0{\cdot}107\left(\frac{n_U \times 60^2 \times 24 \times 21 \times d}{4\mu} \sum_U R\right) c_U.$$

Similarly, the number of 2 stars per cm² due to thorium is

$$0{\cdot}143\left(\frac{n_{Th} \times 60^2 \times 24 \times 21 \times d}{4\mu} \sum_{Th} R\right) c_{Th},$$

and we add these and equate them to the observed density of 2 stars.

One can make use of the 3, 4 and 5 star densities to provide checks.

The effect of allowing for the minimum observable range would be to decrease the ratios, but would affect the thorium ratios rather less than the uranium because on the whole the relevant thorium ranges are greater; thus there will be an increased accuracy in distinguishing uranium from thorium.

The stars can only be recognized easily when the track-density is low, so that the calculation as it stands applies to rocks poor in uranium and thorium; even for such rocks the method would not be suitable if the radioactive elements were localized in very small grains, as often happens. For markedly inhomogeneous rocks, the method in combination with petrographic technique (Poole and Bremner 1949) would have its virtues: for example, one of the extra star-density equations could be used to eliminate μ.

ACKNOWLEDGMENT

The author's sincere thanks are due to Professor J. H. J. Poole for his very valuable encouragement.

REFERENCES

Bateman, H., 1910, *Proc. Camb. Phil. Soc.*, **15**, 423.
Coppens, R., 1950, *J. Phys. Radium*, **11**, 21.
Evans, R. D., 1934, *Phys. Rev.*, **45**, 29.
Joliot-Curie, I., 1946, *J. Phys. Radium*, **7**, 11.
Poole, J. H. J., and Bremner, J. W., 1948, *Nature, Lond.*, **161**, 884; 1949, *Ibid.*, **163**, 130.
Seaborg, G. T., 1944, *Rev. Mod. Phys.*, **16**, 1.

The Planar Vibrations of Ethylene and Tetra-deutero-ethylene: A Critical Analysis of the Potential Function

By P. TORKINGTON
British Rayon Research Association, Urmston, Lancs.

MS. received 23*rd February* 1950, *and in final form* 24*th May* 1950

ABSTRACT. A careful analysis of the planar modes of vibration of ethylene and ethylene-d_4 is carried out in order (*a*) to determine finally the value of the C=C stretching force constant in these key molecules, (*b*) to find what interactions, particularly those between the two ends of the molecules, are real, and (*c*) to determine the vibrational forms and the potential energy distributions in the normal modes, and how they are affected by altering the potential function. Solutions are obtained both with and without correction for anharmonicity, and estimates are made of the effects of other corrections which may be necessary. The limits found for the C=C stretching constant are $9{\cdot}336, 9{\cdot}388 \times 10^5$ dyne/cm., with a most probable value of 9·343, the carbon atoms being uncorrected for anharmonicity. The zero-order constant is unlikely to be greater than 9·57. There is detectable real interaction between the two ends of the molecule, for both stretching and bending coordinates. Interactions are discussed.

§ 1. INTRODUCTION

RECENTLY (Torkington 1949 a, 1950 a) it was shown that the non-planar vibrations of substituted ethylenes could only be explained satisfactorily if the C–H bending force constants varied with the substituents. Some evidence has been obtained for similar variations in the planar C–H bending modes (Torkington 1949 b), and it is intended to apply a similar treatment to the skeletal vibrations of substituted ethylenes; as a first step the planar vibrations of the parent compound tetra-chloro-ethylene were recently subjected to a complete analysis (Torkington 1950 b). Now it becomes necessary to fix the value of the C=C stretching constant in ethylene itself, this involving a careful analysis of the potential function of ethylene and ethylene-d_4, because the required constant is sensitive to some of the various small interactions which are theoretically possible. Ethylene has previously been treated quite fully, but none of the investigations is satisfactory, for reasons mentioned below. To avoid repeating the present calculations, the problem is approached from several different angles and necessary key results given. The procedures are outlined so that any required stage can be rapidly checked or adjusted.

§ 2. PREVIOUS INVESTIGATIONS

Brief summaries of previous investigations will be found in publications by Herzberg (1945) and Wu (1946); a review of work up to 1939 was given by de Hemptinne and Manneback (1939).

The experimental measurements are summarized below:

Levin and Meyer (1928)	C_2H_4	I.R.	Gas
Daure (1929)	C_2H_4	R.	Liquid
Dickinson, Dillon and Rasetti (1929)	C_2H_4	R.	Gas
Bhagavantam (1936)	C_2H_4	R.	Gas

Bonner (1936)	C_2H_4	R.	Liquid
Sutherland and Conn (1937)	C_2D_4	I.R.	Gas
Glockler and Renfrew (1938)	C_2H_4	R.	Liquid
de Hemptinne, Jungers and Delfosse (1938)	C_2H_4	R.	Liquid
	C_2D_4	R.	Liquid (and partial spectra of all compounds $C_2H_nD_{4-n}$)
Conn and Sutherland (1939)	C_2D_4	I.R.	Gas
Gallaway and Barker (1942)	C_2H_4	I.R.	Gas
	C_2D_4	I.R.	Gas

Photographic infra-red bands have been reported by Badger and Binder (1931), by Gänswein and Mecke (1936), and by Thompson (1939); a weak infra-red band at approximately 800 cm^{-1} was reported by Rasmussen (1942) and confirmed by Thompson and Harris (1944). The specific heat of ethylene was measured by Eucken and Parts in 1933, and by Burcik, Eyster and Yost in 1941. From measurements on a photographic infra-red band Badger (1934) deduced the dimensions of C_2H_4 to be: $r_{C-H}=1{\cdot}04$ A., $r_{C=C}=1{\cdot}37$ A., $\widehat{HCH}=126°$. Thompson (1939) obtained 1·085, 1·331 A. and 118°. From an analysis of the rotational structure of infra-red absorption bands obtained with high resolving power in the fundamental region, Gallaway and Barker (1942) obtained the dimensions now accepted for C_2H_4 and C_2D_4: $r_{C-H}=1{\cdot}071$ A., $r_{C=C}=1{\cdot}353$ A., $\widehat{HCH}=119°\,55'\pm30'$.

The vibrational assignments for ethylene and ethylene-d_4 now accepted as correct (Herzberg 1945) are based largely on the high-resolution work of Gallaway and Barker (1942), though the assignments of Conn and Sutherland (1939) were essentially the same. Previously, only the A_g and B_{3u} modes were certain. The B_{1g} and B_{2u} (planar) rocking modes were usually both taken to be in the region of 950 cm^{-1} (for C_2H_4), though it is the non-planar modes which are of this magnitude.* Earlier assignments for ethylene are discussed by Mecke (1932) and by Teller and Topley (1935); the former had assigned the non-planar modes correctly. Correlation with C_2D_4 is discussed fully by Conn and Sutherland (1939).

There have been numerous investigations of the potential function of ethylene. Mecke (1932), using a simplified valence force field, obtained a value of $8{\cdot}0\times10^5$ dyne/cm. (quoted as 52 volts), for the C=C stretching force constant. Sutherland and Dennison (1935) treated the molecule as two coupled CH_2 groups; the potential function for each group was not of valence type. The only cross-term corresponded to $\Delta r_{C-H}.\Delta\theta_{CH_2}$ interaction. Only the parallel, A_g and B_{3u}, vibrations were treated, and the force constants were assumed the same in both symmetry factors. The frequencies were adjusted to fit a relation deduced from this assumption, the adjustments (to the C–H stretching modes) being $3019\rightarrow3039$ and $2988\rightarrow2968$. The value $9{\cdot}79\times10^5$ dyne/cm. was deduced for the C=C stretching constant. Delfosse (1935) used a standard valence-type potential based on the symmetry coordinates of Brester as developed by Manneback (1935), which, together with the nomenclature, was carried over essentially unchanged by later European workers. He obtained a value 8·64 for $k_{C=C}$. Bonner (1936) employed a potential due to Wilson. Here the bending coordinates were expressed in terms of the acute angle between a C–H bond and the C=C

* Wu (1946) still attempts this assignment.

axis. Interactions between the stretchings of adjacent C–H bonds and the deformations of adjacent angles were included, but none involving C=C stretching. Because of this omission, no real roots could be found for the cubic factor, but a best solution was reached by a variational method (which was not explained) giving $k_{C=C}=8{\cdot}2$. The treatment included all twelve fundamentals, but wrong assignments were employed for the B_{1g}, B_{2u} and B_{2g} modes; the A_u (twisting) mode was correctly assigned from the Raman line at 1656 cm^{-1}, reported here for the first time. Manneback and Verleysen (1936, 1937), using Delfosse's potential function with eleven constants for the nine planar vibrations, obtained $k_{C=C}=8{\cdot}674$, this being chosen as the best value from the range 8·37 to 8·97; negative constants were used for $\Delta r_{C=C}.\Delta r_{C-H}$ and for $\Delta r_{C=C}.\Delta\theta_{CH_2}$ interactions. Predictions of the frequencies of deuterated ethylenes were made, and the forms of the vibrations calculated. Considering the complexity of the potential function, the predicted spectra were not in good agreement with the values observed later by de Hemptinne, Jungers and Delfosse (1938). Thompson and Linnett (1937), using a valence force field with one interaction term for $\Delta r_{C=C}.\Delta\theta_{CH_2}$ interaction, obtained a value $k_{C=C}=9{\cdot}8$, associated with a negative interaction constant. Calculations of the frequencies of C_2D_4 by Conn and Sutherland (1939) showed that this potential function was not as satisfactory as previous ones with a smaller C=C stretching constant. Fox and Martin (1938) used in addition a constant for interaction between the stretchings of adjacent C–H bonds, but gave no value for $k_{C=C}$, which was eliminated from their equations in order to study the CH_2 groups. Lemaitre, Tchang and Manneback (1937) and Tchang (1938), using the maximum number of interaction terms and one constant to correct for anharmonicity, were able to predict the frequencies of C_2H_4 and of the six deuterated ethylenes, in so far as their spectra were complete, with an error less than 0·5% in general and always less than 1·5%. The anharmonicity correction was introduced because it was obvious that the different degrees of anharmonicity in motions involving hydrogen and deuterium atoms were the chief cause of the discrepancies in the predictions of Manneback and Verleysen. In the method of Tchang, the masses m_H and m_D are replaced by effective masses $m_{H,D}'=m_{H,D}+Cm_{H,D}^{1/2}$, where C is an anharmonicity constant for the isotopic pair; it is given a value such that the isotope product rule for the frequencies of each symmetry factor is obeyed. The formula can be deduced from the expression for the energy levels of an anharmonic oscillator (see Kilpatrick and Pitzer 1947). A review of this work on ethylene and deuterated ethylenes was published by de Hemptinne and Manneback in 1939; the value quoted there for the C=C stretching constant was 9·356. In view of the fact that the B_{1g} and B_{2u} bending modes were assigned incorrectly, and that the dimensions of Badger were used in the calculations, it must be supposed that the relatively high accuracy of frequency prediction attained by Tchang is due at least in part to accidental coincidence. Only one analysis has been carried out with the correct assignments and dimensions (Kilpatrick and Pitzer 1947)*. Results for C_2H_4 and C_2D_4 were obtained both with and without Tchang's correction for anharmonicity, using only the one cross-term employed by Thompson and Linnett. The anharmonicity constant is calculated by fitting the A_g factors

* Apart from preliminary calculations by the author (Torkington 1949 b); see also Linnett, Heath and Wheatley (1949) and § 7.

perfectly, but its use does not greatly improve the fits for the other symmetry factors. The values obtained for k_{C-C} were 9·66 and 9·23 respectively, with and without the correction for anharmonicity. Two obvious criticisms of the treatment are as follows: (i) If it is granted that small differences between corresponding constants in different symmetry factors are to be allowed, then there is no justification for assuming zero for all except one of the off-diagonal elements of the symmetry force constant matrix, for a difference between two corresponding constants is equivalent to an interaction constant in the expanded valence-force potential function. (ii) The Raman data for C_2H_4 refers to the gas, that of C_2D_4 to the liquid; some correction is surely necessary before evaluating the anharmonicity constant.

§3. THE VIBRATIONAL ASSIGNMENTS AND POTENTIAL FUNCTION

The assignments given by Herzberg were accepted as a working basis; they are summarized in Table 1; all values are in cm^{-1}.

Table 1. Vibrational Assignments for Ethylene and Ethylene-d_4 (Planar Modes)

	A_g		B_{1g}		B_{2u}		B_{3u}	
	C_2H_4	C_2D_4	C_2H_4	C_2D_4	C_2H_4	C_2D_4	C_2H_4	C_2D_4
$\nu_{C=C}$	1623·3	1515						
ν_{CH}, ν_{CD}	3019·3	2251	3075	2304	3105·5	2345	2989·5	2200·2
δ_{CH_2}, δ_{CD_2}	1342·4	981					1443·5	1077·9
δ_{CCH}, δ_{CCD}			1050	883	995	712		

All the frequencies of C_2H_4 are taken from measurements of the gas, with the exception of the B_{1g} stretching frequency; the value for this mode adopted here is taken from a weak Raman line of the liquid. This latter value is preferred to 3272·3 cm^{-1}, which occurs as a very weak Raman line of the gas, among other reasons because it allows a reasonable fit with the isotope product rule. The B_{1g} bending modes of both compounds are deduced from an infra-red combination band, measured for the gases. The B_{2u} and B_{3u} frequencies of C_2D_4 are taken from measurements of the gas; the B_{2u} bending mode is in some doubt. The value given here is that deduced by Herzberg by application of the isotope relations to the corresponding frequency for C_2H_4. Various maxima have been reported in this region, at 723·4, 727 and 740 cm^{-1} (Herzberg 1945); the very strong B_{1u} maximum at 720 cm^{-1} is too close for a certain value to be obtained. The B_{1g} and A_g frequencies of C_2D_4 (with the exception of the B_{1g} bending mode, see above) are taken from the Raman spectrum of the liquid. There are no data available on liquid-vapour shifts for C_2D_4, but a certain amount for C_2H_4 has been summarized by Wu (1946). The probable Raman frequencies of liquid C_2H_4 are 1620, 3008, 1341 (A_g) cm^{-1}.

The coordinates used are identical with those employed for tetra-chloroethylene, (Torkington 1950b), and the same order of frequencies is adopted. In general, formulae will not be repeated and the paper should be referred to.

The atomic masses used were: $m_H = 1{\cdot}00813$, $m_D = 2{\cdot}01473$, $m_C = 12{\cdot}00398$. Conversion factor: $4\pi^2c^2m_C = 0{\cdot}70691_3$ gm.cm^{2}sec^{-2}.

§ 4. PRELIMINARY ANALYSIS

Results for the three second-degree factors, assuming the off-diagonal elements of the force constant matrix to be zero, have been given previously (Torkington 1949 b) and will not be repeated here. Comparison of the two sets of constants obtained (*a*) by solving explicitly and (*b*) by factoring off the C–H and C–D stretching modes by the method of Wilson (1941) suggests that the error intro-

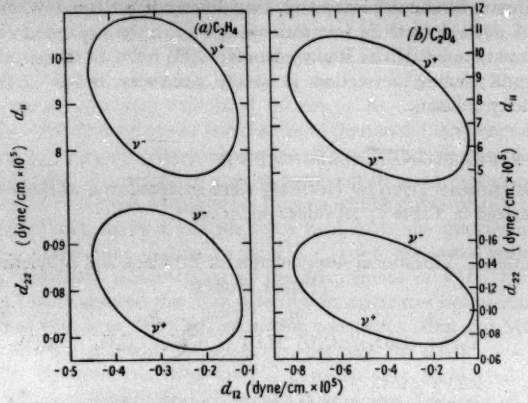

Figure 1. Allowed solutions for the force constants of (*a*) C_2H_4, (*b*) C_2D_4 from the second-degree approximation to the A_g factors.

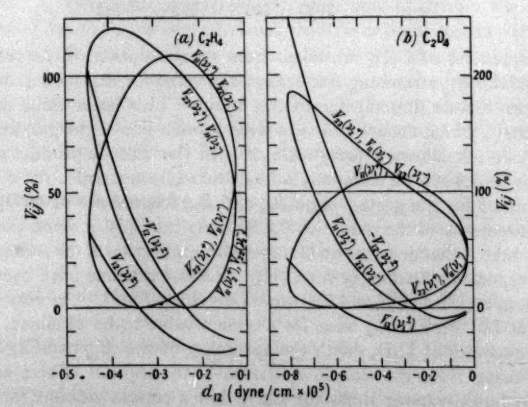

Figure 2. Distributions of the potential energy in the second-degree approximation to the A_g factors for (*a*) C_2H_4, (*b*) C_2D_4.

duced by factoring off these modes in the A_g factor will be quite small. To obtain insight into the various allowed potential functions for each molecule, therefore, the A_g factors will be treated as second-degree equations. The procedure has been standardized (Torkington 1949 c); the results of the analysis are conveniently summarized in Figures 1, 2 and 3. By correlating the two sets of constants it is seen that d_{12} must be restricted to its range in ethylene, d_{22} to

the range 0·098 to 0·071, and hence d_{11} to 8·5 to 10·5. The potential energy distributions and displacements should be noticed. No common solution of the two second-degree equations is to be expected, since there will be some error introduced in factoring off ν_{C-D}, but we may obtain a preliminary fit for ethylene by correlating the A_g and B_{3u} factors; assuming no interaction between the two

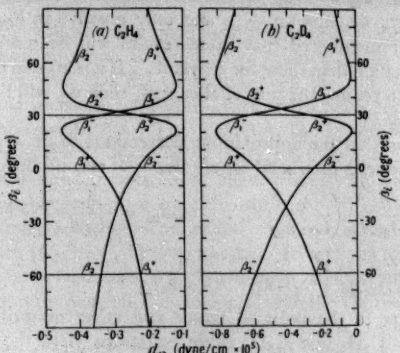

Figure 3. The directions of the displacement vectors in the second-degree approximation to the A_g factors for (*a*) C_2H_4, (*b*) C_2D_4.

($\beta_i^{\pm}$ = arc tan $(y_1/x_1)(\nu_i^{\pm})$, with the numbering and coordinates as for C_2Cl_4 (Torkington 1950 b); $\parallel$ and $\perp$ signify along and perpendicular to $r_{O-H,D}$.)

Coordinates: Δ_1, C=C stretching; Δ_2, CH_2 (CD_2) deformation. $\nu_{1,2}^+$ and $\nu_{1,2}^-$ are the modes of vibration in which d_{11} has respectively the greater and the smaller value for a given value of d_{12}. (See Torkington 1949 c.)

ends of the molecule, the CH_2 deformation constant d_{22} will be the same in both factors. Carrying over the factored constant for δ_{CH_2}, we obtain solutions at

$$\left.\begin{array}{ll}(a)\ d_{12}=-0{\cdot}161, & d_{11}=9{\cdot}784\\ (b)\ d_{12}=-0{\cdot}317, & d_{11}=10{\cdot}86\end{array}\right\}, \qquad d_{22}=0{\cdot}0690,$$

but for C_2D_4 the B_{3u} CD_2 deformation constant is less than the minimum A_g constant, and there is no real solution. If we attempt to fit the two second-degree equations with common constants d_{11}, d_{12}, we obtain the two solutions

(*a*) $d_{12}=-0{\cdot}1223$, $d_{11}=8{\cdot}535$, $d_{22}=0{\cdot}07778$ (C_2H_4); $0{\cdot}07527$ (C_2D_4).
(*b*) $d_{12}=-0{\cdot}4206$, $d_{11}=10{\cdot}53$, $d_{22}=0{\cdot}07842$ (C_2H_4); $0{\cdot}07639$ (C_2D_4).

It would be expected that the greater anharmonicity in a mode involving displacement of hydrogen relative to the same mode in the deuterium compound would lead to the uncorrected constant having the higher value in the latter; data on the increments have been given previously (Torkington 1949 b). Inspection of solutions (*a*) and (*b*) above shows that the factoring of ν_{C-D} must introduce an error which more than compensates for this effect. That this is so is obvious from the following:

	C_2H_4	C_2D_4	
$\lambda_1\lambda_2\lambda_3/\lvert\mathbf{A}\rvert$	0·8426	0·8701	(from cubic equation)
$\lambda_1\lambda_2/\lvert\mathbf{A}'\rvert$	0·6489	0·6275	(from second-degree equation)

$$d_{22}=(\lambda_1\lambda_2/\lvert\mathbf{A}'\rvert+d_{12}^2)/d_{11},$$

where $|\mathbf{A}|$ is the determinant of the matrix $\mathbf{A}$, $=128\epsilon^2$, and $|\mathbf{A}'|$ is the determinant of the reduced matrix $\mathbf{A}'$, $=64\epsilon^2/(1+2\epsilon)$, ($\epsilon = m_C/m_{H,D}$). Referring to the energy curves for ethylene, we see that the component in the potential energy from the cross-term is negative in $\nu_{C=C}$ and positive in δ_{CH_2} from $d_{12}=-0{\cdot}12$ to $-0{\cdot}23$, positive in $\nu_{C=C}$ and negative in δ_{CH_2} from $d_{12}=-0{\cdot}34$ to $-0{\cdot}45$, and negative in both modes from $d_{12}=-0{\cdot}23$ to $-0{\cdot}34$. Over the same range in C_2D_4 the cross-term is always negative in $\nu_{C=C}$ and only positive in δ_{CD_2} for $|d_{12}|<0{\cdot}24$. But it should be remembered that these results will be more sensitive to the factoring approximation than those for ethylene. If it is argued that the cross-term must always tend to reduce the potential energy, then d_{12} will be restricted to the range $-0{\cdot}24$ to $-0{\cdot}34$.

It can be shown that the approximate corrections to be applied to constants obtained from a reduced matrix $\mathbf{A}'$ where this is of second degree are as follows:

$$\Delta d_{11}' = \frac{A_{12}^2}{A_{11}A_{22}}\left(\frac{\lambda_2}{\lambda_1-\lambda_2}\right)d_{11}', \qquad \Delta d_{22}' = \frac{A_{13}^2}{A_{11}A_{33}}\left(\frac{\lambda_3}{\lambda_1-\lambda_3}\right)d_{22}',$$

$$\Delta d_{12}' = \frac{A_{12}A_{13}}{2A_{11}A_{23}}\left[\frac{\lambda_2}{(\lambda_1-\lambda_2)}+\frac{\lambda_3}{(\lambda_1-\lambda_3)}\right]d_{12}'$$

where the d_{ij}' refer to the reduced factor and other quantities to the initial cubic factor. For C_2H_4 and C_2D_4 these equations yield the following results expressed as percentages:

	C_2H_4	C_2D_4
$\Delta d_{11}(k_{C=C})$	1·64	6·41
$\Delta d_{22}(f_{CH_2})$	0·11	0·365
Δd_{12}	1·32	4·11

Note that the actual sign of the increment to the interaction constant is negative. Clearly, factorization of ν_{C-H} gives a good approximation for ethylene, but, as expected, the approximation for C_2D_4 is not nearly as close. A factored high frequency is in general associated with interaction constants which retain the factored coordinate rigid in the residual modes (Torkington 1948, 1949 d); in C_2H_4 and C_2D_4 there are such arbitrary constants for $\Delta r_{C=C}.\Delta r_{C-H,D}$ interaction of magnitudes 0·39 and 0·68 respectively. The corrections to be applied to $k_{C-H,D}$ when these are reduced to zero are proportional to these values, and inversely proportional to the element in the kinetic energy matrix for C–H, D stretching, so that the correction for C_2D_4 will be about four times that for C_2H_4.

§5. THE CUBIC A_g FACTORS

Proceeding to the unreduced cubics, we first attempt solutions in which constants are carried over from the B_{3u} factors. The equations have been given for C_2Cl_4 (Torkington 1950 b, equation (20)); here the constants k, f and d are for C–H stretching (C–D stretching), CH_2 (CD_2) deformation, and for interaction between these two coordinates, and d_{11}, d_{12} and d_{13} are for C=C stretching, $\Delta r_{C=C}.\Delta r_{C-H}$ interaction, and for $\Delta r_{C=C}.\Delta\theta_{CH_2}$ interaction (and for the corresponding interactions in C_2D_4). Using observed frequencies from Table 1, the constants on the right-hand side of the equations take the following values:

	C_2H_4	C_2D_4
$C_1' = \frac{1}{2}[(\lambda_1+\lambda_2+\lambda_3)-(\lambda_1'+\lambda_2')]$	8·953	8·207
$C_2' = (1/8\epsilon)[(\lambda_1\lambda_2+\lambda_1\lambda_3+\lambda_2\lambda_3)-\lambda_1'\lambda_2']$	13·943	13·724
$C_3' = (1/128\epsilon^2)\lambda_1\lambda_2\lambda_3$	0·8426	0·8701

with the force constants in units of 10^5 dyne/cm. With $d_{12}=d_{13}=0$ the corresponding values obtained for $k_{C-C}(=d_{11})$ are:

	C_2H_4	C_2D_4	
From C_1'	8·95	8·21	× 10^5 dyne/cm.
From C_2'	9·01	8·58	
From C_3'	9·60	9·39	

The values from C_3' will be quite good approximations, since the left-hand side of the corresponding equation contains only squares of d_{12} and d_{13}. If it is permissible to carry over the B_{3u} constants, then the differences $(C_i'^{H}-C_i'^{D})$ will arise from anharmonicity; for zero-order frequencies there would be only one value for each constant C_i'. The term $\lambda_1\lambda_2/|\mathbf{A}|$ in the B_{3u} factors (corresponding to C_3') takes the values 0·08781 (C_2H_4), 0·09262 (C_2D_4), from which it appears that there is considerably more anharmonicity in the B_{3u} than in the A_g modes. If the anharmonicities were the same in both C–H (C–D) stretching modes, which will have the greatest effect, they would be eliminated in the constant C_1'. Since $(C_1'^{H}-C_1'^{D})$ is so appreciable, and the carrying over of the B_{3u} constants will be at least a good approximation, apart from considerations of anharmonicity, the only possible conclusion is that the degree of anharmonicity is much greater in the B_{3u} than in the A_g modes. The larger negative correction to $C_1'^{H}$ to reduce to zero-order frequencies would then bring $C_1'^{H}$ and $C_1'^{D}$ to a common value. Confirmation, if considered necessary, is obtained by adjusting the B_{3u} frequencies of C_2D_4 only, so that the constants for both molecules are identical (and the isotope product rule satisfied). The frequencies are then corrected to '*C–H anharmonicity*'. The increments are: $\Delta\nu_{C-D}=-39{\cdot}3$, $\Delta\delta_{CD_2}=-9{\cdot}3\ cm^{-1}$. Using the corrected frequencies, the corresponding increments to the A_g frequencies can be found, using the first two equations. They are: $\Delta\nu_{C-D}=+12{\cdot}4$, $\Delta\delta_{CD_2}=-18{\cdot}6\ cm^{-1}$. These values give $\Delta C_3'^{D}=-0{\cdot}0231$, which is satisfactory. The degree of anharmonicity will be proportional to the difference $(d_{ij}^{D}-d_{ij}^{H})$ (referred to subsequently as the anharmonicity increment) and hence will be greater the greater the negative increment $\Delta\nu_{C-D}$ required to bring $(d_{ii}^{D}-d_{ii}^{H})$ to zero. The absolute frequency increments given above are probably of no great significance, but the results can be interpreted as implying that there is much more anharmonicity in the B_{3u} stretching mode than in the corresponding A_g mode, though probably not in the bending mode.

With the observed vibration frequencies for ethylene, and substituting $k=1{\cdot}2712$, $f=0{\cdot}06907$, $d=0$ from the B_{3u} factor, we obtain the solutions $d_{11}=9{\cdot}962$, $d_{13}=-0{\cdot}158_5$; and $d_{11}=11{\cdot}081$, $d_{13}=-0{\cdot}320_0$, both going with $d_{12}=-0{\cdot}044_2$. The solution with the smaller values of d_{11} and d_{13} may be compared with the approximate solution obtained from the reduced equation and the factored B_{3u} constant. Because of the large component from ν_{C-H} which occurs in the cubic, and the unknown anharmonicity, it seems better to take the solution from the reduced equation as a standard for A_g/B_{3u} fitting. If we attempt to solve the cubic for C_2D_4 similarly, no real roots can be found. This does not necessarily mean that carrying over the B_{3u} constants is not a reasonable approximation, because of the following considerations. By eliminating d_{11}, the following two second-degree equations in d_{12} and d_{13} are obtained:

$$\frac{(d_{12}-k)^2}{K_1}+\frac{(d_{13}+2\sqrt{3}f)^2}{K_1/4}=1\ ;\quad \frac{(d_{12}-k)^2}{K_2}+\frac{(d_{13}+2\sqrt{3}f)^2}{(f/k)K_2}=1,$$

where $K_1=k^2+48f^2+(k+4f)C_1'-C_2'$; $K_2=k^2+12kf+kC_1'-(C_3'/f)$.

These are equations of ellipses having a common centre; the condition that there should be real solutions of d_{12}, d_{13} is that they should intersect, viz. $K_1 < K_2$ with $kK_1 > 4fK_2$. With C_2H_4 this condition is just satisfied, and there are four real points of intersection in close pairs; with C_2D_4 the condition is just not satisfied, and one ellipse lies wholly within the other. It is possible to separate the variables d_{12}, d_{13}, obtaining the following simple equations:

$$\left.\begin{aligned} d_{12}^2 - 2kd_{12} - (k^2C_1' - kC_2' + 4C_3')/(k-4f) &= 0, \\ d_{13}^2 + 4\sqrt{3}fd_{13} + (C_3' - fC_2' + 4f^2C_1')/(k-4f) &= 0. \end{aligned}\right\}.$$

A shift of $-6\,\mathrm{cm}^{-1}$ in the A_g C–H stretching mode reduces d_{12} to zero, while having only a negligible effect on the other constants. For the moment, then, we will attach no significance to d_{12}. It should perhaps be mentioned here that part at least of the large increment $(C_1'^{H} - C_1'^{D})$ may be attributable to Fermi resonance; there are a number of other Raman lines in the region of ν_{CH} whose intensity Herzberg ascribes to resonance with the A_g C–H stretching mode. A shift of $-28\,\mathrm{cm}^{-1}$ would reduce $C_1'^{H}$ to the order of $C_1'^{D}$. Such a large shift is extremely unlikely, but certainly one of $6\,\mathrm{cm}^{-1}$ seems possible. This uncertainty as to the reality of small interaction constants is of course quite general; many small values quoted in the literature are unaccompanied by any data on the frequency-shifts associated with their elimination. With reasonable corrections for liquid–vapour shifts to C_2D_4 there are still no real roots when the B_{3u} constants with $d=0$ are carried over. The procedure adopted at this stage is to solve for increments Δk, Δf and Δd_{13} with respect to solutions satisfying ethylene, so that the corrected constants satisfy the equations for C_2D_4, the ethylene solutions being taken from Figure 1 and corrected as explained in the last section. The following set of equations is obtained for the increments, from equations (19) of the paper on tetra-chloro-ethylene (Torkington 1950 b):

$$\begin{bmatrix} (2\epsilon_D+1) & 4(2\epsilon_D+3) & 4\sqrt{3} \\ \{d_{11}+8(\epsilon_D+2)f+4\sqrt{3}d_{13}\} & 4\{d_{11}+2(\epsilon_D+2)k\} & 4(\sqrt{3}k-2d_{13}) \\ fd_{11} & kd_{11} & -2kd_{13} \end{bmatrix} \begin{bmatrix} \Delta k \\ \Delta f \\ \Delta d_{13} \end{bmatrix}$$

$$= \begin{bmatrix} \{2(\epsilon_H-\epsilon_D)(k+4f)-(C_1^{H}-C_1^{D})\} \\ \{8(\epsilon_H-\epsilon_D)kf-(C_2^{H}-C_2^{D})\} \\ (C_3^{D}-C_3^{H}) \end{bmatrix}$$

where $\epsilon_{H,D} = m_C/m_{H,D}$ and $C_1 = \frac{1}{2}(\lambda_1+\lambda_2+\lambda_3)$, $C_2 = (\lambda_1\lambda_2+\lambda_1\lambda_3+\lambda_2\lambda_3)/8\epsilon$, $C_3 = \lambda_1\lambda_2\lambda_3/128\epsilon^2$, the superscripts H, D referring to C_2H_4, C_2D_4.

Since it has been found a reasonable approximation to the factor for ethylene, the same constant k is used throughout; the value taken was 1·277, this being obtained from the A_g/B_{3u} fit, using a correction for kinetic coupling (Torkington 1949 d, e). The results, in units of 10^5 dyne/cm., are shown in the following Table; since the treatment is only approximate, though the approximation will

d_{11}	8·67	9·48	9·60	9·95	10·45
k	1·277	—	—	—	—
f	0·07787	0·07167	0·07090	0·06906	0·06722
d_{13}	−0·124	−0·139	−0·144	−0·163	−0·206
Δk	−0·0028	−0·0018	−0·0016	−0·0011	−0·0004
Δf	0·00103	0·00235	0·00252	0·00301	0·00387
Δd_{13}	0·057	0·00095	−0·0061	−0·0239	−0·0453

be quite good, the observed frequencies of C_2D_4 were employed in the fitting. The increments obtained will of course be the anharmonicity increments introduced previously; since no such increment is to be expected in d_{11}, this does not appear as a variable; d_{12} and d are neglected.

An obvious first point in the table is the consistently negative increment Δk; a small correction for liquid→vapour to C_2D_4 would change the sign of this increment, but unless there were an additional positive correction to ν_{CD}, or a negative correction to ν_{CH}, such as the Fermi resonance correction discussed previously, it would still not be sufficiently positive (compare the data given in a preliminary analysis of these molecules by Torkington (1949b)). The trends of the anharmonicity increments for f and d_{13} suggest that the correct solution for the pair of molecules will be in the region of $d_{11}=9{\cdot}5$, where d_{13} changes sign and becomes small and negative. d_{11} will not have a smaller value, for then $|d_{13}^{D}|$ would be less than $|d_{13}^{H}|$, and it will not be as great as 9·6, for then the increment for d_{13} is as large proportionately as that for f; it is unlikely that this would be the case, since d_{13} is for an interaction involving a coordinate (C=C stretching) whose anharmonicity is invariable. The anharmonicity increment for f amounts to 3 to 4% (cf. 2% for the B_{3u} factor), and the absolute values for f exceed the B_{3u} constants in both molecules by about 0·003. The results are consistent within the degree of approximation to be expected for this variational treatment, and suggest that there is a real positive constant for interaction between deformations of CH_2 or CD_2 groups separated by a double bond, and that the correct values for d_{11} and d_{13} are near 9·5 and $-0{\cdot}14$ respectively. Note also that there is probably less anharmonicity in the B_{3u} deformation than in the corresponding A_g mode—certainly not more—and so there must be much more anharmonicity in the B_{3u} stretching mode than in the corresponding A_g mode, or a negative Fermi resonance correction to the latter, confirming previous conclusions. Correction to zero-order frequencies would probably not eliminate the constant $f(A_g)-f(B_{3u})$ for interaction between the deformations of the two CH_2, (CD_2), groups.

So far, we have solved for ethylene using the constants from the B_{3u} factor, found d_{12} negligible in the first instance, obtained a series of approximate solutions for C_2H_4 and, from the anharmonicity increments required in order that the constants should satisfy the equations for C_2D_4, deduced that $f(A_g)>f(B_{3u})$ and that the correct potential function representing the observed frequencies has $d_{11}\simeq 9{\cdot}5$, $d_{13}\simeq -0{\cdot}14$. Since any correction for anharmonicity is likely to be found arbitrary, it is convenient to obtain ranges of explicit solutions at this stage, in case it is subsequently found preferable to correct the constants directly, rather than the frequencies or atomic masses. The procedure adopted was as follows. The constant f can be expressed as a function of k only, d and d_{12} being neglected, and d_{13} as a function of k and d_{11}:

$$f=(1/4)[(2\epsilon+1)k-C_1+C_2/k]-C_3/k^2,$$

$$d_{13}=(1/4\sqrt{3})[2(\epsilon+2)\{C_1-(2\epsilon+1)k\}+\{(2\epsilon+3)/k\}(4C_3/k-C_2)-d_{11}].$$

With a given value of k, f may be obtained immediately and d_{13} expressed as a function of d_{11}, of such form that the identity involving the constants and C_1 is satisfied for all values of d_{11}, but the identities for C_2 and C_3 are only satisfied at the correct value of d_{11}. This latter is soon found. The calculations may be repeated for as many values of k as required. (This is a rapid and exact method

for solving equations from cubic factors.) The results are conveniently plotted against d_{11}; they are shown in Figures 4, 5 and 6, (*a*) for the observed frequencies from Table 1, curves (i) and (iii); (*b*) for C_2D_4 with empirical corrections for liquid–vapour frequency shifts, curve (iv); (*c*) for C_2H_4 with an empirical correction of $-10\,cm^{-1}$ to ν_{CH}, for Fermi resonance, curve (ii), Figure 4; (*d*) for

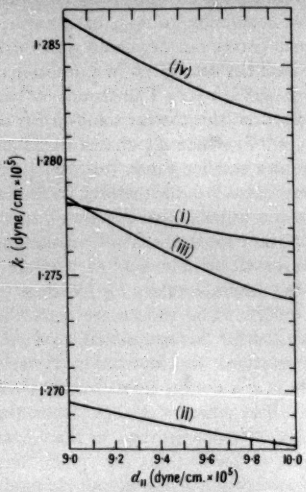

Figure 4. Solutions for k in the A_g factors:
(i) C_2H_4, observed frequencies;
(ii) C_2H_4, with $\Delta\nu_{CH} = -10\,cm^{-1}$;
(iii) C_2D_4, observed frequencies;
(iv) C_2D_4, corrected to gas.

Coordinates: Δ_1, C=C stretching; Δ_2, C–H (C–D) stretching; Δ_3, CH_2 (CD_2) deformation.

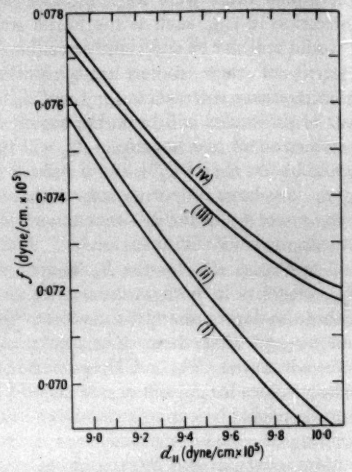

Figure 5. Solutions for f in the A_g factors:
(i) C_2H_4, observed frequencies;
(ii) C_2H_4, with $\Delta\delta_{CH_2} = -\Delta\nu_{C=C} = +10\,cm^{-1}$;
(iii) C_2D_4, observed frequencies;
(iv) C_2D_4, corrected to gas.

Coordinates: Δ_1, C=C stretching; Δ_2, C–H (C–D) stretching; Δ_3, CH_2 (CD_2) deformation.

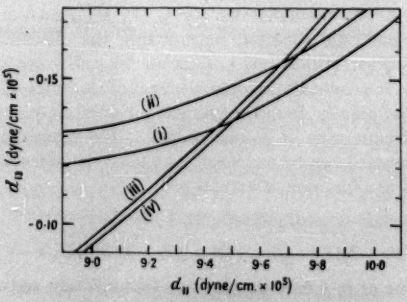

Figure 6. Solutions for d_{13} in the A_g factors;
(i) C_2H_4, observed frequencies;
(ii) C_2H_4, with $\Delta\delta_{CH_2} = -\Delta\nu_{C=C} = +10\,cm^{-1}$;
(iii) C_2D_4, observed frequencies;
(iv) C_2D_4, corrected to gas.

Coordinates: Δ_1, C=C stretching; Δ_2, C–H (C–D) stretching; Δ_3, CH_2 (CD_2) deformation.

C_2H_4 with empirical corrections of $+10$, $-10\,cm^{-1}$ to δ_{CH_2} and $\nu_{C=C}$ respectively, to show the effect of Fermi resonance between these modes, curve (ii), Figures 5 and 6. Note should be taken of the relative magnitudes of k and the effect of the corrections (*b*) and (*c*)—see the previous discussion—and of the trends of the anharmonicity increments for f and d_{13}. For f the trend is always positive; hence there is no solution for the pair of molecules with common constants without correction for anharmonicity. For d_{13} there is a change of sign which can be used to select solutions. Further, the correction for Fermi resonance between $\nu_{C=C}$ and δ_{CH_2} in C_2H_4 increases d_{11} and decreases f, although the frequency increments are in the opposite directions. This is due to the importance of the coupling term; $|d_{13}|$ becomes larger. The results are summarized below, all values being in units of 10^5 dyne/cm.

Correlation :

	C_2H_4 (obs.)	C_2D_4 (obs.)	C_2H_4 (obs.)	C_2D_4 (corr.)	C_2H_4 (corr.)	C_2D_4 (obs.)	C_2H_4 (corr.)	C_2D_4 (corr.)
f	0·0717$_5$	0·0740	0·07130	0·0740	0·0708	0·0729$_5$	0·07050	0·0729$_5$
d_{11}	9·45$_9$		9·51$_5$		9·69		9·75	
d_{13}	−0·1340		−0·136$_5$		−0·157		−0·160	

'obs.' refers to the observed frequencies in Table 1, (C_2H_4 gas, C_2D_4 liquid); 'corr.' refers to corrected frequencies, for ethylene with $\Delta\nu_{C=C} = -10\,cm^{-1}$, $\Delta\delta_{CH_2} = +10\,cm^{-1}$, and for C_2D_4 with the following empirical corrections for liquid–vapour shifts: $\Delta\nu_{C-D} = +6{\cdot}3$, $\Delta\nu_{C-C} = +2{\cdot}9$, $\Delta\delta_{CD_2} = +0{\cdot}75\,cm^{-1}$, these being deduced from those for C_2H_4 on the assumption that for isotopic molecules such shifts will be proportional to the square of the frequency. k is omitted from the table. Correction of ν_{C-H} by $-10\,cm^{-1}$ has only a negligible effect on the fits for the remaining constants. It may be noted that the corrections to C_2D_4 give shifts of the solutions as follows: $\Delta f = -0{\cdot}00030$ to $-0{\cdot}00045$ for C_2H_4, zero for C_2D_4; $\Delta d_{11} = +0{\cdot}06$, $\Delta d_{13} = -0{\cdot}0025$ to $-0{\cdot}0030$; and that the corrections to C_2H_4 give $\Delta f = -0{\cdot}00080$ to $-0{\cdot}00095$ for C_2H_4, $-0{\cdot}00105$ for C_2D_4; $\Delta d_{11} = +0{\cdot}24$, $\Delta d_{13} = -0{\cdot}023$. The solutions with common values of d_{13} have been given; in fact, this constant would be expected to have a small anharmonicity increment. It would probably not exceed 2%; the increment for B_{3u} deformation amounts to 1·7%. The shift of the solution for $\Delta d_{13} = -0{\cdot}003$ is $\Delta d_{11} = +0{\cdot}06$, $\Delta f = -0{\cdot}00040$ to $-0{\cdot}00030$ for C_2H_4, $-0{\cdot}00030$ to $-0{\cdot}00020$ for C_2D_4. The anharmonicity increments for f are between 3 and 4%; all the absolute values exceed the B_{3u} constants, by 0·0027 to 0·0014 for C_2H_4, 0·0037 to 0·0027 for C_2D_4. (These differences apply to the solutions in the table for common d_{13}; additional correction to d_{13} leaves the result essentially the same.) The values of k at $d_{11} = 9{\cdot}45$, with the observed frequencies, are 1·2772 (C_2H_4); 1·2759 (C_2D_4). The slopes $(\partial k/\partial d_{11})$ are of the order $-0{\cdot}002$ to $-0{\cdot}0015$ for C_2H_4, $-0{\cdot}005$ to $-0{\cdot}003$ for C_2D_4. The increments for the corrections (*a*) of $-10\,cm^{-1}$ to ν_{C-H}, (*b*) of the liquid–vapour shifts to C_2D_4, are respectively $-0{\cdot}0086$ and $+0{\cdot}0078$. The anharmonicity increments at $d_{11} = 9{\cdot}5$ referred to the corrected C_2D_4 constant are 0·0063 and 0·0149 for the observed and corrected C_2H_4 frequencies. For the B_{3u} stretching mode it is 0·0469. It would appear from these results that some correction for Fermi resonance to the A_g stretching mode was necessary, but that the anharmonicity could not be as great as in the B_{3u} mode. Further, the increments to k required for coincidence with the B_{3u} stretching constants are respectively $-0{\cdot}0058$, $+0{\cdot}0425$ for C_2H_4, C_2D_4, referred to the results for the

observed frequencies. The corrections available do not lead to consistent values, which suggests that small real interactions, either d or d_{12}, or both, have been neglected.

It is convenient to give here the derivatives determining the dependence of the frequencies on the force constants (Torkington 1949d, 1950b, Appendix II). The solution used was the standard anharmonicity-corrected one with $C=0{\cdot}09307$, obtained in § 6.

		$(\partial\lambda_k/\partial d_{ij})$					
k	ij	11	12	13	22	23	33
1	C_2H_4	1·518	0·690	11·92	0·314	5·418	93·57
	C_2D_4	1·476	1·375	6·560	1·280	6·109	29·15
2	C_2H_4	0·140	−2·517	0·852	45·19	−15·29	5·172
	C_2D_4	0·478	−3·318	2·207	23·02	−15·31	10·17
3	C_2H_4	0·342	−0·173	−5·840	0·087	2·944	99·61
	C_2D_4	0·046	−0·056	−1·839	0·070	2·273	74·13

Coordinates: Δ_1, C=C stretching; Δ_2, C–H (C–D) stretching; Δ_3, CH_2 (CD_2) deformation. The derivatives are matrix elements; for off-diagonal force constants multiply by 2 for $d_{ij}=d_{ji}$.

§ 6. CORRECTION FOR ANHARMONICITY

The only planar factor for which the vibration frequencies for both C_2H_4 and C_2D_4 in the gaseous state are certain is B_{3u}; the anharmonicity constant in Tchang's formula takes the value 0·09307. Using the data in Table 1, the B_{2u} factor (for which only δ_{CD_2} is uncertain) gives 0·089. These two values seem sufficiently close to justify accepting 0·09307 as the true planar anharmonicity constant. The procedure adopted was to fit the frequencies to this value, using the most probable increments. The calculated values in cm^{-1} are C_2H_4: B_{1g} 3086, 1056; C_2D_4: A_g 2262·4, 1518, 983; B_{1g} 2310·4, 874; B_{2u} 724·2. The value for $\delta(B_{2u})$ for C_2D_4 may be compared with the reported maxima at 723·4 and 727 cm^{-1}. The liquid–vapour shifts for the A_g C_2D_4 frequencies from the above are $\Delta\nu_{C-D}=11{\cdot}4$, $\Delta\nu_{C=C}=3{\cdot}0$, $\Delta\delta_{CD_2}=2{\cdot}0\,cm^{-1}$. The last two must be fair approximations, but $\Delta\nu_{C-D}$ is probably too large; the data for ethylene give $\Delta\nu_{C-H}=11\,cm^{-1}$. But the solution will not be very sensitive to ν_{C-D} except for k and possibly d_{12}; the point is considered later. The B_{1g} factor is the most uncertain. The value obtained for C_2H_4 by taking $\Delta\nu_{C-H}=11$ for liquid→vapour is 3086; a value of 1056 is obtained if the excess of $(\delta(B_{1g})+\delta(B_{2u}))$ over 2047·0 (an infra-red combination of the gas) is assumed to be 4 cm^{-1}. The value 4 cm^{-1} is derived from that for $\delta(B_{1u})+\delta(B_{2g})$, the infra-red combination band at 1889·6, assuming the liquid–vapour shift for $\delta(B_{2g})$ to be 1·4 cm^{-1}. Similar arguments were used to fix $\delta(B_{1g})$ for C_2D_4 at 874 cm^{-1}; the fitted value for $\nu(B_{1g})$ then gives a liquid–vapour shift of 4·4 cm^{-1}, which is probably about 2 cm^{-1} too small.

With these assignments, and using $C=0{\cdot}09307$ (equivalent to $m_H'=1{\cdot}10158$, $m_D'=2{\cdot}14683$) the following solution is obtained:

$$A_g\begin{bmatrix}9{\cdot}3429 & 0{\cdot}2582 & -0{\cdot}1463\\ & 1{\cdot}3988 & -0{\cdot}0347\\ & & 0{\cdot}08035\end{bmatrix}\quad B_{1g}\begin{bmatrix}1{\cdot}4006 & 0{\cdot}100\\ & 0{\cdot}1103\end{bmatrix}\quad B_{2u}\begin{bmatrix}1{\cdot}3798 & 0{\cdot}050\\ & 0{\cdot}1556\end{bmatrix}\quad B_{3u}\begin{bmatrix}1{\cdot}3647 & -0{\cdot}0347\\ & 0{\cdot}07670\end{bmatrix}$$

The constant d in the A_g factor is carried over from the B_{3u} factor; this seemed the best assumption to make. The dependence of the remaining constants on d is shown in Figure 7. The curves for k and f are symmetrical about $d=0$; f is

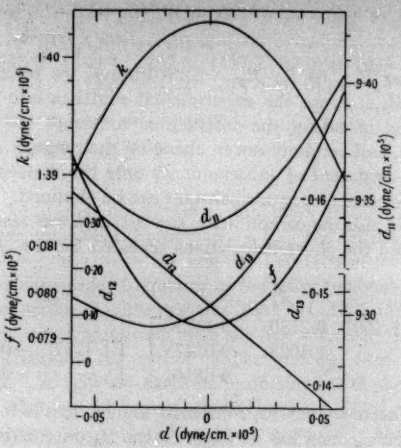

Figure 7. The dependence of the force constants of the A_g factor on d ($\equiv d_{23}$), in the region of the exact solutions with corrections for anharmonicity in the motions of the hydrogen and deuterium atoms (C=0·09307).

Coordinates: Δ_1, C=C stretching; Δ_3, C—H (C—D) stretching; Δ_5, CH_2 (CD_2) deformation.

always greater than $f(B_{3u})$, and k is always greater than $k(B_{3u})$ for $|d|<0{\cdot}10$. d_{11} and d_{13} have minimum values for small negative values of d, and are not very sensitive to any variation in d over this region; d_{12} varies appreciably, and changes sign at $d=+0{\cdot}030$.

It is of interest to compare the above results with those of Tchang (1938) who used effective masses $m_H'=1{\cdot}088$, $m_D'=2{\cdot}126$, corresponding to $C\simeq 0{\cdot}08$. In the A_g factor he obtained a small positive constant in place of the negative d (d_{23} of the above matrix) and a small negative constant for $\Delta r_{C=C}\cdot\Delta r_{C-H}$ interaction in place of the positive d_{12}. In the B_{1g} and B_{3u} factors his interaction constants are of the same signs as in the present solution; in the B_{2u} factor the constant is of opposite sign. (Note that his angle-bending coordinates for the B_{1g} and B_{2u} factors have senses opposite to those used here.) Discrepancies are to be ascribed to wrong assignments for the B_{1g} and B_{2u} factors, and to the molecular dimensions used. But they suggest that a careful investigation into possible variations of the small interaction constants should be made before the present results are accepted as final. This has been carried out, the steps being as follows. Using the exact solution for the B_{3u} factor of C_2H_4 with zero interaction, the frequencies of C_2D_4 were predicted to be 2190·1, 1082·9 cm^{-1}. The error here is of the order of 0·5%. Next, the angle $\theta=\widehat{HCH}$ required for an exact solution with zero interaction to be possible was calculated for the B_{3u} and B_{2u} factors. The general condition for such a solution for a pair of isotopic second-degree factors is

$$(A_{11}'A_{22}-A_{11}A_{22}')^2(\lambda_1\lambda_2/D)+\{A_{11}'(\lambda_1+\lambda_2)-A_{11}(\lambda_1'+\lambda_2')\}\times\{A_{22}'(\lambda_1+\lambda_2)-A_{22}(\lambda_1'+\lambda_2')\}=0,$$

where $D=|\mathbf{A}|$ and $(\lambda_1\lambda_2/D)=(\lambda_1'\lambda_2'/D')$ is the isotope product constant; primes refer to the isotopic species. If the angle θ is taken as a variable, the result for C_2H_4, C_2D_4 is

$$\cos^2\theta=[(\lambda_1+\lambda_2)(\epsilon'+1)-(\lambda_1'+\lambda_2')(\epsilon+1)]^2/[\{(\lambda_1+\lambda_2)-(\lambda_1'+\lambda_2')\}^2 - B(\epsilon-\epsilon')^2(\lambda_1\lambda_2/D)]^{-1},$$

where $B=256$ for B_{3u}, 64 for B_{2u}. Substituting, we obtain $\theta=112°33'$ for B_{3u}, $115°8'$ for B_{2u}. From the experimental evidence one would not on the whole be justified in taking the interaction constants in the second-degree equations as zero, and certainly not in changing their signs.

In the above treatment of anharmonicity only the masses of hydrogen and deuterium are corrected; only one constant can be obtained. To investigate the effect of correcting also the carbon mass, the constant was assumed the same for all three atoms and the above calculations repeated for the A_g and B_{3u} factors, giving

A_g B_{3u}

$$\begin{bmatrix} 9{\cdot}5691 & 0{\cdot}2150 & -0{\cdot}1429 \\ & 1{\cdot}4028 & -0{\cdot}0347 \\ & & 0{\cdot}08101 \end{bmatrix} \quad \begin{bmatrix} 1{\cdot}3737 & -0{\cdot}0347 \\ & 0{\cdot}07725 \end{bmatrix}$$

The value for C becomes 0·0988, somewhat higher than before.

The additional correction has no effect on the B_{3u} interaction constant which, as before, was carried over to the A_g factor. The values of both pairs of constants k and f are raised somewhat, but the differences $k(A_g)-k(B_{3u})$ and $f(A_g)-f(B_{3u})$ remain essentially the same; d_{12} is decreased, but was certainly not due to neglect of carbon anharmonicity; d_{13} is hardly affected, and d_{11} is increased by about 0·2. For comparison, the calculations for the A_g factor were repeated with $C=0{\cdot}09307$ (for m_H and m_D only) and with an empirical correction $\Delta\nu_{C=C}=+25\ \text{cm}^{-1}$ in C_2H_4 for carbon anharmonicity. The increment for C_2D_4 required for satisfaction of the isotope product rule is then $+26{\cdot}4\ \text{cm}^{-1}$. The increase in $k_{C=C}$ is about the same as that obtained with corrected carbon masses and observed frequencies. Lastly, the A_g factor was solved (*a*) with $\Delta\nu_{C=H}=-10\ \text{cm}^{-1}$, (*b*) with $\Delta\nu_{C=C}=-\Delta\delta_{CH_2}=-10\ \text{cm}^{-1}$ in C_2H_4, ν_{C-D} being adjusted to fit in both cases. The shifts represent possible Fermi resonance.

C_2H_4								
1648·3	—	—	—	3009·3	—	1613·3	—	1352·4
C_2D_4								
1541·4	—	—	—	2258·0	—	—	2265·3	—

$$\begin{bmatrix} 9{\cdot}5545 & 0{\cdot}2870 & -0{\cdot}1384 \\ & 1{\cdot}4010 & -0{\cdot}0347 \\ & & 0{\cdot}08065 \end{bmatrix} \begin{bmatrix} 9{\cdot}3938 & 0{\cdot}2438 & -0{\cdot}1473 \\ & 1{\cdot}3876 & -0{\cdot}0347 \\ & & 0{\cdot}08003 \end{bmatrix} \begin{bmatrix} 9{\cdot}5748 & 0{\cdot}2400 & -0{\cdot}1667 \\ & 1{\cdot}3968 & -0{\cdot}0347 \\ & & 0{\cdot}07931 \end{bmatrix}$$

Units are, as usual, in cm^{-1} and 10^5 dyne/cm.

Fundamental frequencies different from those used so far in this section are given in the appropriate columns of the force constant matrices. It will be seen that it appears to be impossible to eliminate the small positive constant d_{12} for $\Delta r_{C=C}.\Delta r_{C-H}$ interaction if the constant d is carried over from the B_{3u} factor; the dependence of the constants on d will remain essentially as in Figure 7. It remains to attempt to decide whether or not the carbon anharmonicity correction

is an improvement. The only way available is to predict the zero-order frequencies from the uncorrected masses and the force constants obtained here. With $C=0{\cdot}09307$, m_H and m_D corrected, and frequencies going with C_2H_4 (obs.),

	A_g			B_{1g}		B_{2u}		B_{3u}	
C_2H_4	3147·0	1643·0	1390·4	3202·2	1117·2	3238·4	1035·7	3117·5	1502·6
C_2D_4	2318·8	1530·1	1014·0	2361·5	915·9	2416·6	742·7	2263·5	1107·4

With $C=0{\cdot}0988$, m_H, m_D and m_C corrected,

C_2H_4, A_g	3157·3	1660·9	1397·6
C_2D_4, A_g	2334·1	1543·8	1017·7

The effect of the additional correction to the mass of the carbon atoms is to raise the frequencies somewhat, particularly $\nu_{C=C}$; the results with $C=0{\cdot}09307$, applied to m_H and m_D only, with the empirical correction for anharmonicity to $\nu_{C=C}$, is to raise the zero-order frequency of the latter to about the same value as for $C=0{\cdot}0988$ (the actual magnitudes are: 1667·4 (C_2H_4), 1553·9 (C_2D_4)), with the remaining frequencies practically as in the first solution. It might seem that the additional corrections for carbon anharmonicity were superfluous; an increment of 20 cm^{-1} at 1,500 to 1,600 cm^{-1}, obtained with the correction to m_H and m_D, is about what would be expected (Herzberg 1945), while the 40 cm^{-1} for C_2H_4 with the extra $\Delta\nu_{C=C}=+25$ cm^{-1} seems definitely too large, though the possibility that some of this is derived from the 30% CH_2 deformation in the 'C=C stretching' mode must be considered (Figure 2). The increment for the (very nearly) pure CH_2 deformation in the B_{3u} factor for C_2H_4 is 59·1 cm^{-1}, while in the A_g factor it is 48·0 cm^{-1}; in the latter there is only about 75% CH_2 deformation. The corresponding increments in C_2D_4 are 31·0 (A_g) and 29·5 (B_{3u}); here there is no appreciable component from δ_{CD_2} in the C=C stretching mode, but some contribution from ν_{C-D}, since the factoring of this coordinate produces considerable error. The increments to $\nu_{C=C}$ in C_2D_4 are 12·1 and 25·8 cm^{-1} for $C=0{\cdot}09307$, 0·0988 respectively. The carbon anharmonicity constant would not be the same as the constant for hydrogen and deuterium, though the results obtained suggest that it must be of the same order; it would certainly seem necessary to allow for one, but at present there is no alternative mode of approach.

Finally, with a correction of -10 cm^{-1} to the A_g stretching mode, the fitted C–D stretching frequency corresponds to a liquid–vapour shift of $+7{\cdot}0$ cm^{-1}, which must be very nearly correct.

§7. INTERACTIONS IN THE ETHYLENE MOLECULE

It is not intended to treat interactions in the ethylene molecule at any length here, but a few points may be summarized for comparison with C_2Cl_4. The interactions between the stretchings of C–H (C–D) bonds* go with constants $-0{\cdot}0169$ (adjacent), $+0{\cdot}0133$ (cis-), $+0{\cdot}0549$ (trans-), taking the values from the standard anharmonicity-corrected constants with $C=0{\cdot}09307$ and using the previous table of relations (Torkington 1950 b, Table 4). A correction of -10 cm^{-1} to A_g C–H stretching produces an increment $-0{\cdot}0112$ in $k(A_g)$, which increases the negative constant for interaction between adjacent bonds and decreases the cis interaction constant nearly to zero, but only reduces the trans interaction

* *Note added in proof.* See also a recent paper (Torkington 1950 d) on the inclusion of van der Waals forces in molecular potential functions.

constant by approximately 20%. Hence there is probably a positive constant for trans interaction between the two ends of the molecule, but possibly no cis interaction, and a negative constant for interaction between adjacent C–H bonds. The latter is to be expected (of that sign) from the changes in hybridization which occur during vibrations of the CH_2 groups (Heath and Linnett 1948 *) if these are of more importance than the repulsions between the hydrogen atoms, which would lead to a positive constant. The trans interaction may be related to conjugation. The positive d_{12}, for $\Delta r_{C=C} . \Delta r_{C-H}$ interaction, implies H . . . C repulsion. The negative interaction constant in the B_{3u} factor, and therefore, presumably, also in the A_g factor, can be explained if the positive constant for $\Delta r_{C-H} . \Delta\theta_{CCH}$ interaction (see below) is greater than that for $\Delta r_{C-H} . \Delta\theta_{CH_2}$ interaction, where the two angles are adjacent to the same bond; a positive sign is to be expected for such interactions, i.e. in triatomic systems, unless attraction between the two non-bonded atoms is important. The negative constant for $\Delta r_{C=C} . \Delta\theta_{CH_2}$ interaction is equivalent to a positive constant for $\Delta r_{C=C} . \Delta\theta_{CCH}$ interaction (Torkington 1949 f) ; this has the expected sign. Other interactions which seem definite are: $\Delta r_{12} . (\Delta\theta_{15} - \Delta\theta_{35})$, +0·300 ; $\Delta r_{12} . (\Delta\theta_{24} - \Delta\theta_{26})$, −0·100; $\Delta\theta_{15}(\Delta\theta_{24} - \Delta\theta_{26})$, +0·09 (normalized values from the B_{1g} and B_{2u} factors) and $\Delta\theta_{13} . \Delta\theta_{46}$, +0·0037. This last could be accounted for by $H_1 \ldots H_4$, but not by H . . .C, repulsion.

In a recent paper (Linnett, Heath and Wheatley 1949) the vibration frequencies of C_2H_4 and C_2D_4 are accounted for by an orbital valency force field (Heath and Linnett 1948) with eight force constants and one van der Waals repulsion constant; there are no interactions which are not derived from this latter. The value obtained for $k_{C=C}$ was 7·16. The constants can be derived by applying a quite simple transformation to the usual valence force constant matrix; the results of the present paper may therefore be used to obtain accurate values of orbital constants should these be required. The reverse transformation applied to the orbital constants gives $k_{C=C} = 8{\cdot}97$, which is somewhat different from the solution found here. The interesting point of the analysis is the discovery of negative force constants for distortions of π orbitals which occur in the non-planar bending modes. These negative constants arise from the strengthening of the bonding caused by overlapping of the π orbitals during non-planar bending (cf. Wheatley and Linnett 1949). This explains the apparently anomalous relation between electron-distribution and non-planar bending constant found by the author (Torkington 1949 a, 1950 a). It is of interest that the Tchang anharmonicity constants in these modes are much smaller than the planar constants: B_{1u} 0·0171, B_{2g} 0·043; evidently the overlapping of the π orbitals reduces anharmonicity more in the B_{1u} than in the B_{2g} mode, corresponding to the larger negative B_{1u} force constant.

ACKNOWLEDGMENTS

The author wishes to express his gratitude to Courtaulds Limited for making the present programme of work possible, and to the British Rayon Research Association, where the paper was completed, for permission to publish.

Note added in proof. After this paper had been completed, a new assignment for the ethylenes was published (Rank, Shull and Axford 1950, Arnett and Crawford 1950). This is discussed in a recent note by the author (Torkington 1950 c). Any changes would affect only the B_{1g} and B_{2u} factors.

* But Coulson, Duchesne and Manneback (1948) appear to differ.

REFERENCES

ARNETT, R. L., and CRAWFORD, B. L., Jr., 1950, *J. Chem. Phys.*, **18**, 118.

BADGER, R. M., 1934, *Phys. Rev.*, **45**, 648.

BADGER, R. M., and BINDER, J. L., 1931, *Phys. Rev.*, **38**, 1442.

BHAGAVANTAM, S., 1936, *Nature, Lond.*, **138**, 1096.

BONNER, L. G., 1936, *J. Amer. Chem. Soc.*, **58**, 34.

BURCIK, E. J., EYSTER, E. H., and YOST, D. M., 1941, *J. Chem. Phys.*, **9**, 118.

CONN G. K. T., and SUTHERLAND, G. B. B. M., 1939, *Proc. Roy. Soc.* A, **172**, 172.

COULSON, C. A., DUCHESNE, J., and MANNEBACK, C., 1948, *V. Henri Mém. Vol.* (Liège : Desoer).

DAURE, P., 1929, *Ann. Phys., Paris*, **12**, 375.

DELFOSSE, J. M., 1935, *Ann. Soc. Sci., Brux.*, **55**, 114.

DICKINSON, R. G., DILLON, R. T., and RASETTI, F., 1929, *Phys. Rev.*, **34**, 582.

EUCKEN, A., and PARTS, A., 1933, *Z. Phys. Chem.* B, **20**, 184.

FOX, J. J., and MARTIN, A. E., 1938, *Proc. Roy. Soc.* A, **167**, 257.

GALLAWAY, W. S., and BARKER, E. F., 1942, *J. Chem. Phys.*, **10**, 88.

GÄNSWEIN, P., and MECKE, R., 1936, *Z. Phys.*, **99**, 189.

GLOCKLER, G., and RENFREW, M. M., 1938, *J. Chem. Phys.*, **6**, 170, 409.

HEATH, D. F., and LINNETT, J. W., 1948, *Trans. Faraday Soc.*, **44**, 556.

DE HEMPTINNE, M., JUNGERS, J., and DELFOSSE, J. M., 1938, *J. Chem. Phys.*, **6**, 319.

DE HEMPTINNE, M., and MANNEBACK, C., 1939, *Proc. Indian Acad.* A, **9**, 286.

HERZBERG, G., 1945, *Infra-red and Raman Spectra of Polyatomic Molecules* (New York : van Nostrand; London : Macmillan).

KILPATRICK, J. E., and PITZER, K. S., 1947, *J. Res. Bur. Stand., Wash.*, **38**, 191.

LEMAITRE, C., TCHANG, Y. L., and MANNEBACK, C., 1937, *Ann. Soc. Sci., Brux.*, **57**, 120.

LEVIN, A., and MEYER, C. F., 1928, *J. Opt. Soc. Amer.*, **16**, 137.

LINNETT, J. W., HEATH, D. F., and WHEATLEY, P. J., 1949, *Trans. Faraday Soc.*, **45**, 1.

MANNEBACK, C., 1935, *Calcule et Identification des Molécules* (Thesis, Liège) ; 1937, *J. Chem. Phys.*, **5**, 989.

MANNEBACK, C., and VERLEYSEN, A., 1936, *Nature, Lond.*, **138**, 367, *Ann. Soc. Sci., Brux.*, **56**, 349 ; 1937, *Ibid.*, **57**, 31.

MECKE, R., 1932, *Z. Phys. Chem.* B, **17**, 1.

RANK, D. H., SHULL, E. R., and AXFORD, D. W. E., 1950, *J. Chem. Phys.*, **18**, 116.

RASMUSSEN, R. S., 1942, *Phys. Rev.*, **62**, 301.

SUTHERLAND, G. B. B. M., and CONN, G. K. T., 1937, *Nature, Lond.*, **140**, 644.

SUTHERLAND, G. B. B. M., and DENNISON, D. M., 1935, *Proc. Roy. Soc.* A, **148**, 250.

TCHANG, Y. L., 1938, *Ann. Soc. Sci. Brux.*, **58**, 87.

TELLER, E., and TOPLEY, B., 1935, *J. Chem. Soc.*, 885.

THOMPSON, H. W., 1939, *Trans. Faraday Soc.*, **35**, 697.

THOMPSON, H. W., and HARRIS, G. P., 1944, *Trans. Faraday Soc.*, **40**, 295.

THOMPSON, H. W., and LINNETT, J. W., 1937, *J. Chem. Soc.*, 1376.

TORKINGTON, P., 1948, *Nature, Lond.*, **162**, 370, 607 ; 1949 a, *Nature, Lond.*, **163**, 96; 1949 b, *J. Chem. Phys.*, **17**, 1279 ; 1949 c, *Ibid.*, **17**, 357 ; 1949 d, *Ibid.*, **17**, 1026; 1949 e, *Nature, Lond.*, **164**, 113; 1949 f, *Ibid.*, **164**, 186; 1950, a, *Proc. Roy. Soc.* A (in the press); 1950 b, *Proc. Phys. Soc.* A, **63**, 804 ; 1950 c, *J. Chem. Phys.* **18**, 758; 1950 d, *Trans. Faraday Soc.* (in the press).

WHEATLEY, P. J., and LINNETT, J. W., 1949, *Trans. Faraday Soc.*, **45**, 897.

WILSON, E. B., Jr., 1941, *J. Chem. Phys.*, **9**, 76.

WU, T. Y., 1946, *Vibrational Spectra and Structure of Polyatomic Molecules* (Ann Arbor, Michigan : Edwards Bros., Inc.).

On the Elimination of Divergencies from Classical Electrodynamics

By SURAJ N. GUPTA*
Cavendish Laboratory, Cambridge

Communicated by N. Kemmer; MS. received 13th March 1950, and in amended form 29th August 1950

ABSTRACT. It is shown that the divergencies in classical electrodynamics may be removed by subtracting the self-energies of isolated electrons by means of a modification of the usual expression for the force density in an electromagnetic field. The results obtained are equivalent to those of Dirac and Wentzel.

§ 1. INTRODUCTION

It is well known that the classical theory of the point electron involves the difficulty that the self-energy and the self-force of the electron diverge. A way out of this difficulty was first shown by Wentzel (1933, 1934) and Dirac (1938), and more recently other devices have been given for the same purpose (see, for instance, Fremberg 1947). However, we suggest another approach, which seems to be particularly simple.

The present approach is based on the postulate that the *self-energies of isolated electrons are physically meaningless*, and our aim is to carry out a covariant subtraction of these self-energies in such a way that the other usual properties of the electrons are not affected. In particular we have to ensure that the amount of radiation emitted by an electron remains unchanged. It will now be shown that all this can be achieved very easily by introducing a ' counter-term ' in the usual expression for the force density in an electromagnetic field, which will introduce a corresponding counter-term in the energy-momentum tensor.

§ 2. BASIC EQUATIONS OF CLASSICAL ELECTRODYNAMICS

Classical electrodynamics is based on the Maxwell equations

$$\left.\begin{aligned} \frac{\partial F_{\mu\nu}}{\partial x_\nu} &= \frac{4\pi}{c} J_\mu, \\ \frac{\partial F_{\mu\nu}}{\partial x_\lambda} + \frac{\partial F_{\nu\lambda}}{\partial x_\mu} + \frac{\partial F_{\lambda\mu}}{\partial x_\nu} &= 0 \end{aligned}\right\} \quad \ldots(1)$$

and the Lorentz equation

$$K_\mu = \frac{1}{c} F_{\mu\nu} J_\nu, \quad \ldots\ldots(2)$$

where J_μ is the current density, K_μ is the force density, and $F_{\mu\nu}$ is the electromagnetic field tensor such that

$$(F_{23}, F_{31}, F_{12}) = \mathbf{H}, \qquad (F_{41}, F_{42}, F_{43}) = i\mathbf{E}. \quad \ldots\ldots(3)$$

* State Scholar of the Government of India.

If n electrons are present in the field under consideration, then we have

$$F_{\mu\nu} = \sum_{r=1}^{n} f^{(r)}_{\mu\nu,\,\mathrm{ret}} + f_{\mu\nu,\,\mathrm{ex}}, \qquad \ldots\ldots(4)$$

$$J_\mu = \Sigma_r j_\mu^{(r)} \qquad \ldots\ldots(5)$$

with $$j_\mu^{(r)} = e\int \frac{dz_\mu^{(r)}}{dt}\,\delta(z_1^{(r)} - x_1)\,\delta(z_2^{(r)} - x_2)\,\delta(z_3^{(r)} - x_3)\,\delta(z_0^{(r)} - x_0)\,dt, \qquad \ldots\ldots(6)$$

where $f_{\mu\nu,\,\mathrm{ex}}$ is the external field, $f^{(r)}_{\mu\nu,\,\mathrm{ret}}$ is the retarded field of the rth electron, and $j_\mu^{(r)}$ is the current density at the point x_ν due to the rth electron, whose coordinates are given by $z_\nu^{(r)}$.

Using (1), we may put (2) in the form

$$K_\mu = \frac{\partial T_{\mu\nu}}{\partial x_\nu}, \qquad \ldots\ldots(7)$$

where $T_{\mu\nu}$ is the energy-momentum tensor given by

$$T_{\mu\nu} = \frac{1}{4\pi}\left(F_{\mu\lambda}F_{\lambda\nu} + \tfrac{1}{4}\delta_{\mu\nu}F_{\lambda\rho}{}^2\right). \qquad \ldots\ldots(8)$$

In particular, (8) gives for the energy density u and the Poynting vector $\mathbf{S}$

$$u = T_{44} = \frac{1}{8\pi}(E^2 + H^2), \qquad \ldots\ldots(9)$$

$$\mathbf{S} = ic\,(T_{41}, T_{42}, T_{43}) = \frac{c}{4\pi}[\mathbf{E}\times\mathbf{H}]. \qquad \ldots\ldots(10)$$

Having stated the basic results in classical electrodynamics, we now consider the elimination of divergencies.

§ 3. ELIMINATION OF DIVERGENCIES

As already pointed out, our aim is to carry out a subtraction of the self-energies of isolated electrons from the existing scheme of classical electrodynamics, keeping the amount of radiation emitted by an electron unchanged. For this we first introduce the following definitions :

$$\left.\begin{aligned} f^{(r)}_{\mu\nu,\,\mathrm{sym}} &= \tfrac{1}{2}\left(f^{(r)}_{\mu\nu,\,\mathrm{ret}} + f^{(r)}_{\mu\nu,\,\mathrm{adv}}\right), \\ f^{(r)}_{\mu\nu,\,\mathrm{rad}} &= \tfrac{1}{2}\left(f^{(r)}_{\mu\nu,\,\mathrm{ret}} - f^{(r)}_{\mu\nu,\,\mathrm{adv}}\right), \end{aligned}\right\} \qquad \ldots\ldots(11)$$

so that we may write

$$f^{(r)}_{\mu\nu,\,\mathrm{ret}} = f^{(r)}_{\mu\nu,\,\mathrm{sym}} + f^{(r)}_{\mu\nu,\,\mathrm{rad}}, \qquad \ldots\ldots(12)$$

where $f^{(r)}_{\mu\nu,\,\mathrm{adv}}$ is the advanced field of the rth electron and $f^{(r)}_{\mu\nu,\,\mathrm{sym}}$ and $f^{(r)}_{\mu\nu,\,\mathrm{rad}}$ will be called the symmetric and the radiation fields respectively. As shown by Dirac (1938), at the world-line of an electron its symmetric field diverges *quadratically*, while the radiation field is finite and given by*

$$f_{\mu\nu,\,\mathrm{rad}} = \frac{2}{3}\frac{e}{c^4}\left(v_\mu \ddot{v}_\nu - v_\nu \ddot{v}_\mu\right), \qquad \ldots\ldots(13)$$

where dots denote differentiations with respect to the proper time s of the electron and $v_\mu = dz_\mu/ds$. (Differentiations with respect to the ordinary time t will always be shown explicitly.)

* Our definition of the radiation field differs from that of Dirac by a factor $\frac{1}{2}$. Also note that we are taking the space-time coordinates as x_1, x_2, x_3, ict.

We now modify the expression (2) for the force density as

$$K'_\mu = \frac{1}{c}(F_{\mu\nu}J_\nu - \Sigma_r f^{(r)}_{\mu\nu,\,\mathrm{sym}}\, j^{(r)}_\nu), \qquad \ldots\ldots(14)$$

which immediately leads to a new energy–momentum tensor, for the symmetric field satisfies the Maxwell equations

$$\left.\begin{aligned} \frac{\partial f^{(r)}_{\mu\nu,\,\mathrm{sym}}}{\partial x_\nu} &= \frac{4\pi}{c} j^{(r)}_\mu \\ \frac{\partial f^{(r)}_{\mu\nu,\,\mathrm{sym}}}{\partial x_\lambda} + \frac{\partial f^{(r)}_{\nu\lambda,\,\mathrm{sym}}}{\partial x_\mu} + \frac{\partial f^{(r)}_{\lambda\mu,\,\mathrm{sym}}}{\partial x_\nu} &= 0. \end{aligned}\right\} \qquad \ldots\ldots(15)$$

Therefore we obtain from (14), (1) and (15), in the usual way,

$$K'_\mu = \frac{\partial T'_{\mu\nu}}{\partial x_\nu}, \qquad \ldots\ldots(16)$$

where the new energy–momentum tensor $T'_{\mu\nu}$ is given by

$$T'_{\mu\nu} = T_{\mu\nu} - \Sigma_r t^{(r)}_{\mu\nu,\,\mathrm{sym}}, \qquad \ldots\ldots(17)$$

$t^{(r)}_{\mu\nu,\,\mathrm{sym}}$ being obtained from (8) on replacing $F_{\mu\nu}$ by $f^{(r)}_{\mu\nu,\,\mathrm{sym}}$.

It can be easily verified that the tensor (17) has the desired properties. For let us consider a single isolated electron moving with a uniform velocity. In this case, the retarded and the advanced fields of the electron being equal, and there being no external field, the total field is equal to the symmetric field, and therefore, according to (17), $T'_{\mu\nu}$ vanishes everywhere. On the other hand, (17) gives for the modified Poynting vector

$$\mathbf{S}' = \frac{c}{4\pi}[\mathbf{E}\times\mathbf{H}] - \Sigma_r \frac{c}{4\pi}[\mathbf{E}^{(r)}_{\mathrm{sym}}\times\mathbf{H}^{(r)}_{\mathrm{sym}}], \qquad \ldots\ldots(18)$$

which keeps the amount of radiation emitted by an electron unchanged, because it is well known that an electron does not lose any radiation by virtue of its symmetric field. In fact, by reversing the positive sense of the time axis, we immediately find

$$\int_{-\infty}^{\infty}[\mathbf{E}_{\mathrm{sym}}\times\mathbf{H}_{\mathrm{sym}}]\,dt = -\int_{-\infty}^{\infty}[\mathbf{E}_{\mathrm{sym}}\times\mathbf{H}_{\mathrm{sym}}]\,dt = 0. \qquad \ldots\ldots(19)$$

It only remains to be shown that (14) leads to a finite self-force, and the energy and the momenta of the field are always finite. Since at the world-line of the rth electron we have

$$j^{(s)}_\nu = 0, \qquad \text{for } s \neq r,$$

equation (14) gives for the force density at the world-line of this electron

$$k'^{(r)}_\mu = \frac{1}{c}(F_{\mu\nu} - f^{(r)}_{\mu\nu,\,\mathrm{sym}})\, j^{(r)}_\nu. \qquad \ldots\ldots(20)$$

From (20) and (6) we find

$$m\frac{dv^{(r)}_\mu}{dt} = \int k'^{(r)}_\mu\, dv = \frac{e}{c}\frac{dz^{(r)}_\nu}{dt}(F_{\mu\nu} - f^{(r)}_{\mu\nu,\,\mathrm{sym}}).$$

Multiplying both sides by dt/ds, we get

$$m\dot{v}_\mu^{(r)} = \frac{e}{c} v_\nu^{(r)} \left(f_{\mu\nu,\,\mathrm{rad}}^{(r)} + \sum_{s \neq r} f_{\mu\nu,\,\mathrm{ret}}^{(s)} + f_{\mu\nu,\,\mathrm{ex}} \right). \qquad \ldots\ldots(21)$$

Using (13), and remembering that

$$v_\nu^2 = -c^2, \qquad v_\nu \dot{v}_\nu = -\dot{v}_\nu^2,$$

we obtain

$$m\dot{v}_\mu^{(r)} - \frac{2}{3}\frac{e^2}{c^3}\ddot{v}_\mu^{(r)} + \frac{2}{3}\frac{e^2}{c^5} v_\mu^{(r)} \dot{v}_\nu^{2(r)} = \frac{e}{c} v_\nu^{(r)} \left(\sum_{s \neq r} f_{\mu\nu,\,\mathrm{ret}}^{(s)} + f_{\mu\nu,\,\mathrm{ex}} \right), \qquad \ldots\ldots(22)$$

which is just the equation of motion obtained by Dirac.

Further, we notice that at the world-line of the r th electron we may put

$$F_{\mu\nu} = f_{\mu\nu,\,\mathrm{sym}}^{(r)} + F_{\mu\nu,\,\mathrm{fin}}, \qquad \ldots\ldots(23)$$

where $f_{\mu\nu,\,\mathrm{sym}}^{(r)}$ diverges quadratically and $F_{\mu\nu,\,\mathrm{fin}}$ is finite. Thus, according to (8), $T_{\mu\nu}$ may be written as

$$T_{\mu\nu} = t_{\mu\nu,\,\mathrm{sym}}^{(r)} + t_{\mu\nu,\,\mathrm{mix}} + \text{finite terms},$$

where $t_{\mu\nu,\,\mathrm{mix}}$, which contains the cross-terms of $f_{\mu\nu,\,\mathrm{sym}}^{(r)}$ and $F_{\mu\nu,\,\mathrm{fin}}$, diverges only quadratically. Hence, at the world-line of the r th electron we have

$$T'_{\mu\nu} = t_{\mu\nu,\,\mathrm{mix}} + \text{finite terms}. \qquad \ldots\ldots(24)$$

Since $T'_{\mu\nu}$ has only a singularity of the second order at the world-line of any electron, its space-integral is always finite.

§ 4. CONCLUSION

We add a few remarks about the advanced field. Though the advanced field has been in use for a long time, its meaning does not seem to be very clear. In our opinion the advanced field cannot be a measurable quantity. It is, therefore, significant to note that the advanced field enters into the present treatment in such a way that it can never be measured. For, according to (14), the force exerted by an electron on other charges placed in its field is always given by its retarded field. It may also be pointed out that though the modified energy momentum tensor involves the advanced field, this does not matter at all. For (17) satisfies the usual mathematical requirements of an energy momentum tensor, and it can be used in the usual way to calculate the amount of radiation emitted by an electron.

Finally, it should be noted that the success of the present treatment depends on the fact that at the world-line of the electron $f_{\mu\nu,\,\mathrm{rad}}$ is finite and $f_{\mu\nu,\,\mathrm{sym}}$ does not have a singularity of an order greater than two. Since these results hold even for the meson field (Majumdar and Apte 1948), this treatment is equally applicable there.

ACKNOWLEDGMENTS

I wish to express my thanks to Dr. N. Kemmer for many helpful discussions, and to Professor P. A. M. Dirac for valuable comments.

REFERENCES

Dirac, P. A. M., 1938, *Proc. Roy. Soc.* A, **167**, 148.
Fremberg, N. E., 1947, *Proc. Roy. Soc.* A, **188**, 18.
Majumdar, R. C., and Apte, A. S., 1948, *Phys. Rev.*, **74**, 538.
Wentzel, G., 1933, *Z. Phys.*, **86**, 479; 1934, *Ibid.*, **87**, 726.

On the Renormalization of Quantum Electrodynamics

By J. C. WARD
Clarendon Laboratory, Oxford

Communicated by F. E. Simon; MS. received 4th September 1950

ABSTRACT. The subtraction procedure of Dyson is modified in order to eliminate a certain difficulty in the renormalization programme, namely the so-called ' b ' divergencies. The conclusions of Dyson concerning the finiteness of the renormalized S matrix are confirmed.

It has been shown to be very probable that the divergencies which arise in quantum electrodynamics manifest themselves in unobservable mass and charge renormalization effects alone (Dyson 1949). The demonstration of this behaviour rested, however, on a correct, but hitherto unproved, hypothesis concerning the behaviour of divergencies associated with self-energy Feynman graphs, the ' b ' divergencies in Dyson terminology. By a slight change of Dyson's renormalization procedure, it is possible to avoid this difficulty, and the proof of the finiteness of the renormalized matrix is complete. We shall use the notation of Dyson, and refer the reader to his paper for the meaning of the notation used.

The difficulties referred to above arise because it is possible to regard a reducible self-energy part of a graph as constructed from irreducible components in many different ways, according as vertex parts are considered to be inserted at one vertex or the other of the irreducible second order graph, and each possible way in fact contributes separately to the resulting divergencies.

A method of avoiding the ambiguity of construction of reducible self-energy parts will therefore be explained here, which makes use of the formal identity (Ward 1950)

$$-\frac{1}{2\pi}\frac{\partial\Sigma^*}{\partial p_\mu}=\Lambda_\mu(p,p).$$

If we define $p^\lambda=p\lambda+p'(1-\lambda)$ where p' is the energy-momentum vector of a free electron then

$$\Sigma^*(p)=-2\pi\int_0^1 d\lambda(p_\mu-p_\mu')\Lambda_\mu(p^\lambda,p^\lambda)$$

where the effects of the contribution of the mass renormalization term to Σ^* have been taken into account.

$\Lambda_\mu(V^i,p^\lambda,p^\lambda)$ will now contain the infinities arising from inserted self-energy and vertex parts in the V^i as well as the divergence associated with the V^i themselves. However, there is now no overlapping of divergent parts, and the finite parts may be separated out unambiguously in sequence.

An analogous procedure may be adopted for the reduction of photon S.E. parts.

It is here necessary to define a new linearly divergent operator $\Delta_\mu(t_1,t_2)$ by the equation

$$\Delta_\mu(t_1,t_2)=\sum_{\text{all }X^i}\Delta_\mu(X^i,t_1,t_2).$$

X^i is a graph obtained from a completely unreduced photon S.E. part by insertion of an external photon line in an electron line carrying the external photon variable of the S.E. part, and $\Delta_\mu(X^i, t_1, t_2)$ the corresponding operator.†

Then $$\Pi^* = -2\pi \int_0^1 d\lambda\, t_\mu \Delta_\mu(\lambda t, \lambda t).‡$$

Again, $\Delta_\mu(\lambda t, \lambda t)$ need only be summed over the irreducible X^i, the overlapping divergencies have disappeared, and the divergencies may be removed in sequence in the usual way.

The resulting finite operators $S_{F1}, D_{F1}, \Gamma_{\mu 1}$ obtained by this process of successive approximation are defined by the way in which they reproduce themselves when substituted into the integral equations of the theory, together with infinite parts. This is represented by the equations

$$\left.\begin{aligned} S_{F1} &= S_F - 2\pi S_F \int_0^1 d\lambda (p_\mu - p_\mu')\{\Lambda_\mu(p^\lambda, p^\lambda) - \Lambda_\mu(p', p')\} S_{F1} && \ldots\ldots(1)\\ D_{F1} &= D_F - 2\pi D_F \int_0^1 d\lambda\, t_\mu \left\{\Delta_\mu(\lambda t, \lambda t) - \Delta_\mu(0,0) - (\lambda t_\sigma)\left(\frac{\partial \Delta_\mu}{\partial(\lambda t_\sigma)}\right)_0\right\} D_{F1} && \ldots\ldots(2)\\ \Gamma_{\mu 1} &= \gamma_\mu + \Lambda_\mu(p_1, p_2) - \Lambda_\mu(p', p') && \ldots\ldots(3) \end{aligned}\right\} \text{A}$$

On the other hand the divergent operators Γ_μ', S_F', D_F' reproduce themselves identically when substituted into the integral equations, as is described by the equations

$$\left.\begin{aligned} S_F' &= S_F + S_F \Sigma^* S_F' && \ldots\ldots(4)\\ D_F' &= D_F + D_F \Pi^* D_F' && \ldots\ldots(5)\\ \Gamma_\mu &= \gamma_\mu + \sum_{\text{all irreducible } V^i} \Lambda_\mu(V^i) && \ldots\ldots(6) \end{aligned}\right\} \text{B}$$

$$\Sigma^* = -2\pi \int_0^1 d\lambda (p_\mu - p_\mu') \Lambda_\mu(p^\lambda, p^\lambda)$$

$$\Pi^* = -2\pi \int_0^1 d\lambda\, t_\mu \Delta_\mu(t^\lambda, t^\lambda).$$

It is now easy to prove that

$$\left.\begin{aligned} S_F' &= Z_2 S_{F1}(e_1)\\ D_F' &= Z_3 D_{F1}(e_1)\\ \Gamma_\mu' &= Z_1^{-1} \Gamma_{\mu 1}(e_1) \end{aligned}\right\} \text{C}$$

where $e_1 = Z_1^{-1} Z_2 Z_3^{1/2} e$, provided that Z_1, Z_2 and Z_3 are suitably chosen constants. This is seen by substituting these expressions for S_F', D_F', and Γ_μ' into the set of equations B.

Notes added in proof.

† This prescription for the necessary function $\Delta_\mu(t, t)$ is correct only for photon S.E. parts having a single electron loop carrying the photon variable. This has been pointed out to the author by P. T. Matthews. Δ_μ is really to be defined by the equation $-\frac{1}{2\pi}\frac{\partial \Pi^*}{\partial t_\mu} = \Delta_\mu$, which is to be regarded as an implicit definition of Δ_μ. It will be noted that Δ_μ may occur once in the integral equations of the theory, since the definition of Δ_μ implies that it may have to be inserted at one of the irreducible graphs defining Δ_μ. Hence one has to define a new divergent function $W_\mu = 2it_\mu + \Delta_\mu$ and a corresponding finite function $W_{\mu 1} = 2it_\mu + \Delta_{\mu 1}$. It is then straightforward to prove that $W_\mu = Z_3^{-1} W_{\mu 1}(e_1)$ with the value of Z_3 given in the text.

‡ The photon self-energy $\Pi^*(0)$ has been put equal to zero.

By counting up the number of vertices and lines of the irreducible graphs which define Λ_μ and Δ_μ, one finds that

$$\Sigma^*(e_1) = -2\pi Z_1^{-1} \int_0^1 d\lambda (p_\mu - p_\mu') \Lambda_\mu(p^\lambda, p^\lambda, e_1)$$

$$\Pi^*(e_1) = -2\pi Z_1^{-1} Z_2 Z_3^{-1} \int_0^1 d\lambda\, t_\mu \Delta_\mu(\lambda t, \lambda t, e_1)$$

with the S_{F1}, D_{F1}, $\Gamma_{\mu 1}$ functions substituted into Λ_μ and Δ_μ.
Equations B therefore become :

$$\left.\begin{aligned} Z_2 S_{F1}(e_1) &= S_F - 2\pi S_F(p_\mu - p_\mu') Z_1^{-1} Z_2 \int_0^1 d\lambda \Lambda_\mu(p^\lambda, p^\lambda) d\lambda S_{F1}(e_1) \quad \ldots\ldots (4') \\ Z_3 D_{F1}(e_1) &= D_F - 2\pi D_F t_\mu Z_1^{-1} Z_2 \int_0^1 d\lambda \Delta_\mu(\lambda t, \lambda t)\, D_{F1}(e_1) \quad \ldots\ldots (5') \\ Z_1^{-1} \Gamma_{\mu 1}(e_1) &= \gamma_\mu + Z_1^{-1} \Lambda_\mu(e_1) \quad \ldots\ldots (6') \end{aligned}\right\} \text{B}'$$

These have to be identical with equations A. Equations (3) and (6′) are the same if $Z_1 \gamma_\mu = \gamma_\mu - \Lambda_\mu(p', p')$. Substituting this result into (1), one finds that (1) and (4) are the same if $Z_1 = Z_2$ and finally (2) and (5) are the same if $Z_3 = 1 + c$ where

$$c\delta_{\mu\sigma} = i \int_0^1 d\lambda\, \lambda \left(\frac{\partial \Delta_\mu}{\partial(\lambda t_\sigma)} \right)_0 . \quad \text{(Note } \Delta_\mu (0, 0) = 0 \text{ by invariance.)}$$

Hence the relations C are proved. The finiteness of the renormalized S matrix now follows in the manner indicated by Dyson.

There may of course be doubt about the validity of the formal methods of manipulating infinite quantities used above. The author believes that it is possible to construct a consistent and unambiguous calculus in this way, as long as sufficient notice is taken of the requirements of Lorentz and gauge invariance at each stage. It is to be hoped that future developments will enable us to avoid dealing with unnormalized charges and masses, and the divergencies that appear here will then find their rightful place as abstractions from physical reality, namely the charges and masses of non-interacting particles.

REFERENCES

DYSON, F. J., 1949, *Phys. Rev.*, **75**, 1736.
WARD, J. C., 1950, *Phys. Rev.*, **78**, 182.

Equations of Motion in General Relativity

By A. PAPAPETROU
I.C.I. Research Fellow, University of Manchester

Communicated by L. Rosenfeld; MS. received 20th January 1950

ABSTRACT. This paper contains a new derivation of the equations of motion of bodies moving slowly in their (weak) gravitational field, up to terms of the order $(v/c)^2$. In contrast to the method developed previously by Einstein and co-workers, in which only the field outside the bodies has been considered, in the present paper a new method is used in which the field outside as well as inside the bodies, and the internal structure of the bodies, is taken into consideration. The equations of motion derived by this new method are identical with those obtained by Einstein and co-workers, but the new method is essentially simpler and the necessary calculations much less lengthy.

§ 1.

It was proved by Einstein and Grommer (1927) that in general relativity the field equations contain the equations of motion of bodies inside the gravitational field they produce. Subsequently the problem of deriving these equations of motion from the field equations has been treated in detail, especially in the last 12 years. When one tries to survey the work done in these years one sees that two distinct methods have been used. The first is the method developed by Einstein and co-workers (1938, 1940, 1949), its characteristic feature being that all the calculations refer to the space ***outside*** the bodies, for the interior of which only the assumption of spherical symmetry is used. The second method has been introduced by Fock (1939) and, in contrast to the previous one, it also considers the gravitational field ***inside*** the material bodies.

Though far more developed than the second, the method of Einstein and co-workers is very restricted from the physical point of view, since it is only applicable to bodies with spherical symmetry. That this is a real restriction one can see immediately by considering the motion of stellar bodies. When we treat this problem according to general relativity, the first approximation confirms the results of the Newtonian theory of gravitation, while the second approximation leads to the (very small) relativistic effects. Now in the Newtonian theory the oblateness of, for example, a planet will cause a rotation of the line of apsides of a satellite. This effect is usually much larger than the similar relativistic effect (i.e. the relativistic rotation of the line of apsides, which is independent of the oblateness of the central body). Thus in this case it will be indispensable to consider the oblateness of the central body. But any departure from spherical symmetry can only be treated by considering the internal structure of the bodies in detail, which has been excluded from the very beginning in the method of Einstein and co-workers.

Besides the astronomical problem one might hope to use the equations of motion for discussing the motion of elementary particles in a gravitational field, and this seems to be the ultimate aim of Einstein and co-workers. But the only case of practical interest is the motion of photons in the gravitational field of a star; and for this case the method of these authors is entirely inadequate, since the

photon moves with the velocity $v=c$, while the method is based on the assumption $v \ll c$. A further argument might be mentioned here. The photon—and all other elementary particles—has a spin and therefore it is doubtful whether the use of a model having a spherical symmetry is justified even for a calculation in first approximation.

In contrast to this Fock considers from the very beginning the astronomical problem only, and he also includes in the discussion the internal structure of the bodies. This has the immediate consequence that the physical meaning of his calculations can be followed in detail. Additionally there is no longer any difficulty (except the more extensive calculations needed) in discussing bodies without spherical symmetry. However Fock has not reached the full efficiency of his method because he has insisted upon using the field equations alone. Thus he finds the equations of motion to the first approximation as the integrability condition of the field equations in the second approximation by actually integrating them in this approximation, that is, when—as we shall see in the following—he has calculated nearly all quantities necessary for the determination of the equations of motion in second approximation.

§ 2.

We shall show in the following that one can give to Fock's method a much more compact and effective form. We mention in anticipation that this will be possible when we use, together with the field equations, the well-known relation

$$\frac{\partial \mathfrak{T}_\mu^{\ \nu}}{\partial x^\nu} - \tfrac{1}{2}\mathfrak{T}^{\nu\sigma}\frac{\partial g_{\nu\sigma}}{\partial x^\mu} = 0, \qquad \ldots\ldots (2.1)$$

thus allowing the simultaneous calculation of $g_{\mu\nu}$ and $\mathfrak{T}_\mu^{\ \nu}$. In the following calculations this relation will play a role just as fundamental as that of the field equations. For this reason we shall give it a name (which will be justified later): we shall call it the *dynamical equation* of the theory of gravitation.

It is not difficult to see why the dynamical equation has not been used in this problem up to now. Orthodox general relativity considers $g_{\mu\nu}$ as the fundamental quantity, and this determines everything else. The field equations are considered to be well defined only for the empty space, where they are

$$R_{\mu\nu}=0. \qquad \ldots\ldots (2.2a)$$

In regions of space containing matter, i.e. where $R_{\mu\nu}\neq 0$, we put

$$R_{\mu\nu}-\tfrac{1}{2}g_{\mu\nu}R=-\kappa T_{\mu\nu} \qquad \ldots\ldots (2.2)$$

and this is then the equation of definition of $T_{\mu\nu}$, which consequently appears as an auxiliary quantity. Under these conditions the dynamical equation becomes a mere mathematical identity and this is the reason why one has tried to derive the equations of motion from the field equations only. In its extreme form this point of view has been accepted in the papers of Einstein and co-workers who refuse to allow any considerations on $T_{\mu\nu}$ and insist on deriving the equations of motion from the field equations for the empty space surrounding the material bodies (which they characteristically call singularities of the gravitational field). To a certain degree this point of view has also influenced Fock, who, at first, considers $T_{\mu\nu}$ merely to find out the general structure of $g_{\mu\nu}$; then he calculates the $g_{\mu\nu}$ independently of the $T_{\mu\nu}$, and only later does he determine $T_{\mu\nu}$ from the already calculated $g_{\mu\nu}$.

An entirely different situation arises in the more moderate interpretation of general relativity as a theory of gravitation in flat space, which has been suggested by Rosen (1940) and Papapetrou (1948). In this interpretation $g_{\mu\nu}$ is only the potential of gravitation (and no longer the metrical fundamental tensor) and consequently $T_{\mu\nu}$ will have at least an equally primary physical meaning as that of $g_{\mu\nu}$. The field equations will now be (2.2), reducing to the form (2.2*a*) in the case of empty space. Further, we must now consider equation (2.1) as an equation having a primary physical meaning and not as a mathematical identity only. A first argument for this point of view is the following. If we assume for $T_{\mu\nu}$ the form corresponding to incoherent matter,

$$\mathfrak{T}^{\mu\nu} = \rho u^{\mu} u^{\nu},$$

where $u^{\mu} = dx^{\mu}/ds$ is the four-dimensional velocity of the element of matter, then equation (2.1) leads to the conclusion that the orbits of these elements of matter are the geodesics of the field $g_{\mu\nu}$ (de Donder 1926). But this is a statement of such physical importance that one cannot understand why it should be derived from a mathematical identity without physical meaning. We shall show in the following that the use of the field equations (2.2) together with the dynamical equation (2.1) for the simultaneous calculation of $g_{\mu\nu}$ and $T_{\mu\nu}$ will provide us with an extremely effective method for determining the equations of motion; this result may be considered as a new argument in favour of the moderate interpretation of general relativity.

§ 3.

In this section we shall summarize the physical and mathematical assumptions on which the following calculations will be based.

There will be two fundamental physical assumptions. We shall consider a system of bodies whose velocities are small compared with c and assume that the gravitational field is weak; i.e. $g_{\mu\nu}$ will differ very little from the values $\eta_{\mu\nu}$ of the metrical tensor of special relativity. The difference $g_{\mu\nu} - \eta_{\mu\nu}$ will be written as a power series of a small parameter. Following Fock we formally take as parameter the quantity $1/c$.

The next physical assumption which we shall use in the following is that the mutual distances of the bodies are large compared with their dimensions; i.e. if the distances are of the order of magnitude of a length L and the dimensions of l,

$$L \gg l. \qquad \ldots\ldots (3.1)$$

This is an assumption which we introduce in order to avoid complicated calculations. The reason is obvious. Stars consist of matter in the fluid state (this being a suitable assumption even for planets, though they have a thin solid crust) and consequently, if the condition (3.1) was not fulfilled, the form of each star would depend on the relative positions of all the others; the problem of their motion would, then, become a very difficult one even in the Newtonian theory of gravitation. But when the condition (3.1) is fulfilled, the form of each star will depend only on the conditions existing on this star; and in the stationary case it will be a spheroidal one, the oblateness of the spheroid being due to the proper rotation of the star.

For a further simplification of the calculations, we shall treat the case of spherical bodies only. (The only difficulty in treating spheroidal bodies is that the calculations are more lengthy.) This will be true if the bodies have

no proper rotations; consequently the last simplification must be combined with the assumption that the motion of each body is a pure translation.

Mathematically, we first have to choose the independent variables (coordinates) and the unknown functions which we shall have to calculate. Following Fock we take as independent variables the space-coordinates x^i $(i=1, 2, 3)$ and the time $x^0=t$. As unknown functions we shall take the quantities $\mathfrak{g}^{\mu\nu}$ and $\mathfrak{T}_\nu^\mu$. Generally latin indices will take the values 1, 2, 3 only, while greek indices will take the values 1, 2, 3 and 0. A subscript comma will indicate ordinary differentiation:

$$f_{,i}\equiv\frac{\partial f}{\partial x^i}\,,\quad f_{,0}\equiv\frac{\partial f}{\partial x^0}=\frac{\partial f}{\partial t}\,.$$

We must now introduce another assumption, which according to Einstein and co-workers is merely a matter of mathematical convenience, but which in our opinion might have a deep physical meaning. We must choose the so-called *coordinate condition*, which from the mathematical point of view is necessary in order to restrict the variety of forms which a given solution of the field equations can take (because these are tensor equations). But the physical aspect is very much different: Our problem is to derive equations of motion from general relativity, and to express them in terms of space and time of Newtonian mechanics. Obviously not every frame will be suitable for this purpose; the coordinate condition will have to exclude the unsuitable frames, or, in other words, to determine what we might call the inertial frames in general relativity. One must expect that the choice of this condition will influence the equations of motion, at least in the higher approximations.*

In this paper we shall accept the coordinate condition used by Fock:

$$\mathfrak{g}^{\mu\nu}{}_{,\nu}=0, \qquad \ldots\ldots(3.2)$$

which has several remarkable properties (see Papapetrou 1948). It is worth stressing that by using (3.2) we shall in the second approximation arrive at the same equations of motion as Einstein and co-workers did, though these authors have used a different coordinate condition. The reason for this coincidence and the deeper meaning of the coordinate condition should be discussed in more detail, since there seems to be an important problem behind them. If the equations of motion in second approximation really depend on the coordinate condition, then the observational data will give support to some special coordinate condition; but such a result would be a decisive argument in favour of the interpretation of general relativity as a theory of gravitation in flat space.

§ 4.

Before starting our calculations we still have to express the field equations and the dynamical equation in terms of $\mathfrak{g}^{\mu\nu}$ and $\mathfrak{T}_\nu^\mu$; additionally in the field equations we have to consider the condition (3.2). We shall not repeat here the calculations necessary for the transformation of the field equations, but we take the final

* In a recent paper Einstein and Infeld (1949) have tried to prove that in the second approximation the equations of motion are independent of the choice of the coordinate condition. But their proof extends only to a special class of coordinate conditions; the initial condition being given by their equation (9.8),

$$\gamma_{00,0}-\gamma_{0n,n}=0, \qquad \gamma_{mn,n}=0,$$

they keep it unchanged in the first approximation, allowing a change of this condition only in the second approximation. However, the important question is what will happen to the equations of motion in the second approximation if we change the coordinate condition for the first-order terms.

formulae from Fock.* With a slight difference in the notation $\mathfrak{g}^{\mu\nu}$ will in second approximation be of the form

$$\left.\begin{aligned}\mathfrak{g}^{00} &= \frac{1}{c} + \frac{4U^{00}}{c^3} + \frac{4S^{00}}{c^5} + \dots,\\ \mathfrak{g}^{0i} &= \frac{4U^{0i}}{c^3} + \frac{4S^{0i}}{c^5} + \dots,\\ \mathfrak{g}^{ik} &= -c\delta_i^{\,k} + \frac{4S^{ik}}{c^3} + \dots.\end{aligned}\right\} \quad \dots\dots(4.1)$$

The field equations up to terms proportional to $1/c^3$ are

$$\left.\begin{aligned}-\kappa\mathfrak{T}_0^{\,0} &= \frac{2}{c}\Delta U^{00} + \frac{2}{c^3}\Delta S^{00} - \frac{2}{c^3}U^{00}{}_{,00} - \frac{7}{c^3}U^{00}{}_{,l}U^{00}{}_{,l} - \frac{8}{c^3}U^{00}\Delta U^{00},\\ -\kappa\mathfrak{T}_0^{\,k} &= \frac{2}{c}\Delta U^{0k} + \frac{2}{c^3}\Delta S^{0k} - \frac{2}{c^3}U^{0k}{}_{,00} + \frac{6}{c^3}U^{00}{}_{,0}U^{00}{}_{,k}\\ &\quad - \frac{8}{c^3}(U^{0k}{}_{,s} - U^{0s}{}_{,k})U^{00}{}_{,s} - \frac{8}{c^3}U^{00}\Delta U^{0k},\\ -\kappa\mathfrak{T}_i^{\,0} &= -\frac{2}{c^3}\Delta U^{0i},\\ -\kappa\mathfrak{T}_i^{\,k} &= -\frac{2}{c^3}\Delta S^{ik} - \frac{2}{c^3}U^{00}{}_{,i}U^{00}{}_{,k} + \delta_i^{\,k}\frac{1}{c^3}U^{00}{}_{,l}U^{00}{}_{,l}\end{aligned}\right\} \quad (4.2)$$

with $\kappa = 8\pi G/c^2$. (G is Newton's gravitational constant.) These are the only results which we shall take over from Fock; all other calculations necessary for the derivation of the equations of motion will be given in this paper.

It will be more convenient to express the dynamical equation in terms of $\mathfrak{g}^{\mu\nu}$ and $\mathfrak{g}_{\mu\nu}$. A simple transformation of (2, 1) gives

$$\mathfrak{T}^{\nu}{}_{\mu,\nu} = \tfrac{1}{2}\mathfrak{T}_{\varrho}{}^{\sigma}\mathfrak{g}^{\varrho\tau}\frac{1}{\{\sqrt{(-g)}\}^2}\mathfrak{g}_{\sigma\tau,\mu} - \tfrac{1}{2}\mathfrak{T}_{\sigma}{}^{\sigma}\frac{1}{\sqrt{(-g)}}\{\sqrt{(-g)}\}_{,\mu}. \quad (4.3)$$

The quantities $\mathfrak{g}_{\mu\nu}$ and $\sqrt{-g}$ can be found by straightforward calculation from (4.1) and are

$$\left.\begin{aligned}\mathfrak{g}_{00} &= c^2 - \frac{4S^{ll}}{c},\\ \mathfrak{g}_{0i} &= \frac{4U^{0i}}{c} + \frac{4S^{0i}}{c^3},\\ \mathfrak{g}_{ik} &= -\delta_i^{\,k}c\left(1 + \frac{4U^{00}}{c^2} + \frac{4S^{00} - 4S^{ll}}{c^4}\right) - \frac{4S^{ik}}{c^3};\end{aligned}\right\} \quad \dots\dots(4.4)$$

$$\sqrt{(-g)} = c\left[1 + \frac{2U^{00}}{c^2} + \frac{2}{c^4}(S^{00} - S^{ll} - (U^{00})^2)\right]. \quad \dots\dots(4.5)$$

It is convenient for the following to write equation (4.3) separately for $\mu = 0$ and $\mu = i$:

$$\mathfrak{T}_0^{\,k}{}_{,k} + \mathfrak{T}_0^{\,0}{}_{,0} = \tfrac{1}{2}\mathfrak{T}_{\varrho}{}^{\sigma}\mathfrak{g}^{\varrho\sigma}\frac{1}{\{\sqrt{(-g)}\}^2}\mathfrak{g}_{\sigma\tau,0} - \tfrac{1}{2}\mathfrak{T}_{\sigma}{}^{\sigma}\frac{1}{\sqrt{(-g)}}\{\sqrt{(-g)}\}_{,0}, \quad \dots\dots(4.6)$$

$$\mathfrak{T}_i^{\,k}{}_{,k} + \mathfrak{T}_i^{\,0}{}_{,0} = \tfrac{1}{2}\mathfrak{T}_{\varrho}{}^{\sigma}\mathfrak{g}^{\varrho\sigma}\frac{1}{\{\sqrt{(-g)}\}^2}\mathfrak{g}_{\sigma\tau,i} - \tfrac{1}{2}\mathfrak{T}_{\sigma}{}^{\sigma}\frac{1}{\sqrt{(-g)}}\{\sqrt{(-g)}\}_{,i}. \quad \dots\dots(4.7)$$

* For those readers who are unable to see Fock's paper we summarize the main steps of these calculations in Appendix I.

Following Fock we shall denote the different bodies by $a, b, \ldots$ (at the same time avoiding the use of these letters as tensor indices). If we integrate (4.7) over the volume of the body a, the term $\mathfrak{T}_i^k{}_{,k}$ drops out (since $\mathfrak{T}_\nu^\mu = 0$ outside the body) and we get

$$\frac{d}{dt}\int_a \mathfrak{T}_i^0 dV = \int_a \tfrac{1}{2}\mathfrak{T}_\varrho^\sigma \mathfrak{g}^{\varrho\tau}\frac{1}{\{\sqrt{(-g)}\}^2}\mathfrak{g}_{\sigma\tau,i}dV - \int_a \tfrac{1}{2}\mathfrak{T}_\sigma^\sigma \frac{1}{\sqrt{(-g)}}\{\sqrt{(-g)}\}_{,i}dV. \qquad \ldots\ldots(4.8)$$

We shall see in the next section an essential difference in the usefulness of (4.7) and (4.8).

We stress that, contrary to the method of Einstein and co-workers, in which the field equations are separated into equations for each approximation step—thus making conditions of integrability necessary for each step—in our calculations for the solution of the equations in the lth approximation we shall take all terms of order $l' \leqslant l$. No conditions of integrability will be needed since the equations will be integrated directly.

§ 5.

We shall first derive the equations of motion to the first approximation. This will show the efficiency of our method, and at the same time it will give us some quantities which we shall use later. We start by writing down the leading terms in the expressions of $\mathfrak{T}_\nu^\mu$ which we take to be of the same form as the components $\mathfrak{T}_\nu^\mu$ of a perfect fluid in special relativity:

$$\left.\begin{aligned} &\mathfrak{T}_0^0 = \rho c^2,\\ &\mathfrak{T}_0^k = \rho c v^k,\\ &\mathfrak{T}_i^0 = -\frac{\rho}{c}v^i,\\ &\mathfrak{T}_i^k = -\frac{\rho}{c}v^i v^k - \frac{1}{c}\delta_i^k p; \end{aligned}\right\} \qquad \ldots\ldots(5.1)$$

v^i is the (3-dimensional) velocity of the fluid at the point which we are considering. Since our system consists of a number of discrete bodies, the mass density ρ will be of the form

$$\rho = \sum_a \rho_a, \qquad \ldots\ldots(5.2)$$

with $\rho_a \neq 0$ only inside the body a. Because of the spherical symmetry of the body a the density ρ_a at the point $\mathbf{r}$ (coordinates x^i) will be a function of the distance r_a between this point and the centre $\mathbf{a}$ (coordinates a^i) of the body a:

$$\rho_a(\mathbf{r}) \equiv \rho_a(r_a) \quad (r_a = |\mathbf{r}-\mathbf{a}|). \qquad \ldots\ldots(5.3)$$

If l_a denotes the radius of the body a, then $\rho_a = 0$ for $r_a > l_a$.

Since the motion of each body is a pure translation, the velocity of any element of the body a will be equal to the velocity of its centre:

$$\text{inside } a \qquad v^i = \dot{a}^i \equiv \frac{da^i}{dt}. \qquad \ldots\ldots(5.4)$$

It follows that

$$v^i{}_{,k} = 0 \quad (v^i{}_{,0} = \dot{v}^i). \qquad \ldots\ldots(5.5)$$

The pressure p will again be of the form

$$p = \sum_a p_a. \qquad \ldots\ldots(5.6)$$

The partial pressure[1] p_a will be determined from the dynamical equation (4.7) together with the equations of motion. Using (5.2), (5.4) and (5.6) we can put (5.1) into the form

$$\left.\begin{aligned} \mathfrak{T}_0{}^0 &= \sum_a \rho_a c, \\ \mathfrak{T}_0{}^k &= \sum_a \rho_a c \dot{a}^k, \\ \mathfrak{T}_i{}^0 &= -\sum_a \frac{1}{c}\rho_a \dot{a}^i, \\ \mathfrak{T}_i{}^k &= -\sum_a \frac{1}{c}\rho_a \dot{a}^i \dot{a}^k - \delta_i{}^k \sum_a \frac{1}{c} p_a. \end{aligned}\right\} \qquad \ldots\ldots(5.7)$$

We now write down equation (4.6) for a point inside the body a; retaining only terms of order $1/c$ we obtain

$$(\rho_a c \dot{a}^k)_{,k} + (\rho_a c)_{,0} = 0. \qquad \ldots\ldots(5.8)$$

Since for any function $f(x^i)$ it is

$$f_{,k} v^k + f_{,0} \equiv \frac{\partial f}{\partial x^k}\frac{dx^k}{dt} + \frac{\partial f}{\partial t} = \frac{df}{dt}, \qquad \ldots\ldots(5.9)$$

we can write (5.8) in the form $\qquad \dfrac{d\rho_a}{dt} = 0\,; \qquad \ldots\ldots(5.10)$

i.e. in this approximation the mass density ρ_a is constant in time. We then apply equation (4.7), now retaining only terms of order $1/c$ (there are no terms of order c in this equation). The result is

$$-\frac{1}{c}\frac{d}{dt}(\rho_a \dot{a}^i) - \frac{1}{c} p_{a,i} = -\frac{1}{c}\rho_a U^{00}{}_{,i}. \qquad \ldots\ldots(5.11)$$

We see that this relation contains the quantity U^{00}. This quantity together with U^{0k} (which is not necessary for the present calculation, but will be needed later) can be calculated from the first two of the equations (4.2). Taking these equations with the first order terms only and considering (5.1) we get

$$\left.\begin{aligned} \Delta U^{00} &= -4\pi G\rho, \\ \Delta U^{0k} &= -4\pi G\rho v^k. \end{aligned}\right\} \qquad \ldots\ldots(5.12)$$

Because of (5.2) and (5.4) the solutions of these equations are

$$\left.\begin{aligned} U^{00} &= \sum_a u_a, \\ U^{0k} &= \sum_a u_a \dot{a}^k, \end{aligned}\right\} \qquad \ldots\ldots(5.13)$$

with u_a fulfilling the equation $\qquad \Delta u_a = -4\pi G\rho_a \qquad \ldots\ldots(5.14)$

and being therefore the Newtonian potential of the body a. Using (5.10) and (5.13) we can write equation (5.11) in the form

$$\rho_a \ddot{a}^i + p_{a,i} = \rho_a \Big(\sum_b u_{b,i} + u_{a,i}\Big), \qquad \ldots\ldots(5.15)$$

the notation $\sum_b$ meaning summation over all bodies *except* the body a. (But $\sum_a$ will mean summation over all bodies. This convention will be used throughout this paper.)

Equation (5.15) can be split in two if we notice that $u_{b,i}$ is very nearly constant inside the body a because of the assumption (3.1). These two equations will be

$$\ddot{a}^i = \sum_b (u_{b,i})_a, \qquad \ldots\ldots (5.16)$$

$$p_{a,i} = \rho_a u_{a,i}; \qquad \ldots\ldots (5.17)$$

the suffix a outside a bracket will denote the value of the quantity inside the bracket at the centre of the body a:

$$(f)_a \equiv \text{value of } f \text{ at } \mathbf{a}. \qquad \ldots\ldots (5.18)$$

We see that equations (5.16) are the equations of motion to the first approximation —identical with the corresponding Newtonian equations—while (5.17) is a condition determining p_a. Since p_a will be a function of r_a, we can write (5.17) also in the form

$$p_a' = \rho_a u_a', \qquad \ldots\ldots (5.19)$$

the accent meaning derivation with respect to r_a:

$$[f(r_a)]' \equiv \frac{df}{dr_a}. \qquad \ldots\ldots (5.20)$$

Equation (5.19) is again identical with the corresponding Newtonian equation.

Another way of arriving at the equations of motion (5.16) is to use equation (4.8), or, equivalently, to integrate (5.15) over the volume of the body a. The term $p_{a,i}$ makes no contribution because $p_a = 0$ outside the body, and again the integral of $\rho_a u_{a,i}$ will be zero since $u_{a,i} = u_a'(x^i - a^i)/r_a$. We therefore find

$$m_a \ddot{a}^i = \int_a \rho_a \sum_b u_{b,i} dV = m_a \sum_b (u_{b,i})_a,$$

with

$$m_a = \int_a \rho_a dV; \qquad \ldots\ldots (5.21)$$

i.e. the equations of motion (5.16). We now see the difference between equations (4.7) and (4.8). The latter gives the equations of motion alone, while the former gives an additional condition determining $\mathfrak{T}_i^k$ in the approximation which we are considering. We shall make use of this remark in the following calculations. In the second approximation we shall only be interested in the equations of motion and consequently it will be sufficient to use equation (4.8). (We had to make use of the full equation (4.7) in the first approximation, since the quantity p_a will enter in the second order terms of $\mathfrak{T}_0^k$.)

§ 6.

For the derivation of the equations of motion to a second approximation we shall have to follow a step further the procedure outlined in the previous section: calculate $\mathfrak{T}_r^\mu$ and $\mathfrak{g}^{\mu\nu}$ and then apply equation (4.8). Not all the second order terms in $\mathfrak{T}_r^\mu$ and $\mathfrak{g}^{\mu\nu}$ will be needed in this calculation (as in the calculation of the previous section, where only some of the first order terms were used). What is really necessary will be seen when we write equation (4.8) up to terms of order $1/c^3$. Anticipating equation (8.1) we state here that the following quantities will be

needed: (i) from $\mathfrak{T}_\nu^\mu$ the quantities $\mathfrak{T}_0^0$, $\mathfrak{T}_0^k$ and $\mathfrak{T}_i^k$ up to terms of order $1/c$, and the quantity $\mathfrak{T}_i^0$ up to terms of order $1/c^3$; (ii) from $\mathfrak{g}^{\mu\nu}$ the quantities U^{00} and U^{0k} already determined in the previous section and additionally the quantities S^{ii} and S^{00}.

We start with the calculation of $\mathfrak{T}_\nu^\mu$. For $\mathfrak{T}_0^0$ we provisionally keep the previous expression

$$\mathfrak{T}_0^0 = \rho c \qquad \ldots\ldots (6.1)$$

including in ρ terms of first and second order. In $\mathfrak{T}_0^k$ we introduce an additional second order term depending on the pressure p, identical with what we should have for a moving perfect fluid in special relativity :

$$\mathfrak{T}_0^k = \rho c v^k + \frac{1}{c} p v^k. \qquad \ldots\ldots (6.2)$$

The leading terms in $\mathfrak{T}_i^0$ and $\mathfrak{T}_i^k$ will be the same as in (5.1) but with the first order term of ρ instead of the total ρ. The second order terms in $\mathfrak{T}_i^0$ will be determined later.

We first derive an interesting relation which is valid for bodies undergoing arbitrary deformations. For this purpose we combine (4.6) and (4.7) after multiplying the second by v^i. Taking in account (5.9) we find

$$(v^i \mathfrak{T}_i^k + \mathfrak{T}_0^k)_{,k} + (v^i \mathfrak{T}_i^0 + \mathfrak{T}_0^0)_{,0} - v^i{}_{,k} \mathfrak{T}_i^k - v^i{}_{,0} \mathfrak{T}_i^0$$
$$= \tfrac{1}{2} \mathfrak{T}_\varrho{}^\sigma \mathfrak{g}^{\varrho\sigma} \frac{1}{\{\sqrt{(-g)}\}^2} \frac{d\mathfrak{g}_{\sigma\tau}}{dt} - \tfrac{1}{2} \mathfrak{T}_\sigma{}^\sigma \frac{1}{\sqrt{(-g)}} \frac{d\sqrt{(-g)}}{dt}. \qquad \ldots\ldots (6.3)$$

Introducing in this relation the values of $\mathfrak{T}_\nu^\mu$ and $\mathfrak{g}^{\mu\nu}$ and retaining terms up to the order $1/c$ we get (with $v^2 = v^i v^i$)

$$c \frac{d\rho}{dt} + \rho c v^k{}_{,k} - \frac{1}{c} \frac{d}{dt} (\rho v^2) - \frac{1}{c} \rho v^2 v^k{}_{,k} + \frac{1}{c} \rho v^i \frac{dv^i}{dt} + \frac{1}{c} p v^k{}_{,k} + \frac{1}{c} \rho \frac{dU^{00}}{dt} = 0.$$
$$\ldots\ldots (6.4)$$

We now consider the volume element δV containing a given mass element $\rho \delta V$. After a time interval dt this mass element will occupy a volume $\delta V + (d/dt)(\delta V) dt$. The derivative $(d/dt)(\delta V)$ can be calculated easily and is

$$\frac{d}{dt} (\delta V) = \delta V . \operatorname{div} \mathbf{v} \equiv \delta V v^k{}_{,k}. \qquad \ldots\ldots (6.5)$$

If therefore we multiply (6.4) by δV we find

$$\frac{d}{dt} (\rho \delta V) - \frac{d}{dt} \left(\rho \delta V \frac{v^2}{c^2} \right) + \tfrac{1}{2} \rho \delta V \frac{d}{dt} \left(\frac{v^2}{c^2} \right) + \rho \delta V \frac{d}{dt} \left(\frac{U^{00}}{c^2} \right) + \frac{1}{c^2} p \frac{d}{dt} (\delta V) = 0.$$

According to this equation the quantity $(d/dt)(\rho \delta V)$ is of a higher order and consequently we can put $(d/dt)(\rho \delta V) = 0$ in the second order terms. We thus get

$$\frac{d}{dt} \left[\rho \delta V \left(1 - \frac{v^2}{2c^2} + \frac{U^{00}}{c^2} \right) \right] + \frac{1}{c^2} p \frac{d}{dt} (\delta V) = 0, \qquad \ldots\ldots (6.6)$$

a relation which is valid for arbitrarily large deformations, as for example those encountered in pulsating stars.

In our case we have only translational motion for which $(d/dt)(\delta V)=0$. Equation (6.6) becomes therefore, if we consider the interior of the body a (with $v_a^2=\dot{a}^i\dot{a}^i$)

$$\frac{d}{dt}\left[\rho_a\left(1-\frac{v_a^2}{2c^2}+\frac{U^{00}}{c^2}\right)\right]=0.$$

This relation can be written in the form

$$\rho_a\left(1-\frac{v_a^2}{2c^2}+\frac{U^{00}}{c^2}\right)=\rho_a^* \qquad \ldots\ldots(6.7)$$

with $d\rho_a^*/dt=0$. For reasons which will become evident later it is more convenient to introduce another quantity ρ_a^+ by the relation

$$\rho_a^*=\rho_a^+\left(1+\frac{u_a}{2c^2}\right). \qquad \ldots\ldots(6.8)$$

Since the Newtonian potential u_a is also constant in time, $du_a/dt=0$, we shall have $d\rho_a^+/dt=0$. It follows from (6.7) and (6.8)

$$\rho_a=\rho_a^+\left(1+\frac{v_a^2}{2c^2}-\frac{U^{00}}{c^2}+\frac{u_a}{2c^2}\right). \qquad \ldots\ldots(6.9)$$

In all the following calculations we shall use the quantity ρ_a^+ only. We can therefore omit the cross and write instead of (6.1) and (6.2)

$$\left.\begin{aligned}\mathfrak{T}_0^{\,0}&=\sum_a\rho_a c\left(1+\frac{v_a^2}{2c^2}-\frac{U^{00}}{c^2}+\frac{u_a}{2c^2}\right),\\ \mathfrak{T}_0^{\,k}&=\sum_a\rho_a c\dot{a}^k\left(1+\frac{v_a^2}{2c^2}-\frac{U^{00}}{c^2}+\frac{u_a}{2c^2}\right)+\sum_a\frac{1}{c}p_a\dot{a}^k,\end{aligned}\right\} \qquad \ldots\ldots(6.10)$$

with

$$\frac{d\rho_a}{dt}=0. \qquad \ldots\ldots(6.11)$$

In agreement with (5.7) and (5.10) we shall consider ρ_a as the first order term in the expression for the mass density. Thus equations (6.10) give $\mathfrak{T}_0^{\,0}$ and $\mathfrak{T}_0^{\,k}$ separated in their first and second order parts.

Since $\mathfrak{T}_i^{\,k}$ is needed up to terms of order $1/c$ only, it will have the same value as in (5.7):

$$\mathfrak{T}_i^{\,k}=-\sum_a\frac{1}{c}\rho_a\dot{a}^i\dot{a}^k-\frac{1}{c}\delta_i^{\,k}\sum_a p_a. \qquad \ldots\ldots(6.12)$$

Finally we have to calculate $\mathfrak{T}_i^{\,0}$ up to terms of order $1/c^3$. This can be done by using (6.10) as follows. It is

$$\mathfrak{T}_i^{\,0}=\frac{1}{\{\sqrt{(-g)}\}^2}\mathfrak{g}^{0\mu}\mathfrak{g}_{i\nu}\mathfrak{T}_\mu^{\,\nu}=\frac{1}{\{\sqrt{(-g)}\}^2}(\mathfrak{g}^{00}\mathfrak{g}_{i0}\mathfrak{T}_0^{\,0}+\mathfrak{g}^{0k}\mathfrak{g}_{i0}\mathfrak{T}_k^{\,0}+\mathfrak{g}^{00}\mathfrak{g}_{ik}\mathfrak{T}_0^{\,k}+\mathfrak{g}^{0k}\mathfrak{g}_{il}\mathfrak{T}_k^{\,l}).$$

Using (4.1) and (4.4) we see that the second and fourth term in the bracket do not give any terms of order $1/c^3$; taking into account (6.10) and (4.5) we finally find

$$\mathfrak{T}_i^{\,0}=-\frac{1}{c^2}\mathfrak{T}_0^{\,i}-\frac{4}{c^3}\sum_a\sum_b\rho_a u_b(\dot{a}^i-\dot{b}^i). \qquad \ldots\ldots(6.13)$$

This formula displays a very interesting feature, expressed by its last term. Inside the body a the momentum density $\mathfrak{T}_l^0$ has terms proportional to the relative velocity of the body a against each one of the other bodies.

We notice that the values of $\mathfrak{T}_\nu^\mu$ given by (6.10), (6.12) and (6.13) are identical with those following from the values $T^{\mu\nu}$ given by Fock.

§ 7.

The next step is the calculation of S^{ll} and S^{00}. From the last of equations (4.2) we find†

$$\Delta S^{ll} = \frac{\kappa c^3}{2}\,\mathfrak{T}_l^l + \tfrac{1}{2}U^{00}{}_{,l}U^{00}{}_{,l}. \qquad \ldots\ldots(7.1)$$

$\mathfrak{T}_l^l$ is to be calculated from (6.12), while for U^{00} as well as for U^{0k} we have to retain the values (5.13). By taking into account the relation

$$U^{00}{}_{,l}U^{00}{}_{,l} = \tfrac{1}{2}\Delta(U^{00})^2 - U^{00}\Delta U^{00}, \qquad \ldots\ldots(7.2)$$

we can write (7.1) in the form

$$\Delta S^{ll} = \Delta[\tfrac{1}{4}(U^{00})^2 + \sum_a u_a v_a^2] - 4\pi G\sum_a(3p_a - \tfrac{1}{2}\rho_a u_a) + 2\pi G\sum_a \rho_a \sum_b u_b. \qquad \ldots\ldots(7.3)$$

The solution of this equation will be

$$S^{ll} = \tfrac{1}{4}(U^{00})^2 + \sum_a (u_a v_a^2 + s_a + W_a) \qquad \ldots\ldots(7.4)$$

with

$$\Delta s_a = -4\pi G(3p_a - \tfrac{1}{2}\rho_a u_a) \qquad \ldots\ldots(7.5)$$

and

$$\Delta W_a = 2\pi G\rho_a \sum_b u_b. \qquad \ldots\ldots(7.6)$$

We first notice that the quantity s_a has the property that it is a function of r_a which vanishes outside the body a:

$$s_a = 0 \text{ outside the body } a. \qquad \ldots\ldots(7.7)$$

This is so because, as shown in Appendix II, the following relation holds:

$$\epsilon_a \equiv \tfrac{1}{2}\int_a \rho_a u_a dV = 3\int_a p_a dV. \qquad \ldots\ldots(7.8)$$

Because of this property s_a will play no part in the final calculations, as we shall see in the next section. This is also the reason for the introduction of $\rho_a{}^+$ instead of $\rho_a{}^*$ in the previous section: if we retained $\rho_a{}^*$ we should now have a more complicated function s_a.

† One might wonder whether, after having determined the quantities $\mathfrak{g}^{\mu\nu}$ from $\mathfrak{T}_\nu^\mu$ by means of the field equations, the coordinate condition (3.2) would be satisfied automatically. It is easy to see that this will be true in our case. Combining equation (4.2) and taking into account the values $\mathfrak{T}_\nu^\mu$ already determined, we find (neglecting terms of higher order)

$$\Delta(U^{0i}{}_{,0} + S^{ik}{}_{,k}) = 0,$$

$$\Delta\Big[U^{00}{}_{,0} + U^{0k}{}_{,k} + \frac{1}{c^3}(S^{00}{}_{,0} + S^{0k}{}_{,k})\Big] = 0.$$

In contrast to the calculations of Einstein and co-workers, the equation $\Delta A = 0$ leads to the conclusion $A = 0$, since we are considering only continuously distributed sources (no point singularities). Therefore the above equations, together with (4.1), give $\mathfrak{g}^{i\alpha}{}_{,\alpha} = 0$ (up to terms of order $1/c^3$), $\mathfrak{g}^{\alpha}{}_{,\alpha} = 0$ (up to terms of order $1/c^5$).

In order to calculate W_a we develop u_b in power series around the point a_i:

$$u_b=(u_b)_a+(u_{b,k})_a(x^k-a^k)+\ldots, \qquad \ldots\ldots(7.9)$$

the omitted terms being of no importance in this approximation because of the assumption (3.1). We now get

$$W_a=-\tfrac{1}{2}u_a\sum_b(u_b)_a-\tfrac{1}{2}(x^k-a^k)w_a\sum_b(u_{b,k})_a, \qquad \ldots\ldots(7.10)$$

the new function $w_a=w_a(r_a)$ fulfilling the equation

$$w_a''+\frac{4}{r_a}w_a'=-4\pi G\rho_a.$$

The solution of this equation which fulfils the boundary condition is

$$w_a=\frac{4\pi G}{3}\left(\frac{1}{r_a^3}\int_0^{r_a}\rho_a r_a^4\,dr_a+\int_{r_a}^{\infty}\rho_a r_a\,dr_a\right). \qquad \ldots\ldots(7.11)$$

We finally write equation (7.4) in the form

$$S^{ll}=\tfrac{1}{4}(U^{00})^2+\sum_a\left[u_a v_a^2-\tfrac{1}{2}u_a\sum_b(u_b)_a+s_a-\tfrac{1}{2}(x^k-a^k)w_a\sum_b(u_{b,k})_a\right]. \qquad \ldots\ldots(7.12)$$

For S^{00} we find from the first equation (4.2)

$$\Delta S^{00}=-\frac{\kappa c^3}{2}\mathfrak{t}_0{}^0-c^2\Delta U^{00}+U^{00}{}_{,00}+\frac{7}{2}U^{00}{}_{,l}U^{00}{}_{,l}+4U^{00}\Delta U^{00}. \qquad \ldots\ldots(7.13)$$

Taking in account (6.10), (5.13), (5.14) and (7.2) we write this equation in the form

$$\Delta S^{00}=-2\pi G\sum_a\rho_a(v_a^2-\sum_b u_b)+\frac{7}{4}\Delta(U^{00})^2+\sum_a u_{a,00}. \qquad \ldots\ldots(7.14)$$

The solution of this equation will be, if we remember (7.6) and (7.10),

$$S^{00}=\frac{7}{4}(U^{00})^2+\sum_a\left[\tfrac{1}{2}u_a v_a^2-\tfrac{1}{2}u_a\sum_b(u_b)_a-\tfrac{1}{2}(x^i-a^i)w_a\sum_b(u_{b,i})_a+F_a\right], \qquad \ldots\ldots(7.15)$$

with

$$\Delta F_a=u_{a,00}. \qquad \ldots\ldots(7.16)$$

We still have to determine F_a. A straightforward calculation gives

$$u_{a,00}=\frac{1}{r_a}\left(\frac{u'_a}{r_a}\right)'(x^i-a^i)(x^k-a^k)\dot{a}^i\dot{a}^k-\frac{u'_a}{r_a}(x^i-a^i)\ddot{a}^i+\frac{u'_a}{r_a}\dot{a}^i\dot{a}^i. \qquad \ldots\ldots(7.17)$$

This suggests putting

$$F_a=(x^i-a^i)(x^k-a^k)\dot{a}^i\dot{a}^k f_a(r_a)+(x^i-a^i)\ddot{a}^i\phi_a(r_a)+\dot{a}^i\dot{a}^i v_a(r_a). \qquad \ldots\ldots(7.18)$$

For the functions f_a, ϕ_a and v_a we then get the equations

$$\left.\begin{aligned} f_a''+\frac{6}{r_a}f_a'&=\frac{1}{r_a}\left(\frac{u'_a}{r_a}\right),\\ \phi_a''+\frac{4}{r_a}\phi_a'&=-\frac{u'_a}{r_a},\\ v''_a+\frac{2}{r_a}v_a'+2f_a&=\frac{u'_a}{r_a}. \end{aligned}\right\} \qquad \ldots\ldots(7.19)$$

The solutions of these equations are

$$\left.\begin{aligned} f_a &= \frac{u_a}{r_a^2} - \frac{3}{r_a^5}\int_0^{r_a} u_a r_a^2\, dr_a, \\ \phi_a &= -v_a = -\frac{1}{r_a^3}\int_0^{r_a} u_a r_a^2\, dr_a. \end{aligned}\right\} \quad \ldots\ldots(7.20)$$

In addition we shall need the value of F_a outside and at large distances from the body a. One can easily see that for this purpose in the integrals of (7.20) it is sufficient to use the value of u_a outside the body a, even for the part of this integral referring to the interior of the body. Since this value is

$$u_a = G\frac{m_a}{r_a}, \quad \ldots\ldots(7.21)$$

we find, after some simple calculations,

$$F_a = \tfrac{1}{2}Gm_a\left(\dot{a}^k\dot{a}^l\frac{\partial^2 r_a}{\partial x^k \partial x^l} - \ddot{a}^k\frac{\partial r_a}{\partial x^k}\right) \quad \text{for} \quad r_a \gg l_a. \quad \ldots\ldots(7.22)$$

In the final calculations we shall have to use the quantity $S^{II} + S^{00} - 2(U^{00})^2$. We find from (7.12) and (7.15)

$$S^{II} + S^{00} - 2(U^{00})^2 = \sum_a \left[\tfrac{3}{2}u_a v_a^2 - u_a U_a + s_a + F_a - (x^i - a^i)w_a U_{ai}\right] \quad \ldots\ldots(7.23)$$

with the additional notation

$$U_a = \sum_b (u_b)_a, \quad U_{ai} = \sum_b (u_{b,i})_a. \quad \ldots\ldots(7.24)$$

§ 8.

The final step for the derivation of the equations of motion in second approximation is the application of equation (4.8), now up to terms of order $1/c^3$. Taking in account (4.1), (4.4) and (4.5) we find

$$\frac{d}{dt}\int_a \mathfrak{T}_i^0 dV = \int_a \frac{dV}{c^2}\left[(\mathfrak{T}_i^l - \mathfrak{T}_0^0)U^{00}{}_{,l} + \frac{4}{c^2}\mathfrak{T}_0^k U^{0k}{}_{,i} - \frac{1}{c^2}\mathfrak{T}_0^0\{S^{II} + S^{00} - 2(U^{00})^2\}_{,i}\right], \quad \ldots\ldots(8.1)$$

where in the last two terms of the right-hand side we have to take $\mathfrak{T}_0^k$ and $\mathfrak{T}_0^0$ in first order only (since the contribution of the second order terms will be of order $1/c^5$).

The calculation of the integral on the left-hand side is straightforward. Considering the value of $\mathfrak{T}_i^0$ given by (6.13) and (6.10) we find

$$\int_a \mathfrak{T}_i^0 dV = -\frac{m_a}{c}\left[\dot{a}^i + \dot{a}^i\frac{v_a^2}{2c^2} + 3\dot{a}^i\frac{U_a}{c^2} - \frac{4}{c^2}\sum_b \dot{b}^i(u_b)_a\right] + \frac{2}{3c^3}\epsilon_a\dot{a}^i \quad \ldots\ldots(8.2)$$

with m_a and ϵ_a defined by (5.21) and (7.8).

The first integral on the right-hand side of (8.1) is, according to (6.10), (6.12) and (5.13),

$$\int_a \frac{dV}{c^2}(\mathfrak{T}_i^l - \mathfrak{T}_0^0)U^{00}{}_{,l} = -\int_a dV\left[\frac{\rho_a}{c}\left(1 + \frac{3}{2}\frac{v_a^2}{c^2} + \frac{u_a}{2c^2} - \frac{U^{00}}{c^2}\right) + 3\frac{p_a}{c^2}\right] \times (u_{a,i} + \sum_b u_{b,i}). \quad \ldots\ldots(8.3)$$

Since for any function $f(r_a)$ it will be

$$\int_a f u_{a,i}\,dV = \int_a f u_a' \frac{x^i - a^i}{r_a}\,dV = 0, \qquad \ldots\ldots(8.4)$$

while on the other hand we can in this approximation replace $u_{b,i}$ by $(u_{b,i})_a$, we get from (8.3)

$$\int_a \frac{dV}{c^2}(\mathfrak{T}_l^l - \mathfrak{T}_0^0)U^{00}{}_{,i} = \frac{1}{c^3}\int_a dV \rho_a u_{a,i} \sum_b u_b - \sum_b (u_{b,i})_a \int_a dV\left[\frac{\rho_a}{c}\left(1 + \frac{3}{2}\frac{v_a^2}{c^2} - \frac{u_a}{2c^2} - \frac{U_a}{c^2}\right) + 3\frac{p_a}{c^2}\right]. \qquad \ldots\ldots(8.5)$$

Using the power series (7.9) we find

$$\int_a dV \rho_a u_{a,i} u_b = (u_{b,k})_a \int_a dV \rho_a \frac{u'_a}{r_a}(x^i - a^i)(x^k - a^k). \qquad \ldots\ldots(8.6)$$

This can be simplified if we take into account the following relation holding for an arbitrary function $f(r_a)$:

$$\int_a f(r_a)(x^i - a^i)(x^k - a^k)\,dV = \tfrac{1}{3}\delta_i^k \int_a f r_a^2\,dV. \qquad \ldots\ldots(8.7)$$

We then get

$$\int_a \frac{dV}{c^2}(\mathfrak{T}_l^l - \mathfrak{T}_0^0)U^{00}{}_{,i} = -\frac{m_a}{c}\left(1 + \frac{3}{2}\frac{v_a^2}{c^2} - \frac{U_a}{c^2}\right)\sum_b (u_{b,i})_a + \frac{1}{3c^3}\sum_b (u_{b,i})_a \int_a \rho_a u_a' r_a\,dV. \qquad \ldots\ldots(8.8)$$

The second integral on the right-hand side of (8.1) gives immediately, if we consider (6.10) and (5.13),

$$\int_a \frac{dV}{c^4} 4\mathfrak{T}_0^k U^{0k}{}_{,i} = \frac{4}{c^3} m_a \dot{a}^k \sum_b \dot{b}^k (u_{b,i})_a. \qquad \ldots\ldots(8.9)$$

The last integral in (8.1) is, according to (6.10) and (7.23),

$$-\int_a \frac{dV}{c^4}\mathfrak{T}_0^0[S^{ll} + S^{00} - 2(U^{00})^2]_{,i} = -\frac{1}{c^3}\int_a \rho_a dV\{u_{a,i}(\tfrac{3}{2}v_a^2 - U_a) + \sum_b u_{b,i}(\tfrac{3}{2}v_b^2 - U_b) + s_{a,i} + \sum_b s_{b,i} + F_{a,i} + \sum_b F_{b,i} - U_{ak}[(x^k - a^k)w_a]_{,i} - \sum_b U_{bk}[(x^k - b^k)w_b]_{,i}\}. \qquad \ldots\ldots(8.10)$$

The first term in the bracket on the right-hand side of this equation gives zero because of (8.4). In the second we have to put $(u_{b,i})_a$ instead of $u_{b,i}$:

$$\int_a \rho_a dV \sum_b u_{b,i}(\tfrac{3}{2}v_b^2 - U_b) = m_a \sum_b (u_{b,i})_a(\tfrac{3}{2}v_b^2 - U_b). \qquad \ldots\ldots(8.11)$$

The integral of $\rho_a s_{a,i}$ vanishes for the same reason as (8.4) and the integral of $\rho_a \Sigma_b s_{b,i}$ again vanishes because of (7.7). The term $F_{a,i}$ gives, according to Appendix III,

$$\int_a \rho_a F_{a,i}\,dV = -\tfrac{2}{3}\epsilon_a \ddot{a}^i. \qquad \ldots\ldots(8.12)$$

In the next term we have to put $(F_{b,i})_a$ instead of $F_{b,i}$:

$$\int_a \rho_a \sum_b F_{b,i}\,dV = m_a \sum_b (F_{b,i})_a. \qquad \ldots\ldots(8.13)$$

The next term gives, remembering (8.7),

$$\int_a \rho_a U_{ak}[(x^k - a^k)w_a]_{,i}\,dV = U_{ai}\int_a \rho_a(w_a + \tfrac{1}{3}w_a' r_a)\,dV. \qquad \ldots\ldots(8.14)$$

The last term in (8.10) makes no contribution in this approximation because of (3.1) since, according to (7.11), it is

$$(w_b)_a : w_a \simeq l^3 : L^3.$$

Thus we finally obtain

$$-\int_a \frac{dV}{c^4}\,\mathfrak{T}_0^0[S^{ii} + S^{00} - 2(U^{00})^2]_{,i}$$

$$= -\frac{m_a}{c^3}\sum_b (u_{b,i})_a(\tfrac{3}{2}v_b^2 - U_b) + \frac{2}{3c^3}\epsilon_a \ddot{a}^i - \frac{m_a}{c^3}\sum_b (F_{b,i})_a$$

$$+ \frac{1}{c^3}U_{ai}\int_a \rho_a(w_a + \tfrac{1}{3}w_a' r_a)\,dV. \qquad \ldots\ldots(8.15)$$

In order to find the equations of motion we have to introduce the results (8.2), (8.8), (8.9) and (8.15) into (8.1). We notice that there are three kinds of terms. Most of them have the factor m_a, two have the factor ϵ_a and three are still in the form of integrals. The terms with ϵ_a cancel, since because of (6.11) $du_a/dt = 0$ and therefore according to (7.8) $d\epsilon_a/dt = 0$. The terms in the form of integrals give the sum

$$\frac{1}{3c^3}\sum_b (u_{b,i})_a \int_a \rho_a(u_a' r_a + 3w_a + w_a' r_a)\,dV,$$

which is also zero as shown in Appendix IV. We thus are left with the terms having the factor m_a only. Remembering that $dm_a/dt = 0$ because of (6.11), and dividing by $-m_a/c$ we get the equations of motion in the form

$$\ddot{a}^i + \ddot{a}^i\frac{v_a^2}{2c^2} + \dot{a}^i\frac{\dot{a}^k\ddot{a}^k}{c^2} + 3\ddot{a}^i\frac{U_a}{c^2} + 3\dot{a}^i\frac{d}{dt}\left(\frac{U_a}{c^2}\right) - \frac{4}{c^2}\sum_b \ddot{b}^i(u_b)_a - \frac{4}{c^2}\sum_b \dot{b}^i\frac{d}{dt}(u_b)_a$$

$$= \sum_b (u_{b,i})_a + \left(\frac{3}{2}\frac{v_a^2}{c^2} - \frac{U_a}{c^2}\right)\sum_b (u_{b,i})_a - \frac{4}{c^2}\dot{a}^k\sum_b \dot{b}^k(u_{b,i})_a$$

$$+ \sum_b (u_{b,i})_a\left(\frac{3}{2}\frac{v_b^2}{c^2} - \frac{U_b}{c^2}\right) + \frac{1}{c^2}\sum_b (F_{b,i})_a. \qquad \ldots\ldots(8.16)$$

In the second order terms of (8.16) which contain second time derivatives we can introduce the first order value

$$\ddot{a}^i = \sum_b (u_{b,i})_a.$$

We further write

$$\ddot{b}^i = \sum_c (u_{c,i})_b + (u_{a,i})_b, \qquad \ldots\ldots(8.17)$$

denoting by $\sum_c$ the sum over all bodies except a and b. Similarly we write

$$U_b = \sum_c (u_c)_b + (u_a)_b. \qquad \ldots\ldots(8.18)$$

Denoting by r_{ab} the distance between $\mathbf{a}$ and $\mathbf{b}$,

$$r_{ab} = |\mathbf{a}-\mathbf{b}|,$$

we get from (7.22)

$$(F_{b,i})_a = G\frac{m_b}{2}\left(\dot{b}^k\dot{b}^l\frac{\partial^3 r_{ab}}{\partial a^i\partial a^k\partial a^l} - \ddot{b}^k\frac{\partial^2 r_{ab}}{\partial a^i\partial a^k}\right). \quad \ldots\ldots(8.19)$$

If we then take into account the relation

$$\frac{\partial^2 r_{ab}}{\partial a^i\partial a^k} = \frac{\delta_i^k}{r_{ab}} - \frac{(a^i-b^i)(a^k-b^k)}{r_{ab}^3},$$

we find

$$\begin{aligned}\frac{4}{c^2}\sum_b \ddot{b}^i(u_b)_a - \frac{1}{c^2}\sum_b U_b(u_{b,i})_a - \frac{1}{2c^2}\sum_b Gm_b\ddot{b}^k\frac{\partial^2 r_{ab}}{\partial a^i\partial a^k}\\ = -\frac{5}{c^2}\sum_b G^2 m_a m_b\frac{1}{r_{ab}}\frac{\partial}{\partial a^i}\left(\frac{1}{r_{ab}}\right) + \frac{7}{2c^2}\sum_b\sum_c (u_{c,i})_b(u_b)_a\\ - \frac{1}{c^2}\sum_b\sum_c (u_c)_b(u_{b,i})_a + \frac{1}{2c^2}\sum_b{}'\sum_c{}'(b^k-a^k)(u_{c,k})_b(u_{a,i})_a.\end{aligned} \quad \ldots\ldots(8.20)$$

Further, we find by direct calculation,

$$\left.\begin{aligned}&(u_{b,i})_a = Gm_b\frac{\partial}{\partial a^i}\left(\frac{1}{r_{ab}}\right),\\ &\frac{d}{dt}(u_b)_a = (\dot{a}^k-\dot{b}^k)(u_{b,k})_a = Gm_b(\dot{a}^k-\dot{b}^k)\frac{\partial}{\partial a^k}\left(\frac{1}{r_{ab}}\right),\\ &\frac{d}{dt}(U_a) = \sum_b\frac{d}{dt}(u_b)_a = \dot{a}^k\sum_b(u_{b,k})_a - \sum_b\dot{b}^k(u_{b,k})_a.\end{aligned}\right\} \quad \ldots\ldots(8.21)$$

And if we write the first of (7.24) in the form

$$U_a = (u_b)_a + \sum_c (u_c)_a,$$

we find

$$-\frac{4}{c^2}U_a\sum_b(u_{b,i})_a = -\frac{4}{c^2}\sum_b(u_{b,i})_a(u_b)_a - \frac{4}{c^2}\sum_b\sum_c(u_{b,i})_a(u_c)_a. \quad \ldots\ldots(8.22)$$

Introducing all this in (8.16) we get the equations of motion in their final form:

$$\begin{aligned}\ddot{a}_i = \sum_b\Bigg[&Gm_b\frac{\partial}{\partial a^i}\left(\frac{1}{r_{ab}}\right) + \frac{Gm_b}{c^2}\left(\dot{a}^k\dot{a}^k + \tfrac{3}{2}\dot{b}^k\dot{b}^k - 4\dot{a}^k\dot{b}^k - 4\frac{Gm_b}{r_{ab}} - 5\frac{Gm_a}{r_{ab}}\right)\frac{\partial}{\partial a^i}\left(\frac{1}{r_{ab}}\right)\\ &+ \frac{Gm_b}{c^2}\left(4\dot{b}^i\dot{a}^k - 4\dot{a}^i\dot{a}^k + 3\dot{a}^i\dot{b}^k - 4\dot{b}^i\dot{b}^k\right)\frac{\partial}{\partial x^k}\left(\frac{1}{r_{ab}}\right) + \frac{Gm_b}{2c^2}\dot{b}^k\dot{b}^l\frac{\partial^3 r_{ab}}{\partial a^i\partial a^k\partial a^l}\Bigg]\\ &+\sum_b\sum_c\frac{G^2 m_c m_b}{2c^2}\Bigg[\frac{7}{r_{ab}}\frac{\partial}{\partial b^i}\left(\frac{1}{r_{ab}}\right) - \frac{2}{r_{bc}}\frac{\partial}{\partial a^i}\left(\frac{1}{r_{ab}}\right) - \frac{8}{r_{ac}}\frac{\partial}{\partial a^i}\left(\frac{1}{r_{ab}}\right)\\ &+ (b^k-a^k)\frac{\partial}{\partial b^k}\left(\frac{1}{r_{bc}}\right)\frac{\partial}{\partial a^i}\left(\frac{1}{r_{ab}}\right)\Bigg].\end{aligned} \quad \ldots\ldots(8.23)$$

If there would be two bodies only—the bodies a and b—then the double sum $\sum_b\sum_c$ is zero and the summation $\sum_b$ on the right-hand side of (8.23) has only the one term corresponding to b. In this case equation (8.23) becomes identical with the equations of motion given by Einstein and co-workers (1938).

APPENDIX I

After a series of transformations in which the following abbreviations are introduced

$$\Pi^{\mu,\varrho\sigma}=\frac{1}{2g}\left(\mathfrak{g}^{\varrho\tau}\mathfrak{g}^{\mu\sigma}{}_{,\tau}+\mathfrak{g}^{\sigma\tau}\mathfrak{g}^{\mu\varrho}{}_{,\tau}-\mathfrak{g}^{\mu\tau}\mathfrak{g}^{\varrho\sigma}{}_{,\tau}\right),$$

$$\Pi_{\varrho\sigma}{}^{\mu}=g_{\varrho\alpha}g_{\sigma\beta}\Pi^{\mu,\alpha\beta}\ ;$$

$$y_\mu=\{\log\sqrt{(-g)}\}_{,\mu},\quad y^\mu=g^{\mu\varrho}y_\varrho\ ;$$

$$\Gamma^\mu=-\frac{1}{\sqrt{(-g)}}\,\mathfrak{g}^{\mu\varrho}{}_{,\varrho},$$

$$\Gamma_{\mu\nu}=\tfrac{1}{2}(g_{\mu\varrho}\Gamma^\varrho{}_{,\nu}+g_{\nu\varrho}\Gamma^\varrho{}_{,\mu}+g_{\mu\nu,\varrho}\Gamma^\varrho),$$

$$\Gamma^{\mu\nu}=g^{\mu\varrho}g^{\nu\sigma}\Gamma_{\varrho\sigma},$$

g being the determinant of $g_{\mu\nu}$ (or $\mathfrak{g}^{\mu\nu}$), one obtains the general formula

$$R^{\mu\nu}-\tfrac{1}{2}g^{\mu\nu}R=\frac{1}{2g}\,\mathfrak{g}^{\varrho\sigma}\mathfrak{g}^{\mu\nu}{}_{,\varrho\sigma}+\Pi^{\mu,\varrho\sigma}\Pi_{\varrho\sigma}{}^{\nu}+\frac{1}{4g}\,\mathfrak{g}^{\mu\nu}\Pi_{\sigma\tau}{}^{\varrho}\mathfrak{g}^{\sigma\tau}{}_{,\varrho}-\tfrac{1}{2}y^\mu y^\nu+\tfrac{1}{4}g^{\mu\nu}y^\varrho y_\varrho$$
$$-\Gamma^{\mu\nu}-\tfrac{1}{2}(\Gamma^\mu y^\nu+\Gamma^\nu y^\mu)+\tfrac{1}{2}g^{\mu\nu}(g^{\varrho\sigma}\Gamma_{\varrho\sigma}+\Gamma^\varrho y_\varrho).$$

In our calculations we assume (3.2), i.e. $\Gamma^\mu=0$ and consequently the last three terms on the right-hand side of this formula vanish.

In order to find the field equations up to terms of order $1/c^3$ one wants $\Pi^{0,00}$ up to terms of order $1/c^6$ and all other $\Pi^{\mu,\varrho\sigma}$ up to terms of order $1/c^4$. Considering (4.1) one gets by a straightforward calculation:

$$\Pi^{0,00}=-\frac{2}{c^6}\,U^{00}{}_{,0}+\ldots,$$

$$\Pi^{0,0i}=-\Pi^{i,00}=\frac{2}{c^4}\,U^{00}{}_{,i}+\ldots,$$

$$\Pi^{0,ik}=\frac{2}{c^4}\,(U^{0i}{}_{,k}+U^{0k}{}_{,i})+\ldots,$$

$$\Pi^{i,k0}=\frac{2}{c^4}\,(U^{0i}{}_{,k}-U^{0k}{}_{,i})+\ldots,$$

$$\Pi^{i,kl}=\ldots,$$

the dots meaning terms of higher order. It follows that

$$\Pi^{0,\mu\nu}\Pi_{\mu\nu}{}^{0}=-\frac{8}{c^6}\,U^{00}{}_{,l}U^{00}{}_{,l}+\ldots,$$

$$\Pi^{i,\mu\nu}\Pi_{\mu\nu}{}^{k}=\frac{4}{c^4}\,U^{00}{}_{,i}U^{00}{}_{,k}+\ldots,$$

$$\Pi^{0,\mu\nu}\Pi_{\mu\nu}{}^{i}=\frac{4}{c^6}\,U^{00}{}_{,0}U^{00}{}_{,i}-\frac{8}{c^6}\,(U^{0i}{}_{,l}-U^{0l}{}_{,i})U^{00}{}_{,l}+\ldots,$$

$$\Pi_{\mu\nu}{}^{\varrho}\mathfrak{g}^{\mu\nu}{}_{,\varrho}=-\frac{8}{c^3}\,U^{00}{}_{,l}U^{00}{}_{,l}+\ldots.$$

Further, one finds

$$y^i=-\frac{2}{c^2}\,U^{00}{}_{,i}+\ldots,\qquad y^0=\frac{2}{c^4}\,U^{00}{}_{,0}+\ldots,$$

$$y^\varrho y_\varrho=-\frac{4}{c^4}\,U^{00}{}_{,l}U^{00}{}_{,l}+\ldots.$$

Introducing these values into the expressions for $R^{\mu\nu}-\frac{1}{2}g^{\mu\nu}R$ Fock obtains the result

$$\frac{-g}{c^2}(R^{00}-\tfrac{1}{2}g^{00}R)=\frac{1}{2c}\Delta\mathfrak{g}^{00}-\frac{1}{2c^3}\mathfrak{g}^{00}{}_{,00}-\frac{7}{c^6}U^{00}{}_{,l}U^{00}{}_{,l}+\ldots,$$

$$\frac{-g}{c^2}(R^{0i}-\tfrac{1}{2}g^{0i}R)=\frac{1}{2c}\Delta\mathfrak{g}^{0i}-\frac{1}{2c^3}\mathfrak{g}^{0i}{}_{,00}+\frac{6}{c^6}U^{00}{}_{,0}U^{00}{}_{,i}-\frac{8}{c^6}(U^{0i}{}_{,s}-U^{0s}{}_{,i})U^{00}{}_{,s}+\ldots,$$

$$\frac{-g}{c^2}(R^{ik}-\tfrac{1}{2}g^{ik}R)=\frac{1}{2c}\Delta\mathfrak{g}^{ik}-\frac{1}{2c^3}\mathfrak{g}^{ik}{}_{,00}+\frac{2}{c^4}U^{00}{}_{,i}U^{00}{}_{,k}-\frac{1}{c^4}\delta_i{}^kU^{00}{}_{,l}U^{00}{}_{,l}+\ldots.$$

From these equations by lowering the one index and considering (4.1), (4.4) and (4.5), we obtain our equation (4.2).

APPENDIX II

We have $3\int_a p_a dV=12\pi\int_0^\infty p_a r_a{}^2dr_a=4\pi\int_0^\infty d(p_a r_a{}^3)-4\pi\int_0^\infty r_a{}^3p'_a dr_a.$

The first integral vanishes because p_a is finite at the centre of a and vanishes outside the body. Taking into account (5.19) we find

$$3\int_a p_a dV=-4\pi\int_0^\infty r_a{}^3\rho_a u_a{}'dr_a.$$

And since according to (5.14)

$$-4\pi G\rho_a=u_a{}''+\frac{2}{r_a}u_a{}',$$

we get

$$3\int_a p_a dV=\frac{1}{G}\int_0^\infty r_a{}^3\left(u_a{}'u_a{}''+\frac{2}{r_a}u_a{}'^2\right)dr_a$$

$$=\frac{1}{2G}\int_0^\infty d(r_a{}^3u_a{}'^2)+\frac{1}{2G}\int_0^\infty r_a{}^2u_a{}'^2dr_a.$$

Again the first integral vanishes because $u_a{}'=0$ for $r_a=0$ and $u_a{}'\sim 1/r_a{}^2$ for $r_a\to\infty$. Therefore

$$3\int_a p_a dV=\frac{1}{2G}\int_0^\infty r_a{}^2u_a{}'^2dr_a.$$

Similarly we find

$$\frac{1}{2}\int_a \rho_a u_a dV=-\frac{1}{2G}\int_0^\infty d(r_a{}^2u_a{}'u_a)+\frac{1}{2G}\int_0^\infty r_a{}^2u_a{}'^2dr_a.$$

The first integral vanishes and we finally get

$$\frac{1}{2}\int_a \rho_a u_a dV=\frac{1}{2G}\int_0^\infty r_a{}^2u_a{}'^2dr_a,$$

which proves (7.8).

APPENDIX III

In the integral $\int_a \rho_a F_{a,i}dV$ only the second term of F_a, equation (7.18), will give a non-vanishing result. We find

$$\int_a \rho_a F_{a,i}\,dV=\int_a \rho_a\ddot{a}^k[(x^k-a^k)\phi_a]_{,i}\,dV=\int_a \rho_a\ddot{a}^k[\delta_i{}^k\phi_a+\frac{1}{r}\phi_a{}'(x^i-a^i)(x^k-a^k)]\,dV.$$

And according to (8.7)

$$\int_a \rho_a F_{a,i} dV = \ddot{a}^i \int_a \rho_a (\phi_a + \tfrac{1}{3}\phi_a' r_a) dV.$$

Now because of (7.20)

$$\phi_a' = \frac{3}{r_a^4}\int_0^{r_a} u_a r_a^2 dr_a - \frac{u_a}{r_a}$$

and

$$\phi_a + \frac{1}{3}\phi_a' r_a = -\frac{u_a}{3}.$$

Therefore, according to (7.8),

$$\int_a \rho_a F_{a,i} dV = -\frac{2}{3}\epsilon_a \ddot{a}^i.$$

APPENDIX IV

We find from (7.11)

$$w_a' = -\frac{4\pi G}{r_a^4}\int_0^{r_a} \rho_a r_a^4 dr_a$$

and

$$3w_a + w_a' r_a = 4\pi G \int_{r_a}^{\infty} \rho_a r_a dr_a = -\int_{r_a}^{\infty} (u_a'' + \frac{2}{r_a} u_a') r_a dr_a$$

$$= -\int_{r_a}^{\infty} d(r_a u_a' + u_a) = r_a u_a' + u_a.$$

Therefore

$$\int_a \rho_a (u_a' r_a + 3w_a + w_a' r_a) dV = \int_a \rho_a (2u_a' r_a + u_a) dV.$$

On the other hand

$$\int_a \rho_a 2u_a' r_a dV = -\frac{2}{G}\int_0^{\infty} (u_a'' + \frac{2}{r_a} u_a') u_a' r_a^3 dr_a$$

$$= -\frac{1}{G}\int_0^{\infty} d(u_a'^2 r_a^3) - \frac{1}{G}\int_0^{\infty} r_a^2 u_a'^2 dr_a = -\frac{1}{G}\int_0^{\infty} r_a^2 u_a'^2 dr_a.$$

And since according to Appendix I

$$\int_a \rho_a u_a dV = \frac{1}{G}\int_0^{\infty} r_a^2 u_a'^2 dr_a,$$

we shall have

$$\int_a \rho_a (u_a' r_a + 3w_a + w_a' r_a) dV = 0.$$

REFERENCES

DE DONDER, TH., 1926, *Théorie des champs gravifiques* (Paris : Gauthier-Villar).
EINSTEIN, A., and GROMMER, J., 1927, *Sitzb. Berl. Akad.*, 2.
EINSTEIN, A., and INFELD, L., 1940, *Ann. Math.*, **41**, 455; 1949, *Canad. J. Math.*, **1**, 209.
EINSTEIN, A., INFELD, L., and HOFFMANN, B., 1938, *Ann. Math.*, **39**, 65.
FOCK, V. A., 1939, *J. Phys., U.S.S.R.*, **1**, 81.
PAPAPETROU, A., 1948, *Proc. Roy. Irish Acad.*, **52**, 11.
ROSEN, N., 1940, *Phys. Rev.*, **57**, 147.

Resonant Nuclear Scattering of Gamma-Rays: Theory and Preliminary Experiments

By P. B. MOON
Department of Physics, The University of Birmingham

MS. received 2nd August 1950

ABSTRACT. Since the lower excited states of nuclei have very small widths ($\ll$ 1ev.), resonant scattering of gamma-rays requires precise matching of the energy available from the gamma-ray with the energy necessary to excite the scattering nucleus.

Resonant scattering should be observable if (1) the emitting and scattering nuclei are of identical type, (2) the gamma-transition goes to the ground state, and (3) the source and scatterer are given such a relative velocity that Doppler effect restores the energy lost by the gamma-ray to nuclear recoils. Thermal velocities of the emitting and scattering nuclei broaden and correspondingly weaken the resonant scattering peak, and the cross section at the optimum speed of $32E/A$ cm/sec. is $3{\cdot}6\times10^{-3}(I\Gamma/E^2)(A/T)^{1/2}$ cm^2, where E and Γ are the energy and intrinsic width of the excited state in electron volts, I the isotopic abundance of the resonantly scattering isotope, A its atomic weight and T the absolute temperature.

Preliminary experiments have been made with the 0·411 Mev. radiation from the nucleus ^{198}Hg, the source being carried by a high-speed rotor up to a speed of about 7×10^4 cm/sec. and the scatterer being liquid mercury (10% ^{198}Hg). A small but apparently significant increase of scattering was found, corresponding to a width Γ of the order of 10^{-5} ev.

No such increase was observed with ^{181}Ta gamma-rays scattered from tantalum carbide.

The negative result for ^{181}Ta and the positive result for ^{198}Hg are consistent with the latest information about the life-times of the excited states concerned, viz. $1{\cdot}1\times10^{-8}$ sec. for ^{181}Ta and less than 2×10^{-10} sec. for ^{198}Hg.

§1. INTRODUCTION

If a source of mass M emits a photon of energy E, the source will recoil with energy $E^2/2Mc^2$; an equal kinetic energy of recoil is involved if the photon is captured by a body of the same mass as the source. This does not prevent the optical excitation of one *atom* by another, because the widths of optical levels are large compared with amount of energy dissipated by recoil; but, owing to the high value of E, it does prevent the emission and capture of a *gamma-ray* from being an effective means of transferring energy of excitation from one *nucleus* to another of identical type. Thus, while the selective scattering of, for example, the mercury resonance line λ2537 by mercury atoms is of quite spectacular prominence, the corresponding nuclear phenomenon has hitherto proved unobservable.

Following Kuhn (1929), various workers have discussed the situation and have looked for the resonant scattering. For example, Pollard and Alburger (1948) have reported a search for resonant scattering of ^{24}Mg gamma-rays ($E=2{\cdot}8$ Mev.) in magnesium. In this instance the energy dissipated in recoil amounts to about 90 ev., while the width of the nuclear resonance is certainly less than 10^{-3} ev. Though the Doppler effect of thermal motions broadens the resonance, and though for heavier elements and less energetic gamma-rays the recoil energy can be of the order of 1 ev. only, the effective energy of the gamma-ray is always relatively far out in the low-energy wing of the resonance curve.

The present paper reports a theoretical and experimental study of the possibility of restoring the resonance with the aid of the Doppler effect, the source being made to move towards the scatterer with an appropriate velocity.

§ 2. THEORY

Electrodynamical theory* shows that the cross section for resonant scattering is

$$\sigma = \frac{\lambda^2}{8\pi} \frac{\Gamma^2}{(E-E_0)^2+\frac{1}{4}\Gamma^2} \qquad \ldots\ldots(1)$$

where $\lambda\,(=\boldsymbol{hc}/E)$ is the wavelength, Γ the width of the resonance, E the effective energy of the gamma-ray and E_0 the resonant energy†; statistical weights are here omitted and the transition is assumed to be between the ground state and the first excited state of the nucleus. With energies in electron volts, equation (1) becomes

$$\sigma = \frac{6\times 10^{-10}}{E^2} \frac{\Gamma^2}{(E-E_0)^2+\frac{1}{4}\Gamma^2}. \qquad \ldots\ldots(2)$$

If the nuclei are initially at rest but free to recoil, $E_0-E=E^2/M\boldsymbol{c}^2$ as indicated in § 1; this is a simple consequence of the conservation of energy and momentum.

Suppose the thermal velocities of the nuclei in the source and the scatterer to be distributed as in a gas at temperature T. The probability that a source nucleus and a scattering nucleus shall have thermal velocity components in the direction of the gamma-ray that differ by v cm/sec^{-1} is then given by

$$P(v)\,dv=(M/4\pi\boldsymbol{k}T)^{1/2}\exp(-Mv^2/4\boldsymbol{k}T)\,dv. \qquad \ldots\ldots(3)$$

The quantity $(4\boldsymbol{k}T/M)^{1/2}$ is a measure of the thermal width in cm/sec^{-1}; it is actually the half-width, at $1/e$ of maximum height, of the distribution curve for the relative velocity components. (The intrinsic gamma-ray width Γ of equation (1) is, in accordance with the usual convention, the *whole* width of the nuclear resonance, measured at *half* maximum height.)

The Doppler energy-displacement corresponding to v is $vE/\boldsymbol{c}$. The scattering cross section is obtained from equation (1) by replacing E by $E+vE/\boldsymbol{c}$, multiplying by $P(v)$ and integrating with respect to v. It is

$$\sigma^{\mathrm{T}} = \frac{\lambda^2}{8\pi}\int_{-\infty}^{\infty} \frac{P(v)\Gamma^2}{(E-E_0+vE/\boldsymbol{c})^2+\frac{1}{4}\Gamma^2}\,dv, \qquad \ldots\ldots(4)$$

where the superscript T is a reminder that we are now including the effect of thermal velocities.

If the source as a whole is moving towards the scatterer with velocity u, the Doppler effect will add an amount $uE/\boldsymbol{c}$ to the effective energy E of the gamma-radiation. Since $E=E_0-E^2/M\boldsymbol{c}^2$, equation (4) now becomes

$$\sigma^{\mathrm{T}} = \frac{\lambda^2}{8\pi}\int_{-\infty}^{\infty} \frac{P(v)\Gamma^2}{(E^2/\boldsymbol{c}^2)(u+v-E/M\boldsymbol{c})^2+\frac{1}{4}\Gamma^2}\,dv. \qquad \ldots\ldots(5)$$

* See, for example, W. Heitler, *Quantum Theory of Radiation* (Oxford: University Press, 1936), equation III, 12.17. By a misinterpretation of this equation, Pollard and Alburger obtained a value for σ that is too great by a factor of $4\pi^2$.

† Except when the difference between them is involved, E and E_0 can be used interchangeably.

In this integral, the factor $\Gamma^2/[(E^2/\mathbf{c}^2)(u+v-E/M\mathbf{c})^2+\frac{1}{4}\Gamma^2]$ has a very sharp maximum* around $v=(E/M\mathbf{c})-u$, and little error will be made by supposing the thermal-distribution factor $P(v)$ to remain constant at the value appropriate to $v=(E/M\mathbf{c})-u$. Writing $E/M\mathbf{c}=u_m$, we thus find from (3) and (5)

$$\sigma^T=\frac{\lambda^2}{8\pi}(M/4\pi\mathbf{k}T)^{1/2}\exp[-M(u_m-u)^2/4\mathbf{k}T]\int_{-\infty}^{\infty}\frac{\Gamma^2\,dv}{(E^2/\mathbf{c}^2)(u-u_m+v)+\frac{1}{4}\Gamma^2}.$$

The quantity beneath the sign of integration is now readily integrable to $2\pi\Gamma\mathbf{c}/E$, whence

$$\sigma^T=\frac{\lambda^2\Gamma}{4}\left(\frac{M\mathbf{c}^2}{4\pi\mathbf{k}TE^2}\right)^{1/2}\exp[-M(u-u_m)^2/4\mathbf{k}T]. \qquad \ldots\ldots(6)$$

Using $\lambda=\mathbf{h}\mathbf{c}/E$, expressing E and Γ in electron volts, and letting A represent the conventional atomic weight and I the isotopic abundance of the resonantly scattering nuclear species among the nuclei in the scatterer, one finds

$$\sigma^T=3{\cdot}6\times10^{-3}\frac{I\Gamma}{E^2}\left(\frac{A}{T}\right)^{1/2}\exp\left[-\frac{A}{T}(u-u_m)^2\right]. \qquad \ldots\ldots(7)$$

The maximum scattering cross section occurs when

$$u=u_m=E/M\mathbf{c}=32E/A \text{ cm.sec}^{-1}$$

and is

$$\sigma_m{}^T=3{\cdot}6\times10^{-3}\frac{I\Gamma}{E^2}\left(\frac{A}{T}\right)^{1/2}\text{ cm}^2. \qquad \ldots\ldots(8)$$

§3. DESIGN OF EXPERIMENT

In the experimental arrangement envisaged (Figure 1), a radioactive source of gamma-rays moves on a circular path and irradiates (principally when

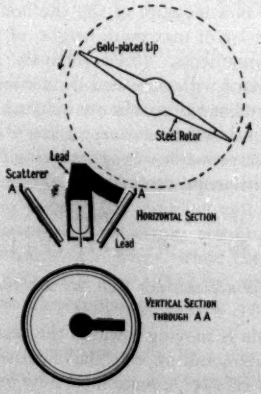

Figure 1. (Not to scale.)

approaching) a scatterer containing nuclei identical in type with those from which the gamma-rays are emitted. A counter, shielded from direct radiation, records

* The width of this maximum, measured at half height, is $\mathbf{c}\Gamma/E$; with typical values such as $E=10^6$ ev., $\Gamma=10^{-4}$ ev., it is of the order of a few centimetres per second and so much smaller than the thermal width $(4\mathbf{k}T/M)^{1/2}$ which is of the order of the velocity of thermal agitation.

the scattered gamma-rays, and the rate of recording should increase as the velocity of the source becomes comparable with the optimum value $32E/A$.

The choice of the isotope to be used as source and scatterer is limited by several considerations. The isotope must have substantial natural abundance for use as scatterer. It must also be available in the excited state (following the decay of its radioactive parent) in order to serve as the source of gamma-rays. The gamma-ray to be studied must go to the ground state; if not the only gamma-ray emitted by the source, it should preferably be the hardest of them, so that the others (together with the much more abundant but softer Compton-scattered radiation) can be removed from the scattered beam by absorbers placed round the counter. The transition should have as large a width Γ as possible; since the width decreases rapidly as the multipole order increases, dipole or electric quadrupole transitions are to be preferred. The optimum speed, $32E/A$, must be within the range of mechanical devices—say, up to 10^5 cm/sec. Since, *ceteris paribus*, Γ increases with E, it is desirable for the atomic weight A to be large so that this last condition can be satisfied with a reasonably high value of E.

A survey of known radioactive transitions yielded two which seemed distinctly the most promising: the 0·411 MEV. transition in ^{198}Au and the 0·48 MEV. transition in ^{181}Ta. The former follows the 2·7 day β-decay of ^{198}Au, the latter the 46 day decay in ^{181}Hf, passing through a 22 μsec. metastable level in ^{181}Ta. Both transitions are believed to go to the ground state, each is the most energetic radiation of appreciable intensity from the nucleus in question, and both are believed to be electric quadrupole. The isotopic abundance of ^{198}Hg is 10%; of ^{181}Ta, 100%. The optimum speeds are $6{\cdot}3 \times 10^4$ cm/sec. and $8{\cdot}5 \times 10^4$ cm/sec. respectively. The thermal breadth of the response curve is in each case such that the intensity of resonant scattering should fall to half its maximum at 80% of the maximum speed and should be negligible below half-speed.

Selecting ^{198}Au for detailed discussion, we find from equation (8) that the maximum cross section for resonant scattering is $4{\cdot}6 \times 10^{-21}\ \Gamma$ cm^2; it is here assumed that $T = 360°$ K., since the rotor which carries the source runs at about 420° K., while the scatterer is at room temperature. It is clearly desirable to use large angles of scattering, so that the Compton photons may be the more easily filtered out. Let us therefore consider scattering through an angle of 115° (the average angle used in the experiments). The angular distribution of the resonant scattering will depend upon the multipole order of the transition but is unlikely to be violently non-uniform, so the resonant scattering cross section per unit solid angle may be taken as equal to $\sigma/4\pi$ or $3{\cdot}6 \times 10^{-22}\ \Gamma$ cm^2. At 115°, Compton scattering and Rayleigh scattering have cross sections per unit solid angle of about 10^{-24} and 10^{-26} cm^2 respectively. If Compton-scattered radiation can be adequately filtered out, an intrinsic width Γ of 10^{-4} ev. should give readily observable resonant scattering, since the Rayleigh scattering has been observed with no great difficulty (Moon 1950, Storruste 1950).

§4. EXPERIMENTS WITH ^{198}Hg

The tips of a doubly tapered steel rod were electroplated with gold, and the whole was irradiated for several days in the Harwell pile (BEPO). A few days after irradiation, the activity was of the order of 100 mc. and was mainly from the gold plating. The rod was then spun in vacuum about an axis perpendicular

to its length, the speed of the tips being taken up to the limit of safety of about 7×10^4 cm.sec^{-1} and down again; the top speed of the centre of mass of the gold was 6×10^4. Meanwhile, observations were made of the rate of counting of a Geiger-Müller counter shielded from direct radiation but exposed (through an $\frac{1}{8}$-inch lead absorber) to gamma-rays scattered from a surrounding thin-walled iron-alloy cone containing liquid mercury (Figure 1). The cone was placed so as to be exposed mainly to gamma-rays from the *advancing* tip of the rotor.

Four complete experiments were made, each lasting for about $1\frac{1}{2}$ hours and each involving the registration of upwards of 250,000 gamma-rays; corrections (unimportant to the final result since acceleration and deceleration occupied about the same time) were made for the experimentally observed decay of the source (about 0·7% per hour). The first two runs were made as described above. In the third, the direction of rotation was reversed; a smaller effect would be expected owing to the less favourable position of the rotor tip when advancing towards the scatterer. The fourth run was made in the forward direction with a scatterer of copper instead of mercury; any increase at high speed would in this case be due to extra-nuclear phenomena such as stretching of the rotor.

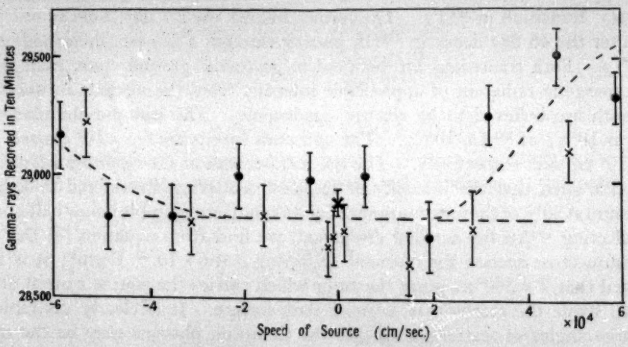

Figure 2. Effect of speed of source on rate of recording of scattered gamma-rays. Negative speeds indicate rotation in opposite sense to that shown in Figure 1.

During a fifth run, with a double thickness of lead round the counter, a vacuum failure before full speed had been reached caused the rotor to strike the wall of the vacuum chamber, with catastrophic results to both.

For purposes of illustration, the results for the second 'forward' run and the 'reverse' run, which were made on the same day, are plotted together in Figure 2. Each point represents the number of particles recorded in a ten-minute interval, and the mean speed during that interval; circles refer to readings taken during acceleration, crosses to readings taken during deceleration, while the heavy cross represents a reading taken at very low speed between the two runs. The vertical lines show the probable error, calculated from the number of particles observed in each interval. The broken lines show a possible analysis into background and resonant scattering, varying with speed in the expected manner and more intense (as it should be) with 'forward' than with 'reverse' rotation. Such an analysis might be over-ambitious and it is preferable to rely on the ratio of the mean counting rate at all speeds above 4×10^4 cm. sec^{-1} to the mean rate at all

lower speeds. The two 'forward' runs gave values for this ratio of $1{\cdot}007_2 \pm 0{\cdot}008$, and $1{\cdot}015_5 \pm 0{\cdot}006$, the probable errors being calculated from the *experimental* fluctuations of counting rate within each of the two speed ranges; since any genuine increase will vary with speed, the errors may be overestimated. The 'reverse' run gave a ratio of $1{\cdot}005_9 \pm 0{\cdot}005$, and the 'blank' run, with a scattering cone of copper instead of mercury, gave a ratio of $0{\cdot}998_2 \pm 0{\cdot}005$.

The difference between the mean of the two 'forward' ratios and that for the blank experiment is $0{\cdot}013 \pm 0{\cdot}007$. This result is distinctly suggestive of the presence of resonant scattering, and it seems worth while to deduce the corresponding values of Γ and of the half-life of the excited state. The figure of 0·013 represents, crudely, the ratio of counts due to resonant scattering to those from Compton scattering, both at a mean angle of 115°, but it must be corrected on account of their different chances of emergence from the thick scatterer, their different transmissions through the absorber surrounding the counter, and the different sensitivities of the counter itself to the two energies in question as well as for background of various origins. It has also to be remembered that only those gamma-rays that leave the source nearly in its direction of motion will receive the full Doppler hardening, and that the experimental ratio is an average over speeds ranging from 4×10^4 cm/sec. to 6×10^4 cm/sec. With these factors taken into account, Γ is found to be about 3×10^{-5} ev., corresponding to a half-life of the order of 10^{-11} sec. for the 0·411 Mev. excited state of ^{198}Hg.

Shortly after these experiments were completed (April 1949), this half-life was reported to be about 2×10^{-8} sec. on the basis of delayed-coincidence measurements (MacIntyre 1949). If this were so, resonant scattering would be about two thousand times less than the present work indicated. Because of this contradiction, plans were made to verify the scattering with a different experimental arrangement. This has now been done with the help of Mr. A. Storruste and Mr. T. H. Bull; the effect has been qualitatively confirmed but the detailed analysis of the results, involving various auxiliary measurements, will take some time to complete. In the meantime, the contradiction has been removed by the work of Bell and Graham (1950), who find the life-time of the excited state to be shorter than the limit of resolution of their apparatus, which is 2×10^{-10} sec.

§ 5. EXPERIMENT WITH ^{181}Ta

A similar experiment was made with ^{181}Ta as the emitting and scattering isotope. The source was about 8 mg. of Hf_2O_3, irradiated in the Harwell pile for two months to obtain about $\frac{1}{2}$ mc. of the 46-day ^{181}Hf. This source was contained in small cup-like cavities in the ends of a rotor which could withstand higher speeds, and the apparatus built for this experiment differed in other details from that used earlier for ^{198}Hg. The scatterer was tantalum carbide. In spite of the decreased statistical accuracy due to the much weaker source, the experiment should afford a more sensitive test of resonant scattering than was possible for ^{198}Hg, since ^{181}Ta has 100% abundance. Two runs, in which the counting rates from 4×10^4 to 9×10^4 and from 0 to 4×10^4 cm/sec. were compared, gave ratios of $1{\cdot}003 \pm 0{\cdot}015$ and $0{\cdot}990 \pm 0{\cdot}014$, with a mean result of $0{\cdot}9965 \pm 0{\cdot}01$. It is to be concluded that the 0·48 Mev. γ-transition either does not go to the ground state or has a width less than 10^{-5} ev. and hence a life-time greater than about 4×10^{-11} sec. After this measurement had been made, a γ-transition of life-time $1{\cdot}1 \times 10^{-8}$ sec. was reported (Barber 1950) which may plausibly be identified with the 0·48 Mev. transition in question.

ACKNOWLEDGMENTS

Much of the apparatus used for the experiments with ^{198}Hg was built by Dr. D. G. Marshall, Mr. J. T. Stringer and the writer for other purposes, and Dr. Marshall kindly controlled and measured the rotor speed during the runs.

Thanks are particularly due to Messrs. N. T. Frost Ltd. for the electrodeposition of a very adherent layer of gold, and to the staff of the Atomic Energy Research Establishment, Harwell, for the irradiation of an unusual specimen to high activity.

REFERENCES

BARBER, W. C., 1950, *Bull. Amer. Phys. Soc.*, **25**, No. 2, p. 9.
BELL, R. E., and GRAHAM, R. L., 1950, *Phys. Rev.*, **78**, 490.
KUHN, W., 1929, *Phil. Mag.*, **8**, p. 625.
MACINTYRE, W. J., 1949, *Phys. Rev.*, **76**, 312.
MOON, P. B., 1950, *Proc. Phys. Soc.* A, **63**, 1189.
POLLARD, E. C., and ALBURGER, D. A., 1948, *Phys. Rev.*, **74**, 926.
STORRUSTE, A., 1950, *Proc. Phys. Soc.* A, **63**, 1197.

Detection of μ-Mesons and other Fast Charged Particles in Cosmic Radiation, by the Čerenkov Effect in Distilled Water

BY J. V. JELLEY

Atomic Energy Research Establishment, Harwell, Didcot, Berks.

MS. received 23*rd August* 1950

ABSTRACT. The Čerenkov effect has been established for the passage of cosmic-ray μ-mesons through distilled water. The light pulses were observed using a photomultiplier and fast amplifier; the experiments were carried out using the detector alone, and in a coincidence-telescope arrangement. The ratio of the light emitted in the downward and upward directions was measured as a function of discriminator bias. In addition measurements were carried out at various depths of water and with various orientations of the detector with respect to the vertical. Estimates of the absolute efficiency were made and other characteristics of the detector are discussed.

§1. INTRODUCTION

DURING the course of investigations into the possibility of utilizing various organic solutions as scintillation detectors in cosmic-ray applications, it was found that several liquids of commercial purity produced light pulses from the passage of single cosmic-ray particles. A study was then made, using distilled water, to ascertain whether some of the pulses could be attributed to the Čerenkov effect (Čerenkov 1934). This effect, the theory of which was worked out by Frank and Tamm (1937), has been investigated by several workers in recent years, notably by Collins and Reiling (1938) who employed a photographic technique, and by Dicke (1947) who used a photomultiplier and an optical system proposed by Getting (1947). The conclusive evidence for the effect has been limited to detection of artifically accelerated electrons and secondary electrons produced by γ-rays. Among those who searched for the phenomenon with cosmic rays Weisz and Anderson (1947) found a small effect while Dicke obtained no effect that could be attributed definitely to Čerenkov radiation.

§ 2. EXPERIMENTAL TECHNIQUE

The arrangement adopted in the experiments to be described is shown in Figure 1. A tray of Geiger counters of effective area 120 cm² was mounted

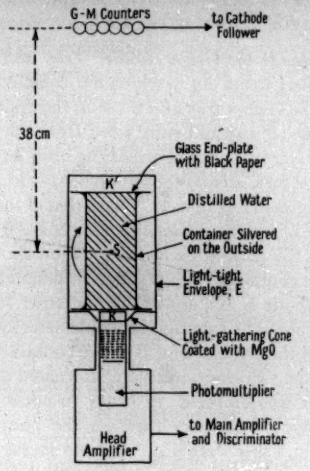

Figure 1. Essential features of apparatus.

vertically above a glass cylindrical container completely filled with distilled water. The container, of length 20 cm. and diameter 8·5 cm., was made of glass, as were also the end plates; the curved body of the container was silvered to reduce loss of light. Black paper over the upper end of the container was arranged to absorb light emerging upwards while, at the lower end, a small light-integrating cone coated with magnesium oxide was mounted to fit snugly round the cathode K of an 11-stage E.M.I. photomultiplier (type 5311). The water container, white cone and phototube were all mounted in an outer light-tight brass envelope E.

The output pulses from the phototube, after passing through a low-gain pre-amplifier situated at the base of the tube, were amplified by a main amplifier, after which they passed through a discriminator to one channel of a coincidence mixer of resolving time $\tau = 1{\cdot}8\,\mu$sec. The other channel was connected to the output of the counter tray via a cathode follower. The amplifier was of special design having both integration and differentiation time-constants of $3{\cdot}2 \times 10^{-8}$ sec.; this extremely narrow bandwidth resulted in a considerable reduction of the phototube noise relative to a pulse as short as that computed for the Čerenkov effect, in this case of the order of 10^{-9} sec. The phototube was operated at 1·9 kv. and the overall gain of the amplifier was about 100.

Water was chosen for the light-producing medium for it was believed there would be a complete absence of the 'scintillation type' mechanism of light production. The cylindrical geometry was chosen as this was symmetrical about the centre S of the container when this and the phototube were inverted.

The experiments were divided into two groups: (i) coincidence experiments, carried out under conditions of relatively low bias at a time when it was not known

how large the light pulses would appear from this type of radiation; (ii) experiments conducted at various conditions of bias using the Čerenkov detector alone and the pulses counted directly at the output of the discriminator.

§ 3. RESULTS

(i) *Coincidences between the Geiger-Müller Tray and Čerenkov Detector*

A number of runs was carried out in which the coincidence rate was measured between the counts in the Geiger tray and those in the phototube; the chance rates were calculated in the usual way and subtracted from the observed rates, for this purpose the single rates were monitored on scaling units and pen recorders. It was realized that a crucial test for Čerenkov radiation lies in its characteristic of emission in directions making angles of less than 41°* with that of the incoming particle (this figure refers to the case of water). Coincidence runs were carried out under two conditions, firstly with the phototube in the position shown in Figure 1 with its cathode at K below the container (this position is denoted by B), and secondly, with the phototube cathode at K′, above the container (denoted by position A). Position A was brought about by rotating the whole detector assembly through 180° in a vertical plane about the centre-point S of the container; the counter tray was not moved. Runs in the two positions were alternated and interlaced with runs in which the container was emptied, in order to allow for those coincidences arising from the passage of particles through the phototube alone in its two positions K and K′. In Table 1 are presented the averaged results of these runs, carried out at three bias settings on the discriminator, 2, 5 and 15 volts; the figures refer to genuine coincidence rates (i.e. chance subtracted) in counts/minute, and the symbols P, C and L refer to the phototube, container and liquid respectively.

Table 1.

Bias	2 volts		5 volts		15 volts	
Phototube position	B	A	B	A	B	A
$(P+C+L)$	$4{\cdot}14\pm0{\cdot}03$	$2{\cdot}29\pm0{\cdot}10$	$4{\cdot}01\pm0{\cdot}11$	$1{\cdot}73\pm0{\cdot}04$	$2{\cdot}54\pm0{\cdot}08$	$0{\cdot}71\pm0{\cdot}03$
$(P+C)$	$0{\cdot}79\pm0{\cdot}03$	$1{\cdot}26\pm0{\cdot}02$	$0{\cdot}47\pm0{\cdot}01$	$0{\cdot}98\pm0{\cdot}03$	$0{\cdot}15\pm0{\cdot}01$	$0{\cdot}40\pm0{\cdot}02$
L	$3{\cdot}35\pm0{\cdot}04$	$1{\cdot}03\pm0{\cdot}10$	$3{\cdot}54\pm0{\cdot}11$	$0{\cdot}75\pm0{\cdot}05$	$2{\cdot}39\pm0{\cdot}08$	$0{\cdot}31\pm0{\cdot}04$
Ratio $[L_B/L_A]$	$3{\cdot}25\pm0{\cdot}32$		$4{\cdot}72\pm0{\cdot}35$		$7{\cdot}7\pm1{\cdot}0$	

The average value of the chance rate, only significant at the 2-volt bias setting, was approximately 0·2/minute; this was deduced from the counter-tray and phototube rates which fluctuated around figures of 400 and 7,000 counts/minute respectively. From the above results the ratio between the counting rates in the B and A positions, L_B/L_A, see Table 1, rises from 3·3 at 2 volts bias to 7·7 at 15 volts. These ratios are good evidence in favour of the Čerenkov effect taking place in water due to the passage of sea-level cosmic-ray particles.

A control experiment was then carried out using a 0·5% solution (by weight) of terphenyl in xylene (Reynolds *et al.* 1950) to replace the water as a source of fluorescence. If it is assumed that the fluorescence radiation is emitted isotropically from each point in the track of a particle one would expect a value for L_B/L_A for the

* In general, the angle of light emission θ is related to the refractive index n, and the ratio of the velocity of the particle to that of light *in vacuo* β, by $\cos\theta = 1/\beta n$. For water ($n=1{\cdot}33$) and $\beta \to 1{\cdot}0$, $\theta = 41°$.

solution of less than unity because of the larger flux of tracks near to the photocathode in position A (Figure 1). The ratio obtained for L_B/L_A in this experiment at a bias of 2 volts was $1{\cdot}26 \pm 0{\cdot}06$. It would have been expected that this ratio would have been unity or less if the Čerenkov effect in this case were negligible; however, the observed ratio is explicable if a comparable contribution is present from the Čerenkov effect in the xylene.

That the ratio L_B/L_A in water is not infinite is interpreted as being due to internal reflections within the container such that even in position A sufficient light is received in a fraction of cases to give a count. The increase of this ratio with discriminator bias confirms this hypothesis. Taking the accepted value for the total cosmic-ray intensity at sea level (Rossi 1948), the coincidence rate of a hypothetical detector 100% efficient and of area 57 cm² placed at S would be about 7/minute. This figure is to be compared with that of about 3·4/minute obtained experimentally for the phototube in position B at 2 volts bias. In the B position with the terphenyl solution a liquid-alone rate L of about 3·5/minute was obtained which agrees with that for the water within the errors.

It is interesting to note that at 2 volts bias a coincidence rate of $0{\cdot}55 \pm 0{\cdot}03$ per minute was obtained for the phototube alone in position B which agrees very closely with that calculated, 0·6/minute, from the total vertical intensity and solid angle, when an area comparable with that of the photocathode is assumed to have an efficiency of 100%. Which elements of the E.M.I. phototube are in fact responsible for this was not investigated. It could well be interpreted as due to the emergence of ' delta rays ' from the cathode surface during the passage of the particles through the glass envelope.

A test was carried out with a lead absorber 10 cm. thick placed above the counter tray to ascertain, by absorption of the soft component, that the observed effects were due to μ-mesons as well as to electrons. With this arrangement the coincidence rate L for the water alone in position B was measured to be $2{\cdot}67 \pm 0{\cdot}11$/minute as compared with the value of $3{\cdot}35 \pm 0{\cdot}04$/minute with no lead. It can therefore be concluded that approximately 80% of the effects obtained were due to μ-mesons.

(ii) *Single Rate Čerenkov Detection*

It was found that above a bias of about 10 volts the single counting rate from the water detector alone depended markedly upon its orientation and that the phototube ' noise ' then made only a small contribution to the total counting rate. A number of bias curves was then taken, see Figure 2, in which the counting rates of the Čerenkov detector alone were measured at values of bias up to 100 volts; the gain of the system and amplifier time-constants were maintained the same as in the coincidence experiments.

Curve (*a*) was obtained for the phototube and empty container in both positions A and B; the counting rates obtained at each bias setting were the same, within the error limits, for the two positions. Curve (*b*) was obtained in position B when the container was filled with distilled water while curve (*c*) was obtained with the detector inverted, position A. Subtraction of curve (*a*) from curves (*b*) and (*c*) yielded bias curves (*d*) and (*e*) for the water alone in positions B and A respectively. In the inset to Figure 2 is shown the ratio of the counting rates L_B/L_A obtained from these last two curves; it will be seen this ratio is as high as 70:1 at a bias of 30 volts. Curve (*f*) was obtained at half depth (i.e. 10 cm. of water); as expected this lay at a

lower level of counting rates. At full depth, curve (*d*), the extrapolated value of the counting rate at zero bias was approximately 170/minute. This is considerably larger than the rate calculated, of the order of 70/minute, for the total cosmic-ray radiation entering an area equal to the cross section of the cylinder integrated over the hemisphere; however, it must be remembered that at all angles of incidence other than the vertical the projected area of the container is larger than 57 cm²; it rises in fact to 170 cm² for particles entering horizontally.

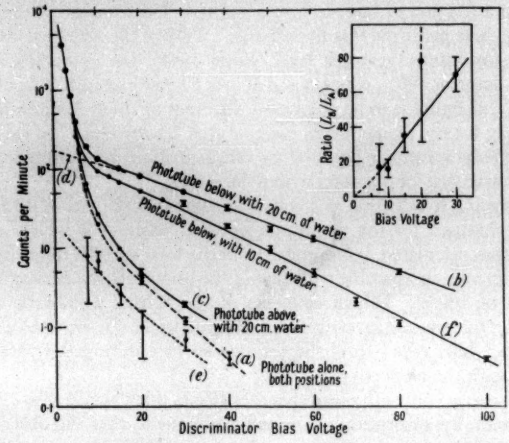

Figure 2. Single-rate bias curves; inset, the ratio L_B/L_A.

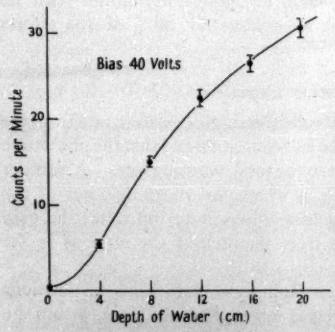

Figure 3. Variation of counting rate as a function of depth of water.

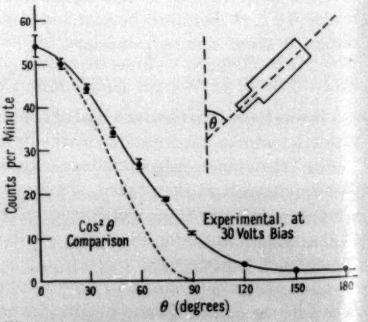

Figure 4. Variation of counting rate as a function of the orientation of the detector with respect to the vertical.

The variation of counting rate with depth of water was carried out, at a fixed bias of 40 volts; a plot of these results is shown in Figure 3.
The curve indicates, at this bias, a detection efficiency of less than unity since an asymptotic value of the counting rate even at 20 cm. depth is not attained.

Finally, the variation of counting rate of the detector was determined as a function of the angle θ between the axis of the system and the vertical. These results, carried out at a bias of 30 volts, are shown in Figure 4.

The general form of the curve agrees with that expected when it is remembered that the light radiated in the water by a relativistic particle is emitted at an angle of approximately 40° with respect to the track of the particle. This means that there is a considerable counting rate when the detector is lying in a horizontal plane, and, for angles of θ such that $180° > \theta > 90°$, detection at reduced efficiency still occurs. For this and other reasons connected with the geometrical form of the detector and the bias conditions, it would not be expected that the form of the curve in Figure 4 should follow the $\cos^2\theta$ distribution law, though for comparison purposes this has been included in the figure.

§ 4. CONCLUSIONS

The Čerenkov effect has been firmly established for the passage of cosmic-ray μ-mesons in distilled water. It now opens up the possibility of developments of methods of measuring directly the velocities of singly charged particles with values of β lying between 0·75 and 1·0 (for water), as first suggested by Getting (1947). It is not easy to understand why the Čerenkov effect with cosmic-ray particles had not previously been obtained using the phototube technique. It may be that in the present experiments the phototube noise was less than in the tube used by Dicke in his earlier experiments, or that the extremely fast amplifier available to the author enabled a very much better signal/noise ratio to be obtained.

Further characteristics of the new detector for cosmic-ray research are (i) extremely high speed of operation, (ii) high efficiency, (iii) negligible sensitivity to nucleon stars and (iv) a very small sensitivity for γ-rays from radioactive sources such as the laboratory background. While properties (i) and (ii) hold for the best scintillation counters, (iii) and (iv) are unique to this instrument.

ACKNOWLEDGMENTS

The author would especially like to thank Dr. B. Pontecorvo for his continual encouragement and interest shown in this work and Mr. F. Bradley for his very considerable technical assistance. The author wishes furthermore to thank the Director, Atomic Energy Research Establishment, for permission to publish these results.

REFERENCES

Čerenkov, P. A., 1934, *C. R. Acad. Sci., U.S.S.R.*, **8**, 451.
Collins, G. B., and Reiling, V. G., 1938, *Phys. Rev.*, **54**, 499.
Dicke, R. H., 1947, *Phys. Rev.*, **71**, 737.
Frank, I., and Tamm, Ig., 1937, *C. R. Acad. Sci., U.S.S.R.*, **14**, 105.
Getting, I. A., 1947, *Phys. Rev.*, **71**, 123.
Reynolds, G. T., Harrison, F. B., and Salvini, G., 1950, *Phys. Rev.*, **78**, 488.
Rossi, B., 1948, *Rev. Mod. Phys.*, **20**, 537.
Weisz, P. B., and Anderson, B. L., 1947, *Phys. Rev.*, **72**, 431.

LETTERS TO THE EDITOR

The Angular Distribution of Protons Emitted in some F(α, p) Ne Resonance Reactions

The angular distributions of the protons emitted in some $^{19}F(\alpha, p)^{22}Ne$ resonance reactions have been studied by using a disintegration camera and the photographic emulsion technique to record the emitted particles. The design of the camera has already been described by Jolley (1949). A collimated beam of α-particles from a polonium source of about 3 millicuries strength is obtained by means of three separated coaxial discs of copper. The energy of this beam on striking the target is adjusted to that of a known resonance level in the compound nucleus ^{23}Na by varying the distance between source and target; air at atmospheric pressure is used as absorber. The target of fluorine consists of a layer of evaporated calcium fluoride on very thin gold foil, the fluoride layer having an estimated thickness of 3 mm. air equivalent.

With the energies of the α-particles set at already established levels of 4·1 and 3·7 MEV., about 2,600 and 900 protons were recorded respectively. The intensity–energy distributions give in each case two distinct peaks together with indications of another smaller peak; these peaks correspond to transitions from the level in the compound nucleus to different levels in the final nucleus. The energies of the peaks for the 4·1 MEV. level are 5·06±0·11

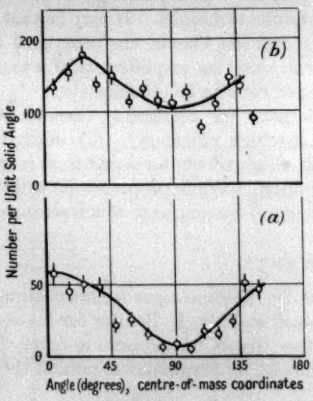

Figure 1.

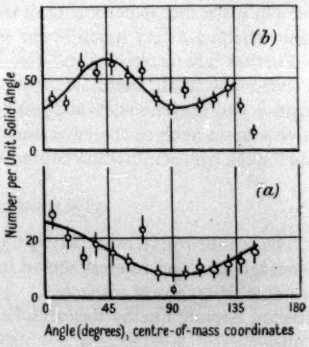

Figure 2.

Angular distribution of protons from the F(α, p)Ne reaction. (*a*) Ground state transitions; (*b*) Second excited state transitions.

Figure 1, $E_\alpha = 4{\cdot}1$ MEV; Figure 2, $E_\alpha = 3{\cdot}7$ MEV.

and 3·67±0·13 MEV. with indications of another peak at about 4·6 MEV.; for the 3·7 MEV. level the peaks are at 4·64±0·10 MEV. and 3·22±0·11 MEV. with indications of another peak at 4·2 MEV. The spacings of these energy levels in the final nucleus ^{22}Ne are 0, 0·4 and 1·41 MEV. above the ground state.

The angular distributions of the protons from these reactions may be seen in Figures 1 and 2. The ground state transitions both show distributions having a minimum at 90° and a maximum at 0° to the direction of the α-beam. The second excited state transitions both show minima at 0° and 90°; there is a maximum at 30° in the case of the 4·1 MEV. resonance and a maximum at 45° for the 3·7 MEV. resonance. Neither of the first excited state transitions is sufficiently intense to allow a determination of the angular distributions.

The recorded distributions are in all cases consistent with symmetry about the equatorial plane but because of the geometrical limitations of the apparatus measurements can be made only between 0° and 135°. There is a striking similarity between the two corresponding angular distributions for the ground state transitions for both resonance levels. This similarity persists in the second excited state distributions and it may be that the two levels of the compound nucleus overlap so that they behave effectively as one level as far as the angular distribution is concerned.

The relative yields for transitions to the ground, first and second excited states are in the ratios 1 : 0·35 : 4 and 1 : 0·16 : 3·1 for the 4·1 and 3·7 MeV. resonances respectively. Early experiments of Chadwick and Constable (1932) gave the yield ratio as 1 : 4 for ground and first excited state transitions. Our value of 1 : 0·35 is in better agreement with results of May and Vaidyanathan (1936) who were unable to record any transitions to the first excited state presumably because of its low intensity.

One of us (J.D.J.) wishes to thank the Department of Scientific and Industrial Research for a maintenance grant which made it possible to carry out this work.

Wheatstone Laboratory,
King's College,
University of London.

J. D. JOLLEY.
F. C. CHAMPION.

Submitted as a paper 27th March 1950;
resubmitted as a letter 15th September 1950.

CHADWICK, J., and CONSTABLE, J. E. R., 1932, *Proc. Roy. Soc.* A, **135**, 48.
JOLLEY, J. D., 1949, *Ph.D. Thesis*, University of London.
MAY, A. N., and VAIDYANATHAN, R., 1936, *Proc. Roy. Soc.* A, **155**, 519.

The Thermal Conductivity of Solid Helium

We have measured the thermal conductivity of solid helium at temperatures between 1·2° and 2·5° K. A german silver tube of 6 mm. I.D., 8 mm. O.D. and 5 cm. long was filled through a capillary with liquid helium at a temperature and pressure corresponding to a

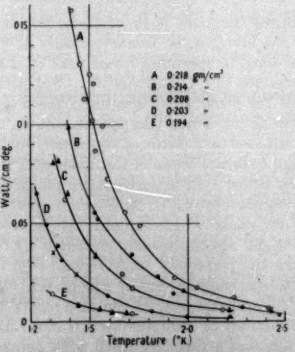

Thermal conductivity of solid helium at constant density.

point on the melting curve, where the density is known. The capillary was then closed off and the tube and its contents cooled down. Provided that the liquid had been sufficiently

compressed initially, the variation of the densities of solid and liquid helium is such that the tube will always be completely filled by the solid. Thus all the measurements have been made at constant densities whose magnitudes were fixed by the initial pressure and temperature of the liquid. One end of the tube was mounted on a cryostat the temperature of which could be varied, and an electric heater was used to supply heat to the other end. The conductivity was then found by measuring the temperature at each end with leaded phosphor-bronze thermometers. The corrections for the conduction of the metal tube, for heat flow down the leads and for end effects were only a few per cent. One set of measurements at a density of 0·208 was also made using a larger tube (9·9 mm. I.D. and 10 cm. long); the points so obtained are shown in the Figure and lie on the same curve as that obtained with the smaller tube.

The Figure shows the thermal conductivity as a function of temperature for various densities; different symbols on the same curve correspond to experiments on different occasions. The only previous value known to us is that of Kikoin (1939), who gives a value of 3×10^{-4} watt units at a temperature of 1·8° K. but does not state the density; this agrees in magnitude with our results.

Although for practical purpose it is convenient to use conductivities, it is better for the theoretical approach to consider their reciprocals, the thermal resistivities. The total resistivity of a cylindrical crystal may be given approximately by

$$W=AT^{v}e^{-\theta/2T}+bT+1/CDT^{3}.$$

The first two terms (Peierls 1929) give the resistance of an infinite crystal due to interactions between the elastic waves, brought about by 'umklapp processes' and imperfections of the lattice, in terms of three constants A, v, b, and the Debye specific heat parameter θ. The last term (Casimir 1938) is due to the scattering of the waves by the boundaries of the crystal and is only important at low temperatures. C is a constant and D the diameter of the crystal.

It appears that in the region of our measurements the principal contribution to the resistance is from the first term. No values of the constants A and v are available save that v is of the order unity, so we write to a first approximation $W\propto e^{-\theta/2T}$, which gives a thermal conductivity $K\propto e^{\theta/2T}$. As the value of θ for solid helium does not vary too much with temperature, we treated it as a constant and chose values of it so as to get the best fit with our experimental points. The appropriate values to fit the curves at densities of 0·218 and 0·194 are 26° and 21° respectively; these are similar to those derived from specific heat measurements (Keesom and Keesom 1936) and vary with the density in the same way.

At really low temperatures the only term of consequence in the expression for the thermal resistivity will be the first one, so that eventually $K=CDT^{3}$. Thus a maximum must occur in the curves at some temperature lower than we have measured. To make an estimate of this temperature we put $CDT^{3}=ae^{\theta/2T}$. Substituting in values for all the constants, we find that for the same sized specimen the maximum should be between 0·5° and 1·0°. Klemens (to be published shortly) has shown that the conductivity in the region of the maximum is reduced by a factor of about ten, due to interactions, so we would expect the conductivity there to have a value of the order of 2 watt units. We hope shortly to extend our measurements below 1° K. to verify these predictions.

Solid helium is very compressible and is, therefore, a good substance on which to study those pressure-dependent constants which cannot yet be evaluated theoretically. The variations in the densities of our specimen were obtained by varying the initial pressure over the liquid through the comparatively small range of 60 to 136 atmospheres, yet this was sufficient to vary the thermal conductivity by a factor ten. We intend to make measurements using much higher filling pressures, of the order of a few thousand atmospheres.

In view of the high conductivity of solid helium it is interesting to review the suggestion made by Dr. C. A. Swenson that a capillary filled with helium might be used as a heat switch below 1° : liquid helium II in the tube would give a very big conductance, while on applying pressure it would solidify and have a much lower conductivity. In the course of measurements on the specific heat of solid helium below 1·0° we suspended a pill of iron alum at 0·3° by a fine capillary (0·13 mm. I.D.) from a cryostat at 0·9°. With

solid helium in the capillary, the heat flow corresponded to a mean conductivity of about 10^{-1} watt units, which is consistent with our other measurements (after allowing for size effect). On releasing the pressure, the liquid equalized the temperatures almost instantaneously, which is consistent with measurements of the heat flow in a capillary just above 1·0° (e.g. Allen and Ganz 1939). Thus a heat switch is possible in this region, but it must be emphasized that the conductivity of the solid helium is still considerable, and precautions need to be taken to prevent too great a heat flow down it. At much lower temperatures, say below 0·3°, it seems likely that the conductivities of both liquid and solid will be small and similar, both being limited by size effect.

We both wish to express our appreciation to Professor F. E. Simon for his kind interest in the work. One of us (K. R. W.) is indebted to the Department of Scientific and Industrial Research for a maintenance grant.

Clarendon Laboratory,
Oxford.
13th November 1950.

K. R. Wilkinson.
J. Wilks.

Allen, J. F., and Ganz, E., 1939, *Proc. Roy. Soc.* A, **171**, 242.
Casimir, H. B. G., 1938, *Physica*, **5**, 495.
Keesom, W. H., and Keesom, A. P., 1936, *Physica*, **3**, 105.
Kikoin, A. K., 1939, *Acta physicochim., U.S.S.R.*, **10**, 307.
Peierls, R. E., 1929, *Ann. Phys., Lpz.*, **3**, 1055.

Factors Involved in the Accuracy and Reproducibility of Depth Measurements on Nuclear Research Emulsions

During the early stages of our work with boron-loaded Nuclear Research emulsions, we observed considerable variations in the apparent thicknesses of the processed emulsions. The plates used were Ilford Type C2, of nominal unprocessed thickness 100 μ. Thicknesses of the 22 processed plates examined ranged from 33–50 μ; over any one plate there were variations of as much as 10 μ (25%), and even measurements on the same area of a plate made at different times varied by as much as 4μ (10%). Since these variations would apply to all depth measurements, the following factors, which we considered may have caused them, were investigated: (i) the reliability of the measuring instrument; (ii) the variation of the emulsion thickness with relative humidity; (iii) the effect of oil immersion on the emulsion.

(i) *The reliability of the measuring instrument.* The thickness of the emulsion was measured by focusing a microscope first on the uppermost grains in the emulsion and then on the lowermost grain in the same area, and reading the distance traversed on the depth-scale of the microscope. The reliability of two microscopes was tested by calibrating the depth-scales using an interference method. One of the microscopes was found to have a periodic error which gave rise to considerable variations in the depth measurements. The other microscope gave a consistently uniform calibration, i.e. $1{\cdot}02_8\,\mu$ per division $\pm 1\%$, and this instrument was used for the rest of this work on depth measurements. The uncertainty of the depth measurements when using this microscope was estimated to be $\pm 1\,\mu$, and variations outside this could be regarded as true variations.

(ii) *The variation of emulsion thickness with relative humidity.* As considerable variations in thickness of emulsions still seemed to be present, we next examined the effect of relative humidity on emulsion thickness. Three plates, two from the same batch A and one from a different batch B, were placed in turn in constant humidity baths ranging from 0–100% relative humidity and measurements were taken on four areas of each plate. All plates examined showed similar increases in emulsion thickness with humidity, the thickness more than doubling itself between 0 and 100% relative humidity*; typical results are shown in

* S. L. Martin (*Aust. J. Sci. Res.*, 1949, **2**, 389) refers to this change of thickness with humidity. He found that the shrinkage factor k=(thickness after processing)/(thickness before processing) changed from about 0·5 at 0% R.H. to about 1·3 at 100% R.H.; this is in agreement with our results.

curves 1 and 2 of the Figure. In order to test the reproducibility of results, measurements were made on one area of each of six plates at the following relative humidities : 0, 43·5, 53, 64, 76 and 88, and then on the same areas, and at the same humidities in the reverse order. Typical results given in curves 3 and 4 show that the measurements repeat themselves within the estimated experimental spread of $2\,\mu$.

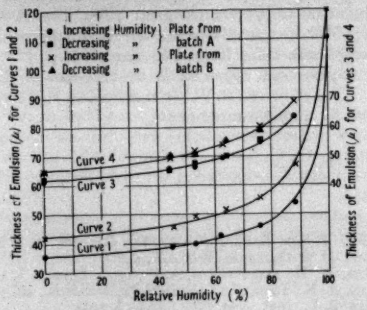

Variation of emulsion thickness with relative humidity.

Since the range of humidities encountered in the Laboratory over a period of five months was found to be 35–80% and the variation in thickness between these two humidities was of the order of 25% for the plates measured, it is necessary to work at constant humidity. As a standard procedure we now place all plates in a constant humidity bath of 53% R.H. (this being approximately the mean R.H. in the Laboratory) for at least 24 hours before making any depth measurements. On removing the plate from the constant humidity bath, the area on which measurements are to be made is immediately covered with cedar wood oil; it has been found that this effectively seals the emulsion and prevents any changes due to varying humidity in the room for normal periods of use, i.e. 5–6 hours. Check measurements at 53% R.H. after a period of two months confirmed that, provided the standard procedure outlined above is used, measurements repeat themselves within the estimated spread of $\pm 1\,\mu$.

Since the emulsion normally adheres to a glass surface, it was anticipated that there would be no appreciable lateral expansion due to change of humidity. This was confirmed by observations at 0 and 88% R.H. on thorium stars produced in the same type of plates.

(iii) *Effect of oil immersion on the emulsion.* During the course of the work it was suspected that when plates were left covered in oil for long periods, swelling was liable to take place due to the absorption of oil by the emulsion. To investigate this, two plates, one from each of the batches previously investigated, were placed in a constant humidity bath of 53% R.H., one test area on each being covered in oil all the time and another area being used as a control. Measurements were taken over a period of nine days. It was found that in one plate, from batch B, both the test area and the control area showed no change in thickness, outside the experimental error of $\pm 1\,\mu$, over the whole period; whereas in the plate from batch A the thickness of the test area showed a tendency to increase slightly with time (the increase exceeding experimental limits after about 7 hours), while that of the control area remained constant. This result is rather inconclusive, but it does appear that plates are liable to absorb the oil if left for long periods, and it is considered advisable to remove the oil from the plates as soon as measurements are finished.

The work described above has been carried out as part of the research programme of the National Physical Laboratory, and this letter is published by permission of the Director of the Laboratory. The authors desire to acknowledge the comments and suggestions they received from their colleagues in the Physics Division, National Physical Laboratory.

Physics Division,
National Physical Laboratory,
Teddington, Middlesex.
11th October 1950.

J. M. McALISTER.
D. W. KEAM.

Measurement of Gamma-Ray Momenta and the Thresholds of the Photo-disintegrations $^{12}C \rightarrow 3\,^4He$ and $^{16}O \rightarrow 4\,^4He$

In a previous letter (Goward and Wilkins 1950 a) the accuracy obtained in measurements of various charged-particle photo-disintegration stars was described. The stars were produced in nuclear emulsions by irradiation with continuous gamma-ray spectra of energies up to 25 MeV. For each star, assuming its identity, the observed momentum unbalance vector Δ was calculated by the relation

$$\Delta=(\Sigma p_r)-p_\gamma, \qquad \ldots\ldots (1)$$

where p_r ($r=1, 2, \ldots$.) are the individual particle momenta, in (MeV. $\times$ mass number)$^{1/2}$ units, and p_γ is the incident gamma-quantum momentum. The value of p_γ was obtained from

$$p_\gamma=0{\cdot}0232(E_T+E_D), \qquad \ldots\ldots (2)$$

where E_T (MeV.) is the total energy of the charged particles and E_D is the reaction threshold calculated from the mass values. The accuracy of measurement, and the certainty with which the stars could be identified, was discussed in terms of $|\Delta|$ statistics.

Momentum unbalance analysis of stars can be adapted to measurement of reaction thresholds E_D. From equation (1) it follows, since Δ should be zero, that Σp_r, resolved along the known gamma-ray direction, gives an independent value for p_γ, and hence E_D may be

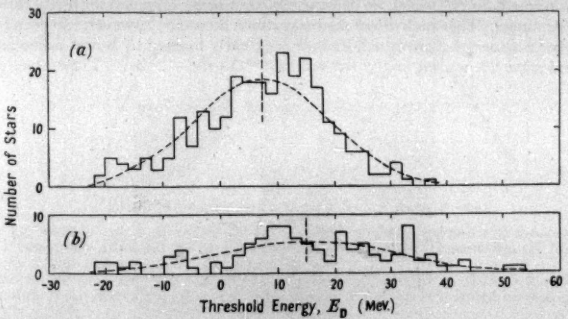

Measurement of thresholds for photo-disintegrations. (*a*) $^{12}C \rightarrow 3\,^4He$; (*b*) $^{16}O \rightarrow 4\,^4He$.

deduced from equation (2). The errors in the individual E_D values are large and a considerable number of stars must be measured to give a reasonably accurate mean value. The method cannot be compared with those using monochromatic gamma-ray sources of known energy, but it is the only recourse when suitable monochromatic sources are not available (e.g. no available monochromatic source gives $^{16}O \rightarrow 4\,^4He$ stars); moreover it provides additional evidence on the correct identification of the stars.

The Figure (*a*) shows a histogram of E_D values obtained, in the above manner, from 275 $^{12}C \rightarrow 3\,^4He$ stars observed in emulsions irradiated with the gamma-ray direction parallel to the emulsion surface. Momentum unbalance statistics for the stars indicated that each p_γ value would be subject to a probable error of about $\pm 0{\cdot}19$ and consequently each E_D value to a probable error of $\pm 8{\cdot}2$ MeV., since the errors in E_T are relatively small; this is confirmed by the fitted curve. The mean value of E_D for the stars of the Figure (*a*) is ($7{\cdot}3 \pm 0{\cdot}5$) MeV., in agreement with the expected value, 7·3 MeV.

The Figure (*b*) shows a histogram of E_D values for 111 $^{16}O \rightarrow 4\,^4He$ stars. Here the individual p_γ values had a probable error $\pm 0{\cdot}23$ (see Goward and Wilkins 1950 b) the increase arising mainly from the additional track to be measured in each star. The fitted curve thus corresponds to a probable error of $\pm 9{\cdot}9$ MeV., and the mean value of E_D obtained from the histogram is ($14{\cdot}8 \pm 1{\cdot}0$) MeV., consistent with the expected value, 14·5 MeV.

It is interesting to observe that the above techniques, applied in a reverse way, provide a test of the equation $p=h\nu/c$ or, in the present units, $p_\gamma=0{\cdot}0232E_\gamma$, where E_γ is the gamma-quantum energy. Assuming the reaction threshold E_D, E_γ is derived from $E_\gamma=E_T+E_D$ and p_γ is derived from the momentum balance analysis. For both the $^{12}C \rightarrow 3\,^4He$ and the $^{16}O \rightarrow 4\,^4He$ stars discussed above, the probable error of the individual (p_γ/E_γ) values is about $\pm 0{\cdot}01$. The combined statistics give $p_\gamma/E_\gamma=0{\cdot}0232\pm 0{\cdot}0005$.

Atomic Energy Research Establishment,
Harwell, Didcot, Berks.
18th September 1950.

F. K. GOWARD.
J. J. WILKINS.

GOWARD, F. K., and WILKINS, J. J., 1950 a, *Proc. Phys. Soc.* A, **63**, 662; 1950 b, *Ibid.*, **63**, 1171.

The Photo-disintegration of Oxygen into Two ^{8}Be Nuclei

Continuing the work reported in a recent note (Goward and Wilkins 1950), measurements have now been made on some 200 $^{16}O \rightarrow 4\,^4He$ photo-disintegration stars. As already reported, analysis of the first 100 stars showed the predominant modes of disintegration to be via intermediate ^{12}C nuclei, no definite evidence being obtained for direct disintegration into two ^{8}Be nuclei. That such direct disintegrations do occur, however, has been established by the larger number of stars, which include six clearly formed by initial disintegration into two ground state ^{8}Be nuclei, i.e. by the reaction $^{16}O+h\nu \rightarrow 2\,^8Be$. These stars are readily

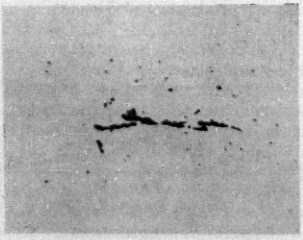

Photo-disintegration $^{16}O \rightarrow 2\,^8Be$.

recognized by the characteristic ' V ' tracks of the alpha-particles finally produced (Wilkins and Goward 1950), identification being confirmed by analysis; a typical example is shown in the photomicrograph.

It is, of course, possible for such a track formation to arise by chance in some other mode of disintegration. A rough estimate indicates that, after analysis, only about 1 star in 1,000 would be misinterpreted in this way in the present experiments.

Atomic Energy Research Establishment,
Harwell, Didcot, Berks.
6th October 1950.

F. K. GOWARD.
J. J. WILKINS.

GOWARD, F. K., and WILKINS, J. J., 1950, *Proc. Phys. Soc.* A, **63**, 1171.
WILKINS, J. J., and GOWARD, K. F., 1950, *Proc. Phys. Soc.* A, **63**, 1173.

Determination of Fission and Neutron Yields, and the Average Neutron Energy in the Photo-disintegration of Uranium

Although the fission and neutron yields in the photo-disintegration of uranium have been measured (Baldwin and Klaiber 1947, Price and Kerst 1950, Baldwin and Elder 1950), the interpretation of the results is obscured by two difficulties : (*a*) the gamma-ray intensities were determined by ionization chambers of somewhat arbitrary design which were not intercalibrated or related adequately to numbers of incident quanta, (*b*) the energy of the neutrons emitted in the photo-disintegration was not determined and no estimate could therefore be made of the likely errors in the neutron yield measurements.

To avoid these difficulties the yields have been remeasured (*a*) using an ionization chamber, with aluminium walls of variable thickness, whose calibration has been studied both practically (Lawson 1950) and theoretically (Flowers, Fossey and Roberts 1950), and (*b*) by determining approximately the average energy of the neutrons. In these remeasurements 23 MeV. bremsstrahlung from a synchrotron (Fry, Gallop, Goward and Dain 1948) was used.

The fission yield was determined by two ion chambers placed back-to-back, one of which contained a uranium film; this system reduced the size of gamma-ray ionization pulses. Only electrons were collected, and, in addition, the chambers were shallow and filled with hydrogen so that only the first portions of the fission-fragment and alpha-particle tracks were recorded (Pontecorvo and West, private communication); these expedients increased the discrimination of fission-particle pulses against alpha-particle pulses and microphony.

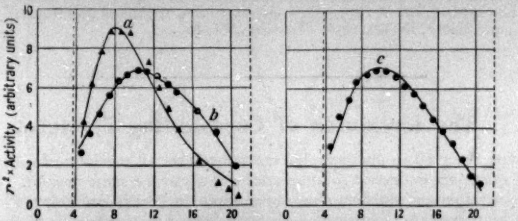

Measured 'C' neutron distributions (shown by dots and triangles) compared with theoretical results from a two-group diffusion theory (full curves): (*a*) for Na–γ–D neutrons, (*b*) for Ra–α–Be neutrons, (*c*) for photoneutrons from uranium.

The theoretical curves are calculated for average energies of 0·25, 4·0 and 1·8 MeV. respectively. Air-water interfaces are indicated on the graphs by dotted vertical lines.

The neutron yield was determined by irradiating about 300 gm. of uranium and slowing down the neutrons in a large distrene tank (68 cm. × 47 cm. × 44 cm.) containing $MnSO_4$ in aqueous solution. The activity induced in the stirred solution was compared with that induced by a standard Ra–α–Be neutron source.

The average neutron energy was measured with the same tank, but the distribution of C neutrons with distance from the uranium target was investigated by activating rhodium foils. The uranium target was separated from the solution in the tank by an air space, so that a rigorous analysis of the slowing down process was not possible. A simple 'two-group' diffusion theory did, however, give reasonable agreement between experiment and theory for Ra–α–Be and Na–γ–D sources (of known neutron energy) placed in the same position as the target, so this theory was used to determine the energy of the photoneutrons from uranium by interpolation. The degree of fit between experiment and theory is shown in the Figure.

The results obtained in the experiments were :

(1) 1 mg. of uranium gives 24·2±2 fissions/röntgen.

(2) 1 mg. of uranium gives 255±25 neutrons/röntgen.

(3) $\int_0^{23} \sigma dE = 1{\cdot}5 \pm 0{\cdot}3$ MeV. barn for the fission yield.

(4) $\int_0^{23} \sigma dE = 11{\cdot}5 \pm 3$ MeV. barn for the neutron yield.

(5) The mean energy of the neutrons emitted is 1·8±0·5 MeV.

In results (1) and (2) the röntgen is defined as the value obtained by extrapolating to zero wall thickness the straight portion of a curve for log (ionization) against aluminium wall thickness. Result (2) is high, compared with previous results (Price and Kerst 1950, Baldwin and Elder 1950), by a factor of at least 1·2, and the ratio of neutron to fission yield, $10{\cdot}5 \pm 2$, from results (1) and (2), is distinctly at variance with the ratio 3·4 determined by less direct methods (Price and Kerst 1950). Result (3) is approximately 4·5 times that of the previous determination (Baldwin and Klaiber 1947). The energy of photo-disintegration neutrons has not been measured previously, so that result (5) is important not only in relation to the yield determination but also in elucidating the mechanism of photo-disintegration. The mean energy is approximately that expected from a normal compound nucleus theory.

Details of the experiments on which this letter is based will be published.

Atomic Energy Research Establishment,
Harwell, Didcot, Berks.
8th September 1950.

F. K. Goward.
E. J. Jones.
H. H. H. Watson.
D. J. Lees.

Baldwin, G. C., and Elder, F. R., 1950, *Phys. Rev.*, **78**, 76.
Baldwin, G. C., and Klaiber, G. S., 1947, *Phys. Rev.*, **71**, 3.
Flowers, B. H., Fossey, E. B., and Roberts, S. J., 1950, *A.E.R.E. Report* T/R 543 (in course of general publication).
Fry, D. W., Gallop, J. W., Goward, F. K., and Dain, J., 1948, *Nature, Lond.*, **161**, 504.
Lawson, J. D., 1950, *A.E.R.E. Report* G/R 555 (in course of general publication).
Price, G. A., and Kerst, D. W., 1950, *Phys. Rev.*, **77**, 806.

The Ionization of Cosmic-Ray Particles

It has been observed in photographic emulsions that all particles of momentum higher than that of minimum ionization produce tracks of about the same density. Further, some tracks of twice minimum ionization have been reported (Bradt and Peters 1950). In some cases it has been possible to separate such tracks into two, further along their length, the components each having minimum ionization. These observations contradict the original ionization theory of Bethe and Bloch, as well as the modifications of Fermi (1940) and of Halpern and Hall (1948) which predict a rise of 50% for mesons of 10^{10} ev. It has been suggested that this rise might merge into the background of the emulsion because it is due to the relativistic broadening of the track. In view of the interest in this question, we present here some preliminary results obtained with a proportional counter, which measures the whole of the broadened track.

The proportional counter, filled to a pressure of 86 cm. Hg with a mixture of argon and 6% ethylene, was inserted in the cosmic-ray spectrometer briefly described elsewhere (Caro, Parry and Rathgeber 1950), between the Geiger counter tray immediately above the magnet and the magnet itself. In a run lasting 14 days we measured the ionization of some 400 particles capable of penetrating 10 cm. of lead and having momenta greater than $2{\cdot}4 \times 10^8$ ev/c. Our results averaged over a series of momentum ranges are shown in the Figure, together with those of Corson and Brode (1938) and Sen Gupta (1943), both of which were obtained by counting droplets in delayed cloud chamber photographs. Also shown, in plain curves, is the total energy loss in argon for electrons, μ-mesons and protons according to Halpern and Hall. Each of the two measurements on electrons has been multiplied by a factor which brings the points near minimum ionization into coincidence with the curve. Our measurements have been brought to the same level as those of Sen Gupta on mesons, which have been multiplied by the same factor as his electron measurements.

It is evident that whilst the measurements on electrons agree with the theory of Halpern and Hall, those on heavy cosmic-ray particles do not. The agreement of the cloud chamber and proportional counter results for heavy particles shows that this discrepancy cannot be due to experimental errors. Moreover, Sen Gupta's results for electrons and heavy particles were obtained during the same experiment. The following speculations might be made to account for this difference between theory and experiment. We shall consider the following suggestions: (i) a breakdown of the laws of electrodynamics which would

make the ionization constant at high momenta; (ii) that the correction of the Bloch–Bethe theory for polarization has been underestimated; (iii) an increasing difference between probable ionization and total energy loss with increasing momentum; (iv) that the proportion of cosmic-ray particles heavier than μ- or π-mesons increases with increasing momentum; (v) that in the ionization process the μ-meson does not behave like a simple charged particle.

The first two of these effects depend only on the velocity of the particle. As the theory gives correct results for electrons it might be expected to apply also to mesons of the same velocity. The third factor was examined by taking, in the theoretical relations, 1,000 ev. as the maximum transferable energy to an electron. This value corresponds to a cluster of 30 ion pairs. The fit for electrons appears to be better than for total ionization, but for mesons the difference remains, especially as the maximum energy transfer recorded by the proportional counter is estimated at 10^6 ev.

As to the fourth point, we know that there is little difference between the ionization of μ- and π-mesons and so an admixture of π-mesons would not become apparent in the results. It is possible to bring the theoretical ionization into agreement with the results at 2×10^9 ev/c. by assuming that all particles of this energy are protons. However even this extreme

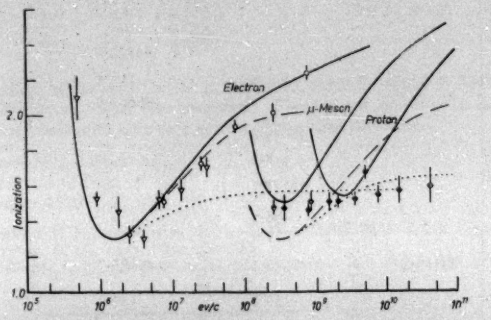

Specific ionization of cosmic-ray particles as a function of momentum.

▽ Electrons (Corson and Brode 1938). ● Mesons (Sen Gupta 1943).
○ Electrons (Sen Gupta 1943). ◆ Mesons (see present note).
———— total energy loss in argon.
— — — — probable ionization in argon normalized at minimum for electrons.
- - - - - - - - probable ionization in photographic emulsions.

assumption does not fit the experimental results over the whole momentum range. In addition it is known that at least up to 10^{10} ev/c. the majority of particles do not have the properties expected of π-mesons or protons, and that practically all particles in the range are μ-mesons. We have thus to conclude that μ-mesons differ from electrons in some respect other than mass.

To compare the above conclusions with the grain density measurements in photographic emulsions we have calculated the probable ionization in silver bromide. The results show that over the momentum range of the double tracks (Carlson, Hooper and King 1950), i.e. above 10^7 ev/c., the probable ionization changes by less than 10%, which agrees with observations. It is also evident that, on the basis of our calculations, the difference between electrons and mesons observed in argon would be more difficult to detect in photographic emulsions.

Physics Department,
University of Melbourne.
25th September 1950.

P. Goodman.
K. P. Nicholson.
H. D. Rathgeber.

Bradt, H. L., and Peters, B., 1950, *Phys. Rev.*, **77**, 54.
Carlson, A. G., Hooper, J. E., and King, D. T., 1950, *Phil. Mag.*, **41**, 701.
Caro, D. E., Parry, J. K., and Rathgeber, H. D., 1950, *Nature, Lond.*, **165**, 688.
Corson, D. R., and Brode, R. B., 1938, *Phys. Rev.*, **53**, 773.
Fermi, E., 1940, *Phys. Rev.*, **57**, 485.
Halpern, O., and Hall, H., 1948, *Phys. Rev.*, **73**, 477.
Sen Gupta, R. L., 1943, *Proc. Nat. Inst. Sci. India*, **9**, 295.

A New Ultra-Violet Band-System of SiF

In the course of a search for the spectrum of AgF, two double double-headed bands, degraded to shorter wavelengths, were observed with heads at 2109 and 2102 A. which do not appear to have been recorded hitherto. Bands already ascribed to SiF (Johnson and Jenkins 1927, Asundi and Samuel 1936, Eyster 1937) were strongly developed on the same plates, and since the separation of the new bands corresponds closely with the ground-state interval $^2\Pi_{3/2}$–$^2\Pi_{1/2}$ in SiF, it seemed likely that they formed part of a new system of this molecule.

Table 1. Deslandres Scheme for Q_1 and P_2 Heads

(The sensitivity varies so steeply with wavelength in this region that estimates of intensity have little meaning, but the 0,0 band appears much the strongest, and the 1,0 band is probably stronger than the 0,1 band.)

v'	$v''=0$		1		2		3
							48952·4
4							158·1
							48794·3
					48823·1		
3					161·5		
					48661·6		
			48689·8				47025·4
2			158·1				158·2
			48531·7				46867·2
			976·7				979·2
			977·9				—
	48558·5	845·4	47713·1	837·4	46875·7	829·5	46046·2
1	160·5		159·3		159·6		
	48398·0	844·2	47553·8	837·9	46715·9		—
	989·3		989·6		988·1		
	989·1		992·1		—		
	47569·2	845·7	46723·5	835·9	45887·6		
0	160·3		161·8				
↑	47408·9	847·2	46561·7				

Table 2

	New system	α-system
$\Delta G''_{0,1}$	845·6 cm^{-1}	845·3 cm^{-1}
$\Delta G''_{1,2}$	837·1	836·0
$\Delta G''_{2,3}$	829·5	827·9
Doublet interval	160·0	160·8

Confirmation of this view was obtained when the system was found to be excited in a high-frequency electrodeless discharge through SiF_4 gas prepared by heating $BaSiF_6$ to about 400° c. in a small furnace attached to the discharge tube. Spectrograms were taken with Hilger Medium and Small quartz instruments on Ilford Q.1 plates. The measurements of the inner heads, probably P_2 and Q_1, are summarized in the Deslandres scheme given in Table 1. In Table 2, the vibrational intervals in the lower state and the mean doublet separation, from Table 1, are compared with the values for the ground-state of SiF taken from Eyster (1937). The agreement is good and confirms the identification of the system.

The constants of the new upper state derived are :

$$\nu_0 = 47495 \text{ cm}^{-1}: \qquad G = 1005{\cdot}5(v+\tfrac{1}{2}) - 5{\cdot}2_8(v+\tfrac{1}{2})^2.$$

Since the doublet separation is so close to the $^2\Pi_{3/2}$–$^2\Pi_{1/2}$ separation, the upper state must be near to Hund's case (*b*). We can therefore proceed to estimate B' from the head–head separations. For both $^0P_{12}-P_2$ and P_1-Q_1 separations, neglecting spin-splitting, Λ-type doubling, and the influence of D terms, we have $\Delta = 2B'B''_{\text{eff}}/(B''_{\text{eff}} - B')$, where B''_{eff} indicates the appropriate effective value for $^2\Pi_{1/2}$ or $^2\Pi_{3/2}$. With Eyster's value $B''_0 = 0{\cdot}5795$, $B''_{\text{eff}} = B''(1 \pm B''/A)$, and an assumed value of α'', equal to 0·004, obtained by comparison with similar molecules, the values of B' given in Table 3 were obtained. Simple averaging gives $B'_v = 0{\cdot}621 - 0{\cdot}00_3(v+\tfrac{1}{2})$.

Table 3. Head-separations and Values of B'(cm^{-1})

v', v''	P_2–$^0P_{12}$	B'	Q_1–P_1	B'	v', v''	P_2–$^0P_{12}$	B'	Q_1–P_1	B'
0, 0	17·1	0·624	15·4	0·624	1, 3	—	—	8·9	(0·647)
0, 1	16·1	0·622	15·5	0·619	2, 1	20·5	0·612	15·7	0·618
0, 2	—	—	15·4	0·615	2, 3	—	—	12·2	0·622
1, 0	19·2	0·619	16·9	0·620	3, 2	15·0	0·620	19·0	0·605
1, 1	17·9	0·617	17·1	0·614	4, 3	—	—	14·1	0·614
1, 2	15·1	0·620	14·7	0·617					

Violet-degraded bands with heads at 48325·0, 48311·3, 48163·5, 48149·6, 47799·1, 47784·9 and 47639·0 cm^{-1} were also observed. They do not appear to fit into the present system : they may belong to a further system of the same molecule.

Physical Chemistry Laboratory,
University of Oxford.
30th September 1950.

W. H. Dovell.
R. F. Barrow.

Asundi, R. K., and Samuel, R., 1936, *Proc. Indian Acad. Sci.* A, **3**, 346.
Eyster, E. H., 1937, *Phys. Rev.*, **51**, 1078.
Johnson, R. C., and Jenkins, H. G., 1927, *Proc. Roy. Soc.* A, **116**, 327.

Calculation of the Oscillator Strengths for certain Band-Systems of N_2 and C_2

In this Letter the oscillator strengths (f-values) for the molecular electronic transitions associated with the second Positive system of nitrogen and the Swan and Deslandres bands of carbon are calculated using the hydrogen-ion approximation.

The constants of the transitions are given below in Table 1, where R represents the mean internuclear distance for the two states in Ångström units and λ_0 the wavelength appropriate to the electronic transition in the same units.

Table 1

	Transition	λ_0	R (A.)	$R(a_0)$
C_2	$^3\Pi_u - {}^3\Pi_g$	5180	1·29	2·44
C_2	$^1\Pi_u - {}^1\Pi_g$	3853	1·29	2·44
N_2	$^3\Pi_u - {}^3\Pi_g$	3371	1·18	2·23

Expressing these transitions in the form of molecular orbitals, it is immediately seen (Mulliken 1932) that they reduce to the form $(\sigma_u 2s) - (\sigma_g 2p)$. The wave functions of the $(\sigma_u 2s)$ and $(\sigma_g 2p)$ molecular orbitals may be approximately represented by a suitable linear combination of atomic wave functions as in the case of the hydrogen ion.

It follows directly that the required wave functions may be written as

$$\Psi(\sigma_u 2s\,|\,\mathbf{r}) = \frac{\psi(2,0,0\,\text{A}\,|\,\mathbf{r}) - \psi(2,0,0\,\text{B}\,|\,\mathbf{r})}{2^{1/2}\{1 - S(2,0,0)\}^{1/2}}, \qquad \ldots\ldots(1)$$

$$\Psi(\sigma_g 2p\,|\,\mathbf{r}) = \frac{\psi(2,1,0\,\text{A}\,|\,\mathbf{r}) - \psi(2,1,0\,\text{B}\,|\,\mathbf{r})}{2^{1/2}\{1 - S(2,1,0)\}^{1/2}}, \qquad \ldots\ldots(2)$$

where the ψ's are normalized atomic wave functions with the principal, azimuthal and magnetic quantum numbers n, l, m as indicated, and with the nucleus to which they apply denoted by A or B in the usual way. The electronic position vector is denoted by $\mathbf{r}$.

The overlap integrals are given by

$$S(n, l, m) = \int_\tau \psi(n, l, m\ \mathrm{A}|\mathbf{r})\psi(n, l, m\ \mathrm{B}|\mathbf{r})\, d\tau, \qquad \ldots\ldots (3)$$

the integration being over all space τ.

Defining the dipole moment factor D as

$$\left| \int_\tau \Psi_i(\mathbf{r}) \mathbf{r} \Psi_f^*(\mathbf{r})\, d\tau \right|^2,$$

and making use of the expressions for $\Psi_i(\mathbf{r})$ and $\Psi_f(\mathbf{r})$ given by equations (1) and (2), it is found that

$$D = \frac{\{P(2, 0, 0;\ 2, 1, 0) - T(2, 0, 0;\ 2, 1, 0)\}^2}{\{1 - S(2, 0, 0)\}\{1 - S(2, 1, 0)\}}, \qquad \ldots\ldots (4)$$

where

$$P(2, 0, 0;\ 2, 1, 0) = \int_\tau \psi(2, 0, 0\ \mathrm{A}|\mathbf{r})\mathbf{r}\psi(2, 1, 0\ \mathrm{A}|\mathbf{r})\, d\tau$$
$$= \int_\tau \psi(2, 0, 0\ \mathrm{B}|\mathbf{r})\mathbf{r}\psi(2, 1, 0\ \mathrm{B}|\mathbf{r})\, d\tau,$$

and

$$T(2, 0, 0;\ 2, 1, 0) = \int_\tau \psi(2, 0, 0\ \mathrm{A}|\mathbf{r})\mathbf{r}\psi(2, 1, 0\ \mathrm{B}|\mathbf{r})\, d\tau$$
$$= \int_\tau \psi(2, 0, 0\ \mathrm{B}|\mathbf{r})\mathbf{r}\psi(2, 1, 0\ \mathrm{A}|\mathbf{r})\, d\tau.$$

The calculation of these integrals was carried out using Slater type atomic wave functions with the appropriate effective nuclear charge. In the case of the S and T integrals it was found necessary to introduce elliptic coordinates in the integration. Table 2 gives the values of the effective nuclear charge for each system together with the values of the integrals in atomic units, the unit of length being equal to the radius of the first Bohr orbit.

Table 2

	$Z=3{\cdot}08e$		$Z=3{\cdot}73e$
	$C_2(^3\Pi_u - {}^3\Pi_g)$	$C_2(^1\Pi_u - {}^1\Pi_g)$	$N_2(^3\Pi_u - {}^3\Pi_g)$
$P(2, 0, 0;\ 2, 1, 0)$	0·94	0·94	0·77
$T(2, 0, 0;\ 2, 1, 0)$	0·37	0·37	0·25
$S(2, 0, 0)$	0·50	0·50	0·45
$S(2, 1, 0)$	−0·30	−0·30	−0·33

Using equation (4) and the familiar expression $f = 304D/\lambda$ for the f-value in terms of the dipole moment factor D (in atomic units) where λ is the wavelength in A., we finally obtain the following results

Table 3

Transition	λ (A.)	D	f-value	Life-time (sec.)
$C_2(^3\Pi_u - {}^3\Pi_g)$	5180	0·50	0·029	$1{\cdot}4 \times 10^{-7}$
$C_2(^1\Pi_u - {}^1\Pi_g)$	3853	0·50	0·039	$5{\cdot}7 \times 10^{-8}$
$N_2(^3\Pi_u - {}^3\Pi_g)$	3371	0·37	0·033	$5{\cdot}2 \times 10^{-8}$

The f-value obtained here for the C_2 triplet system is in close agreement with the experimental value 0·024 obtained by Lyddane and Rogers (1941).

It is to be noted that in these calculations the hybridization of the orbits has been ignored.

Department of Physics,
Imperial College,
London, S.W.7.
20th October 1950.

G. Stephenson.

Mulliken, R. S., 1932, *Rev. Mod. Phys.*, **4**, 1.
Lyddane, R. H., and Rogers, F. T., 1941, *Phys. Rev.*, **60**, 281.

REVIEWS OF BOOKS

Méthodes de calcul dans des problèmes de mécanique. Pp. 102. (Paris: Centre National de la Recherche Scientifique, 1949.) No price.

In the spring of 1948, two international conferences on methods of calculation in problems of mechanics were organized at Marseilles and Paris by the C.N.R.S.; the papers contributed to these conferences have been collated and published in this volume. The contributors and topics are as follows: J. Valensi (Marseilles), "The role of applied mathematics in engineering"; D. N. de G. Allen (London), "Relaxation methods and problems of frameworks", "Relaxation methods and the solution of differential equations", together with "Supplementary notes on the application of relaxation methods"; Th. Vogel (Marseilles), "The escalator method for the calculation of eigenfrequencies"; M. Picone (Rome), "New points of view in harmonic analysis"; L. Couffignal (Paris), "Calculating machines for harmonic analysis according to the method of H. and Y. Labrouste"; J. M. Burgers (Delft), "Problems related to the theory of turbulence"; L. Malavard (Paris), "Some recent applications of the method of electrical analogies"; A. van Vijngaarden (Amsterdam), "Potential flow about a solid of revolution"; F. H. van den Dungen (Brussels), "The application of the calculus of variations in fluid mechanics"; L. Couffignal, "The role of numerical calculation in scientific and technical research".

The papers naturally vary in style and standard but they are, without exception, lucidly written and the book can be thoroughly recommended to a physicist or engineer who wishes to acquire some idea of modern techniques used in the realm of classical mechanics. R. M. D.

Vorstufe zur theoretischen Physik, by R. BECKER. Pp. vii+172. (Berlin: Springer-Verlag, 1950.) 7.50 DM.

This book is interesting from a didactic point of view. Each section can be described as a sort of *verbatim* rendering of a (very good) lecture for beginners. Every detail is carefully written down, including observations of a methodical character, paternal advice, disclosure of useful tricks, and even humorous illustrations with which every teacher intersperses his lectures, but which he usually leaves out when he writes a textbook. The subjects treated are restricted, apart from some slight digressions, to the field of mechanics and thermal phenomena (including kinetic theory). Within this range the selection is the fairly obvious one which, I think, every one of us would make in order to illustrate the application of the most fundamental methods of classical theory. The treatment seems to me somewhat uneven: some sections are extremely elementary, while neighbouring ones are on a decidedly higher level. The discussion of some questions of principle (e.g. the fundamental equation of dynamics) is, in my opinion, too cursory and even slovenly; that of the thermoelectric phenomena is definitely in error. Moreover, there is no reference anywhere to the historical development of the subjects; this is admittedly better than the uncritical repetition of historical mis-statements in which too many authors indulge, but just for pedagogical purposes a judicious use of historical material would be of the greatest help, and would materially enliven the picture. Becker's book will certainly convey to the student a sound understanding of the attitude of mind of the theoretical physicist, but it is a bit too dry to give him even a hint of the beauty of his quest.

L. ROSENFELD.

THE INSTITUTION OF ELECTRICAL ENGINEERS

Proof and Reprint Service

The following details of the Proof and Reprint Service of The Institution of Electrical Engineers, London, have been received, with a request that they should be brought to the attention of our members. Formerly the proofs of a paper allocated for reading before the Institution of Electrical Engineers were made available to members only 10 days before the meeting; thus, if accepted at a time when the current programme of meetings was complete, authors' manuscripts might sometimes lie dormant for several months. Since October 1948 " early proofs " of all papers have been printed without avoidable delay.

As soon as the early proofs of a paper are available, an announcement to that effect, together with a synopsis, appears in the monthly *Journal* of the Institution. Application for such proofs can then be made, and those who avail themselves of this service are given the opportunity of applying for a reprint, from the *Proceedings* of the Institution, of the paper in its final form, together with a report of the discussion. The object of the reprint service is to ensure that the permanent record available to its users shall not consist of an early proof which, however carefully prepared, may contain minor errors and will certainly not include the discussion.

The inclusive charge for an early proof and its associated reprint is 2*s*. 6*d*. (post free). This charge is made whether or not the reprint is required, but a reprint alone can be supplied at the price of 1*s*. 6*d*. (post free) if ordered shortly after the paper has been read in London.

Requests for proofs should be sent, accompanied by a remittance, to The Secretary, The Institution of Electrical Engineers, Savoy Place, London W.C.2, England.

CONTENTS FOR SECTION B

PAGE

Dr. I. J. SHAW. Some Further Investigations of Ionospheric Cross-Modulation . 1

Mr. E. KNIGHTING. Some Meteorological Aspects of Radio Duct Formation . 21

Dr. R. D. CONNOR. The Properties of Spark Counters of the Rosenblum Type . 30

Dr. J. G. OLDROYD, Dr. D. J. STRAWBRIDGE and Dr. B. A. TOMS. A Coaxial-Cylinder Elastoviscometer 44

Mr. L. G. CARPENTER and Mr. W. N. MAIR. The Evaporation of Titanium . . 57

Dr. W. EHRENBERG and Dr. W. E. SPEAR. An Electrostatic Focusing System and its Application to a Fine Focus X-Ray Tube 67

Dr. J. H. VAN DER MERWE and Prof. H. VERLEGER. Low Reflectance Coatings and the Sensitivity Curve of the Eye 76

Letters to the Editor :

Dr. J. G. POWLES. The Interpretation of Dielectric Measurements using the Cole–Cole Plot 81

Dr. P. T. LANDSBERG. Characteristics of Selenium Photocells . . . 82

Dr. E. YEAGER, Dr. J. BUGOSH and Dr. F. HOVORKA. The Measurement of Ultrasonic Vibration Potentials (Debye Effect) with Pulse Techniques . 83

Mr. S. E. BARDEN. A Note on Resonance Damping, at Injection, in Betatrons and Synchrotrons 85

Reviews of Books 87

The Institution of Electrical Engineers. Proof and Reprint Service . . . 93

Contents for Section A 94

Abstracts for Section A 95

ABSTRACTS FOR SECTION B

Some Further Investigations of Ionospheric Cross-Modulation, by I. J. SHAW.

ABSTRACT. The work in this paper forms the continuation and development of the experiments described in a paper by Ratcliffe and Shaw published in 1948. Measurements of the phase and amplitude of the modulation transferred to an unmodulated wave by a modulated disturbing wave in the ionosphere are used to provide information about that part of the ionosphere in which the cross-modulation occurs.

By measuring almost simultaneously the height of reflection of the wanted wave and the characteristics of the transferred modulation, a value of $1{\cdot}4 \times 10^6$ per second for the collision frequency of electrons with molecules at a height of 92 kilometres has been deduced. This measurement has been made possible by the use of a very sensitive automatic apparatus which is briefly described.

Special attention has been paid to the ' gyro-resonance effect ' in cross-modulation first pointed out in a theoretical paper by Bailey in 1937. The experiments appear to show that the predicted enhancement of the cross-modulation when the disturbing station radiates on the local gyro-magnetic frequency does not exist.

A modification of the original theory is given which is of great use in the calculation of the cross-modulation to be expected for a given pair of transmitters. This modified theory is used in the discussion of the gyro-resonance effect and of the observed decrease of the cross-modulation at dawn. The agreement between the calculated and observed magnitudes of cross-modulation is stressed in view of the fact that the calculations involve a knowledge of the absorption of the wanted wave incident obliquely upon the ionosphere.

Some Meteorological Aspects of Radio Duct Formation, by E. KNIGHTING.

ABSTRACT. Three problems of meteorological interest concerning the formation of radio ducts are treated. The first concerns the rate of growth of ducts, with special reference to ducts over the sea; it is shown that ducts form quickly at first and then more slowly as the maximum duct width is approached. The second problem concerns the formation of ducts under conditions of nocturnal cooling; it is shown that there is a limit to the height which the duct may attain. The third problem concerns the width of a radio duct necessary to enclose the track width of a mode associated with a propagated signal of wavelength λ assuming a power law of modified refractive index with height; it is shown that the necessary width is proportional to $\lambda^{2/3}$, and the factor of proportionality, which depends upon the index in the assumed power law, is calculated.

The three problems have a common meteorological basis, for each is concerned with turbulent motion near the earth's surface. The law of turbulent diffusion assumed here is that the coefficient of eddy diffusion is proportional to a power of the height, following the theory developed by O. G. Sutton and others.

The Properties of Spark Counters of the Rosenblum Type, by R. D. CONNOR.

ABSTRACT. The design and operation of Rosenblum-type spark counters having plane, concave and convex cathodes is described, and discussed with reference to the counting characteristics, useful life and background counting rate. The absolute efficiency of the counter in air has been determined for α-particles, knock-on protons, and β-particles, giving values of about 90%, 5% and 0·0002%, respectively. A marked dependence of efficiency on specific ionization and air pressure is evident. The counter is directional in all its forms. The effect of employing gases other than air is also investigated and a qualitative description of the counting characteristics is given. Alpha-particle ranges may be determined using either a single counter or two counters used in anticoincidence as is described in the text.

A Coaxial-Cylinder Elastoviscometer, by J. G. OLDROYD, D. J. STRAWBRIDGE and B. A. TOMS.

ABSTRACT. An instrument is described which was designed to measure the elastic and viscous properties of liquids, primarily of solutions of linear high polymers whose elastic properties had already been observed qualitatively. The liquid is contained in a narrow annulus between two long vertical cylinders. The outer cylinder can be driven in steady rotation at a known speed, or in harmonic angular oscillations of known amplitude and frequency. In steady rotation, the torque on the stationary inner cylinder is measured at different speeds, and interpreted to give a viscosity coefficient as a function of shear stress. In oscillatory motion, the amplitude of oscillation of the inner cylinder, when constrained by a torsion wire, is measured and plotted against the frequency. The shape of the resulting graph can be interpreted so as to distinguish and measure different types of elastic behaviour. The annular gap, the restoring constant of the torsion wire and the amplitude of oscillation of the outer cylinder can be varied in discrete steps. The angular velocity of the outer cylinder can be varied continuously from 0·3 to 3,000 rev/min. in steady rotation, and the frequency can be varied continuously from 0·25 to 25 c/s. in steady oscillation. The performance of the instrument in both steady-state and oscillatory experiments is assessed by comparing observed and predicted results for Newtonian liquids of known viscosity. An example is given of the behaviour of a typical polymer solution in both kinds of experiment, together with a suggested quantitative interpretation of the results.

The Evaporation of Titanium, by L. G. CARPENTER and W. N. MAIR.

ABSTRACT. Data are presented on the evaporation rate of β titanium over the temperature range 1,650–1,810° K.

These are represented by

$$\log ET^{1/2} = -\frac{2{\cdot}42}{T} + 9{\cdot}79,$$

where E is in gm.cm^{-2} sec^{-1} and T is in degrees Kelvin.

The latent heat of vaporization is deduced both from the measured values of evaporation rate, together with known thermodynamic functions of the solid and gas, and also from the temperature coefficient of evaporation rate.

An estimate is made of the variation of total radiation with temperature, and of the vapour pressure at the melting point.

Experimental details are given.

An Electrostatic Focusing System and its Application to a Fine Focus X-Ray Tube, by W. EHRENBERG and W. E. SPEAR.

ABSTRACT. The description is given of an electrostatic focusing system by which electrons emitted from the tip of a hairpin filament are reunited at a distance of 2 to 3 cm. No intermediate potentials are required. An X-ray method is used for the experimental investigation of its properties. The electron spot is a reduced image of the tip of the filament and has a diameter of about 40 μ. On the basis of this system, a fine focus X-ray tube is designed, with a peak specific target loading of about 11 kw/mm^2. Some performance data are given.

Low Reflectance Coatings and the Sensitivity Curve of the Eye, by J. H. VAN DER MERWE and H. VERLEGER.

ABSTRACT. Heterochromatic light is treated and the spectral sensitivity of the human eye is taken into account. In spite of certain simplifying assumptions, conclusions of a general character may be drawn, the most important being that the optical properties required for low reflectance coatings can be obtained by treating the incident light as monochromatic.

Shower A

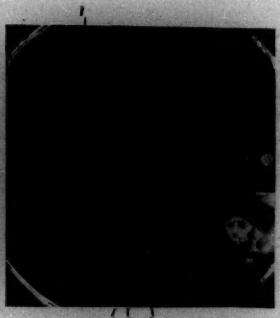

Shower B

Shower C

Shower D

(See back of plate for description.)

Description of Plate

Showers A, B, C and D were observed under 25 cm. of paraffin wax using a magnetic field of 7,500 gauss.

Shower A.

This photograph shows at least two related nuclear interactions in the lead plate induced by a neutral primary. Track 1 is associated with the main interaction; the momentum is of the order of 10^9 ev/c. and the track appears to emerge at an angle of 10° from the core of the main event. The track appears to start in the core and not in the plate to the left of the core. Thus track 1 may have been deflected from the core through an angle of 10° and the process may be similar to that described by Rochester and Butler (1947), that is, the spontaneous decay of a meson with a mass between that of the π-meson and the proton.

Shower B.

A penetrating particle (track 1) is accompanied by a neutral-induced secondary interaction. This event is unusual since two distinct electron cascades were formed; the angle between the cores of these cascades is about 18°. The mean directions are shown by arrows 2 and 3. Unfortunately shower particles are mixed with the electrons, and therefore it is impossible to determine the total energy of each cascade. The cascades may have been produced by the decay of a neutral π-meson.

Shower C.

This event is a simple shower of three collimated penetrating particles, tracks 1, 2 and 3. Track 1 is scattered through 31° in the plate. It is too short for measurement above the plate, but below it is negative with a momentum of 10^9 ev/c.

Shower D.

Tracks 1 and 2 are almost parallel and appear to produce electron cascades of very different energies in the lead plate. Track 1 has a momentum which is too high for measurement and, in addition to the large cascade, produces track 3, which is negative with a momentum of 8×10^8 ev/c. This particle was projected at an angle of 40° to the direction of track 1 and so it is very unlikely to be an electron and must be a meson. Tracks 1 and 3 intersect in the top half of the lead plate and, if the cascade was formed in this region, the total energy in the electronic component is likely to be about 10^{10} ev.

Track 2 is positive with a momentum of $1{\cdot}5 \times 10^9$ ev/c. and is likely to be due to an electron which produced the cascade of three electrons below the plate.

Tracks 1 and 2 are unlikely to be part of an air shower. In order to produce the large cascade, track 1 must have an energy greater than 10^{10} ev., and such an electron would be very close to the core of an air shower.

If the right-hand event is a nuclear interaction, then it is of a very unusual type, and in all probability there are mesons and protons, other than track 3, which must be located in the core of the cascade and so be unobserved. If this is so, the whole event must be of exceptionally high energy.